GL02152

Milestone SPT23KM4: Results of the Analysis of the Timber Mt., Lathrop Wells, and Yucca Mt. Aeromagnetic Data November 29, 1996

WBS 1.2.3.11.2 Surface Geophysics

M. A. Feighner, and E. L. Majer

Earth Sciences Division
Ernest Orlando Lawrence Berkeley National Laboratory
Berkeley, California 94720

Background and Introduction

The depth to basement and basement structures are an important issue for understanding the tectonic setting of Yucca Mt. One of the methods sometimes used to shed information on the basement structure is the inversion of magnetic field data. A data set available in the Yucca Mt area, but not processed prior to the work described in this report, consists of several aeromagnetic surveys flown in the early 1980's. Therefore in August of 1995, at the suggestion of DOE, LBNL procured a study from EarthField Technology Inc. (ETI) in Houston, Texas to process and invert the aeromagnetic data from the Timber Mt., Lathrop Wells, and Yucca Mt. surveys along with the available gravity data. The objective was to obtain information on the depth to basement. Unfortunately, the aeromagnetic data that ETI obtained from the Geophysical Data Center in Denver, Colorado was flawed by an incomplete and mislocated Timber Mt. survey. The error was not detected until after ETI had completed the processing. Therefore, in the summer of 1996 another attempt was made at procuring services to process the aeromagnetic data for a depth-to-basement interpretation. Shown in Appendix I are the scope of work put out for bid to two different vendors, the bid by ETI, and the final contract awarded to ETI. As can be seen, the final contact differed somewhat from the initial scope of work sought, mainly due to the high bids received. However, ETI was contracted to determine the depth to basement by interpreting the aeromagnetic data inverted with the Werner deconvolution method. LBNL checked the data beforehand to insure that the problems of an incomplete and mislocated data set did not occur again. In September of 1996 LBNL, supplied ETI with the three different data sets (see enclosed report of McCafferty). In mid-November of 1996 LBNL was contacted by ETI and informed that in the opinion of ETI the data were not of sufficient quality to derive the information sought, i.e., a reliable depth to basement. LBNL then contacted personnel within the USGS who had supplied the data to the Geophysical Data Center (Vickey Bankey and Tien Grauch) to obtain their opinion on the quality of the data, and suitability for obtaining a reliable depth to basement. They concurred that the data were not suitable for obtaining a depth to basement, mainly due to the fact that the Paleozoic basement in this region of Nevada is almost non-magnetic, and the overlying volcanics further complicate attempts to derive a "depth to basement". It is well known that the Yucca Mt. region is typical of many volcanic regions, in that it is very heterogeneous and structurally complex. The general nature of the volcanics (alternating flow properties

in a vertical and horizontal direction) causes many magnetic anomalies. The magnetic method is, like gravity surveys, a potential field method with magnetic susceptibility being the significant material property variable (like density in gravity). Changes in the physical properties of subsurface rocks leads to anomalies measured by surface instruments. While gravity and magnetics use similar interpretation techniques, the magnetic method is somewhat more complicated. The magnetization of a rock (which is dependent on susceptibility), has both magnitude and direction. Magnetic anomalies can come from variation in magnitude or variation in direction of magnetization and magnetic effects can be caused by certain minerals within the rock mass. Additionally, the total magnetization of a rock mass is composed of induced and remanent magnetization. At Yucca Mountain, previous studies have found the Topopah Tuff is one of the major magnetic anomaly producing formations, depending on faulting and juxtaposition to other formations. Therefore it is very difficult to "see through" the volcanics to derive the basement structure.

what about remanence??

Although a depth to basement was not obtained, an attempt was made to derive fault structure from the magnetic field intensity maps from the merged data sets. All of the subject data and processing described in this report has not been Quality Assured.

Data Processing and Interpretation

The aeromagnetic data was obtained from the National Geophysical Data Center in Boulder, CO. The individual flight lines had been adjusted and merged into a data grid. The merged data represents all the surveys as if flown at a constant altitude of 1000 feet above topography. The data supplied to us were in geographical coordinates and were converted to Nevada State Plane coordinates using the EarthVision software. The entire data set covers a large area and is shown in Figure 1 with the repository boundaries surrounding Yucca Mountain shown for scale. Many high frequency anomalies can be seen that are probably associated with near-surface volcanics. Short wavelength magnetic anomalies arise from shallow magnetic bodies.

Figure 2 shows an enlarged portion of the aeromagnetic data with the surface traces of faults from Sawyer et al. (1995) overlain as white lines. At this scale, there is a correlation between faulting and the magnetic anomalies. The north-south faults in the repository area match alternating highs and lows in the magnetic data. The short wavelength of these features also suggest a shallow source and probably arise from offsets in a shallow magnetic unit. Bath and Jahren (1994) have shown that many north-trending, linear magnetic anomalies are caused by vertical offset of the moderately to highly magnetic Topopah Spring Tuff.

In order to determine the depths of some longer wavelength features, we chose to use two profiles as shown in Figure 3. The first profile is REG-2 & 3, which follows the regional seismic lines, as reported by Brocher et al. (1996). This profile crosses a relatively broad magnetic high in the middle of Crater Flat. The other profile is A-A' and follows a north-south line and crosses a magnetic high. Figure 4 shows the same magnetic data 2-D continued upward to an altitude of 5000 feet above topography. This was done using the software GMT (Wessel and Smith, 1991). This eliminated the high frequency anomalies created by the shallowest magnetic bodies.

at <30° to mag trends, then along a mag discontinuity

AA' E of YMCZ N S @ Calico Hills

Figure 5 shows the magnetic anomaly along REG-2 & 3, along with the anomaly after upward continuation. This produces a smooth profile which can then be used to estimate the depth to the magnetic body. The Peters' Method (Dobrin, 1976) was used to estimate the depth of the magnetic body. In this method, the maximum slope of the anomaly is determined, and then the half-slope points above and below are calculated. This gives a width "S" as shown in

Figure 5. The depth is then simply estimated by (S/1.6). For this profile the S width is 12245 feet, giving a depth of 7653 feet below the level of the anomaly. Since the anomaly was continued upward to 5000 feet, this gives a depth of 2653 below the surface. This is much too shallow for the Paleozoic basement in this area (Majer et al, 1996), and this anomaly is probably due to the Topopah Spring Tuff.

Figure 6 shows the anomaly along Profile A-A'. The slope of the anomaly is even steeper than in Figure 5, resulting in a depth of the magnetic body of 1125 feet below the surface. Paleozoic basement does outcrop along this profile at the location of the magnetic high. However, Ponce and Langenheim (1995) do not consider the Paleozoic to be magnetic in their modeling, since it consists mainly of limestones and dolomites. Again, this anomaly is probably due to shallow magnetic tuffs.

Conclusions

The aeromagnetic anomalies appear to correlate well with mapped faults and seem to indicate faulted offsets in shallow magnetic tuffs, such as the Topopah Spring Tuff. Deeper magnetic anomalies may be present, but are overwhelmed by the shallow or surface volcanic signatures. The Paleozic basement is unlikely to be magnetic due to the non-magnetic nature of limestones and dolomites; thus depth to basement estimates cannot be made for this boundary.

Acknowledgements

This work was supported by the Director, Office of Civilian Radioactive Waste Management, U.S. Department of Energy, through Memorandum Purchase Order EA9013MC5X between TRW Environmental Safety Systems, Inc. and the Ernest Orlando Lawrence Berkeley National Laboratory, under Contract No. DE-AC03-76SF00098. The computations and field work would not have been possible without the continued support of Berkeley Lab's Center for Computational Seismology and Geophysical Measurement Center by the Department of Energy's Office of Energy Research Basic Energy Sciences Geoscience Program and Health and Environmental Sciences Subsurface Science Program.

References

Bath, G.D. and C.E. Jahren, Investigations of an aeromagnetic anomaly on the west side of Yucca Mountain, Nye County, Nevada, USGS-OFR-85-459, 24 pp., 1985.

Dobrin, M. B., Introduction to Geophysical Prospecting, Third Ed, McGraw-Hill, New York, 630 pp., 1976.

Brocher, T.M., P.E. Hart, W.C. Hunter, and V.E. Langenheim, Hybrid-Source Seismic Reflection Profiling Across Yucca Mountain, Nevada: Regional Lines 2 and 3, USGS-OFR-96-28, 97 pp., 1996.

Majer, E.L., M. Feighner, L. Johnson, T. Daley, E. Karageorgi, K.H. Lee, K. Williams, and T. McEvilly, Synthesis of Borehole and Surface Geophysical Studies at Yucca Mountain, Nevada and Vicinity, Volume 1: Surface Geophysics, WBS 1.2.3.11.2, Lawrence Berkeley Nat. Lab, 1996.

Ponce, D.A. and Langenheim, V.E., Gravity and magnetic investigations along selected high-resolution seismic reflection traverses in the central block of Yucca Mountain, Nevada, USGS-OFR-95-667, 23 pp., 1995.

Sawyer, D.A., R.R. Wahl, J.C. Cole, S.A. Minor, R.J. Laczniak, R.G. Warren, C.M. Engle, and R.G. Vega, Preliminary digital geologic map database of the Nevada Test Site Area, Nevada, USGS-OFR-95-0567, 62 pp., 1995.

Wessel, P. and W. H. F. Smith, Free software helps map and display data, Eos Trans. AGU, 72, 441-446, 1991.

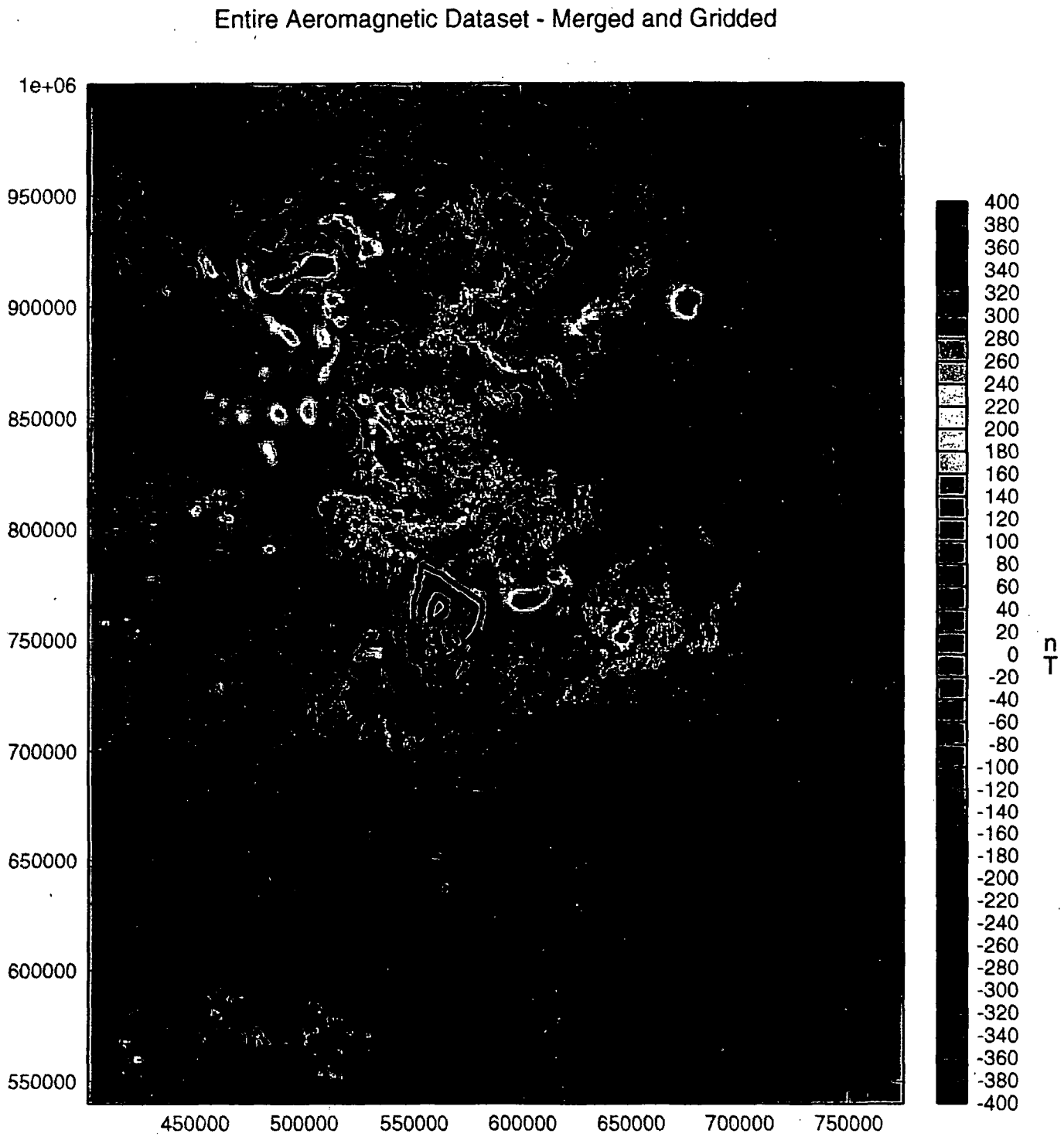

Figure 1. The entire aeromagnetic dataset of the Yucca Mountain Region. The outer black line is the conceptual boundary and the inner black line is the repository boundary. Coordinates are in Nevada State Plane feet.

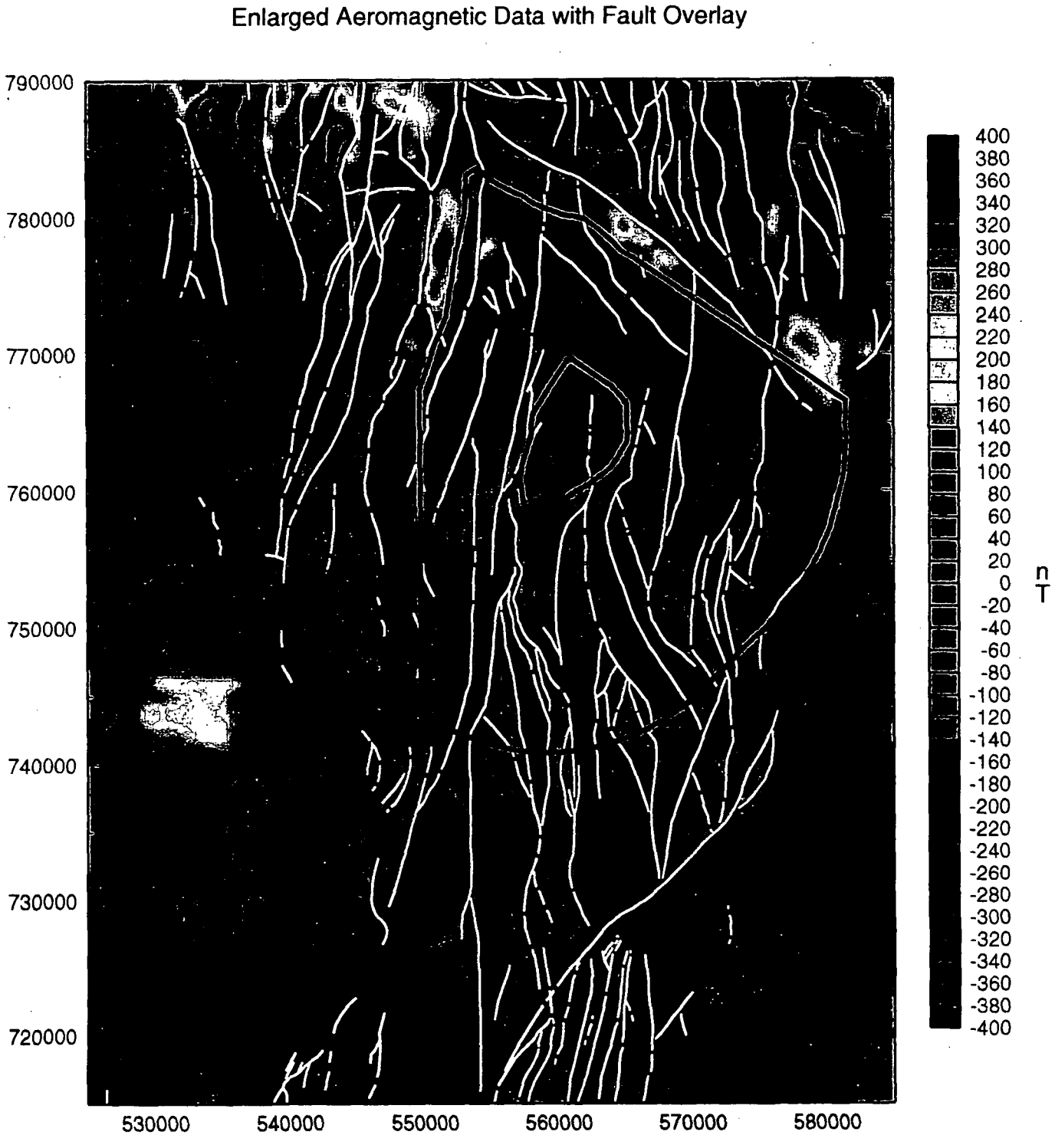

Figure 2. An enlarged section of Figure 1 with faults from Sawyer et al. (1995) overlain as white lines. Coordinates are in Nevada State Plane feet.

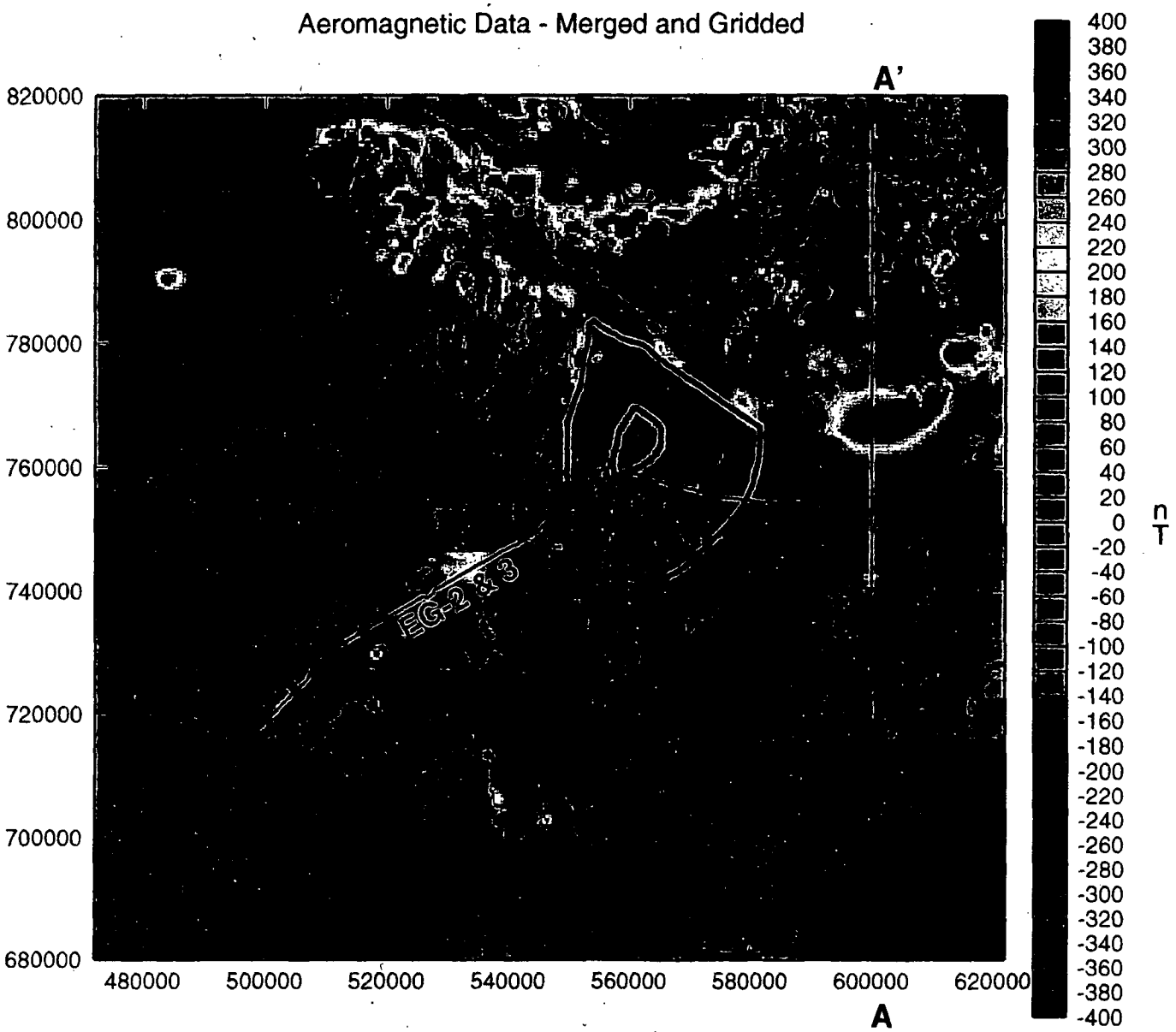

Figure 3. The location of the two profiles: REG-2 & 3 and A-A'. Both profiles cross broader magnetic anomalies to which depth estimates are made. Coordinates are in Nevada State Plane feet.

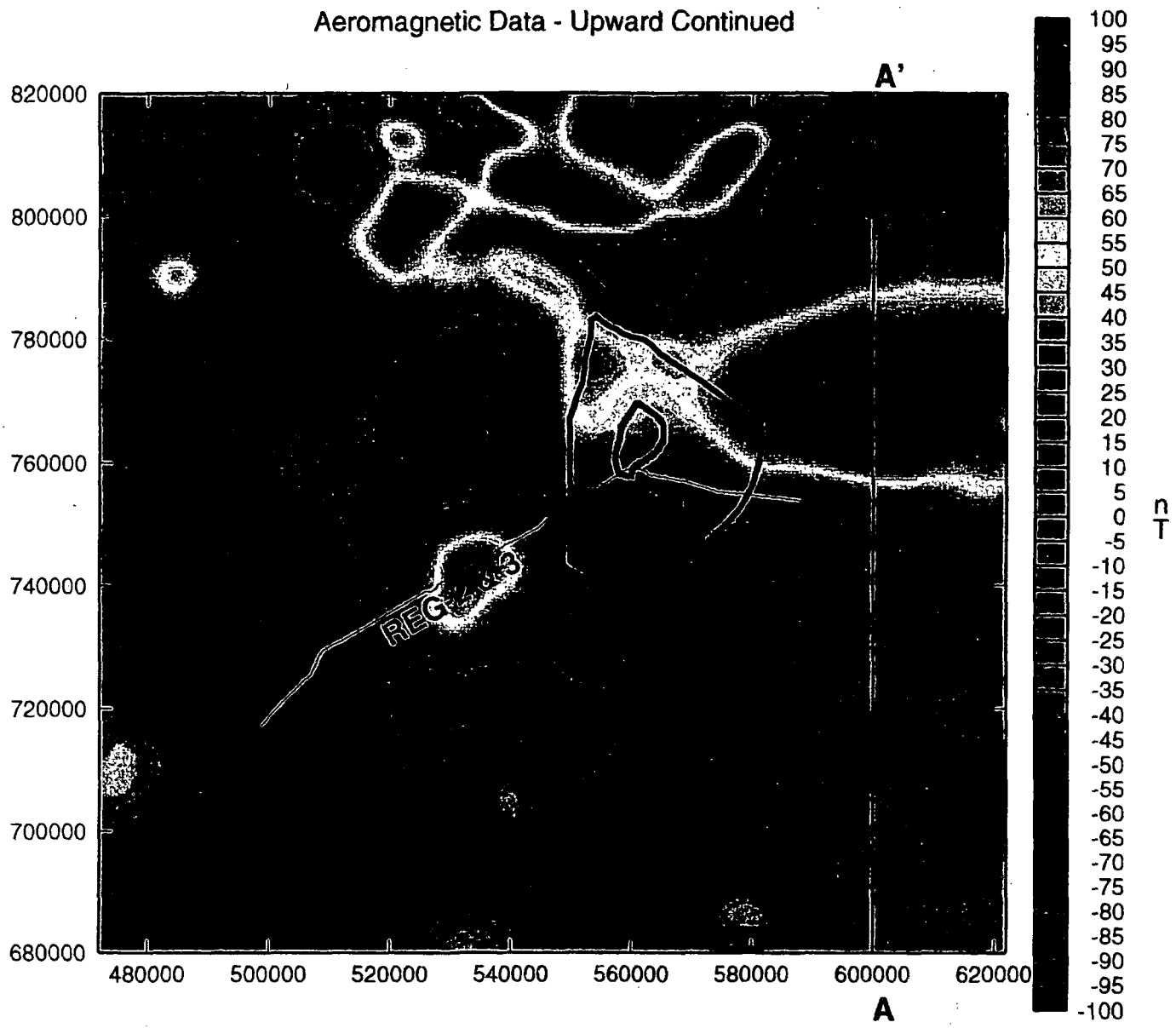

Figure 4. The upward continuation of the magnetic field in Figure 3 to 5000 feet above topography. This was done to eliminate high frequency signals. Coordinates are in Nevada State Plane feet.

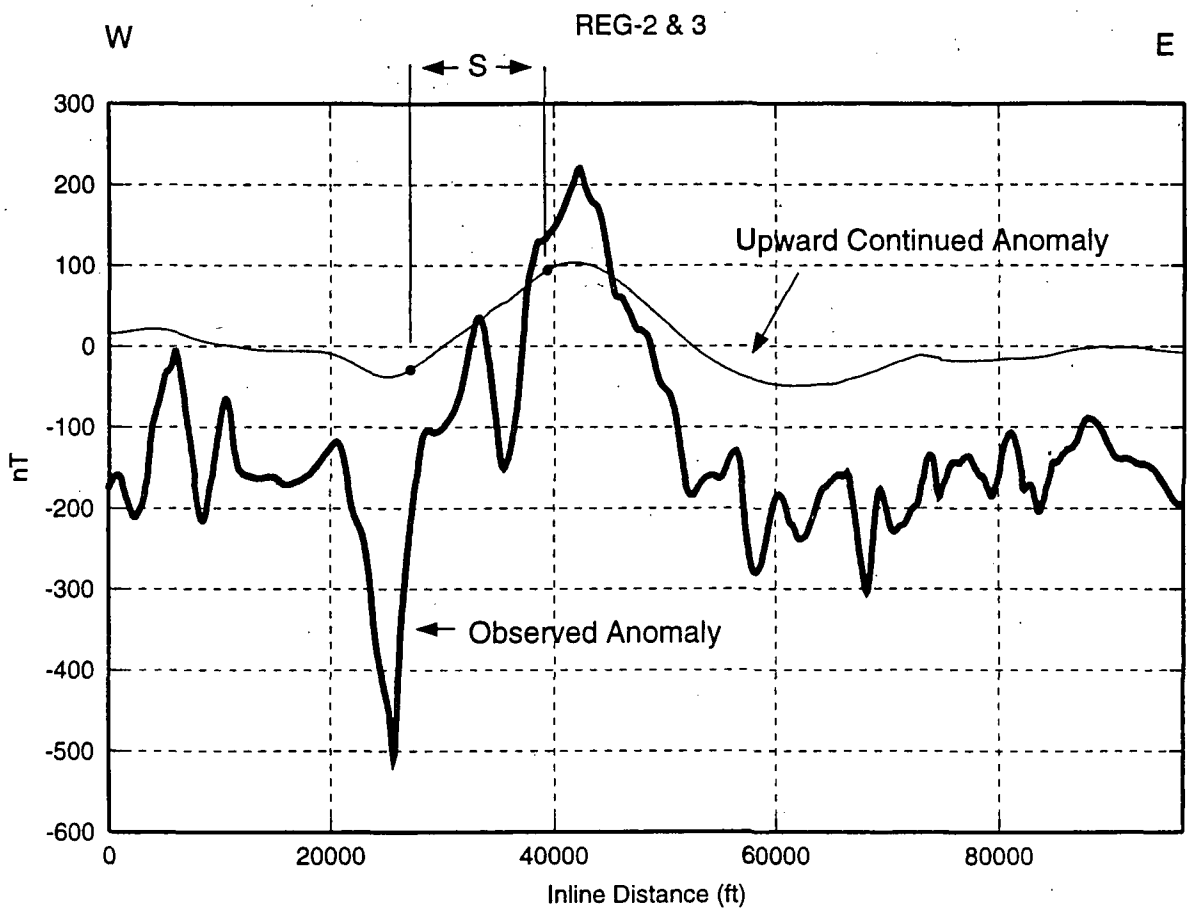

Figure 5. The magnetic anomalies along Profile REG-2 & 3. The half-slope width, S, can be used to estimate the depth of the magnetic body.

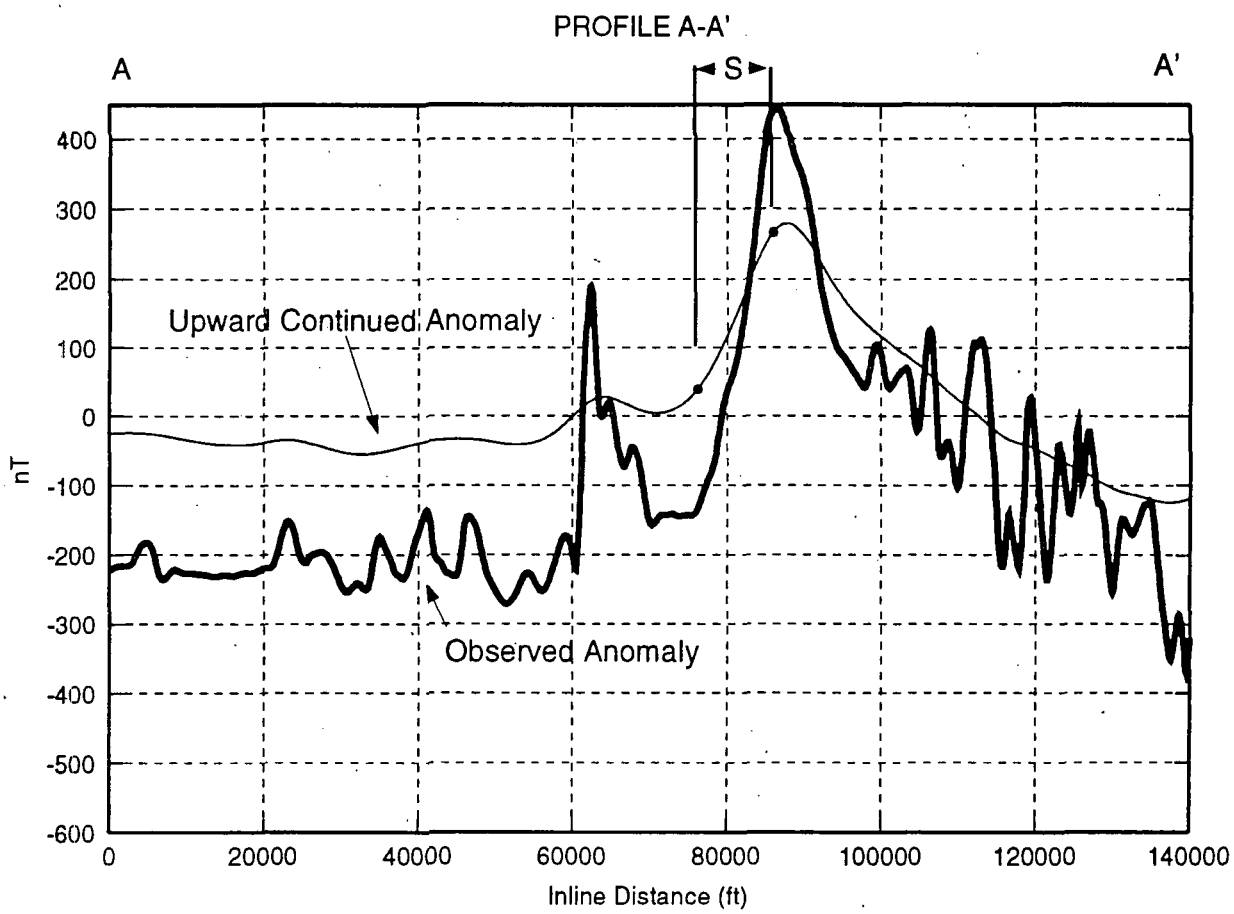

Figure 6. The magnetic anomalies along Profile A-A'. The half-slope width, S, can be used to estimate the depth of the magnetic body.

Appendix I. to Milestone SPT23KM4:

Scope of Work, Earthfield Scope of Work, and Final Contract

Scope of Work

Processing and analysis of aeomagnetic data

There will be three data sets delivered to the vendor
in ASCII format as obtained from the National Geophysical Data Center
1/4 mile spacing on flight lines, see enclosed map for location of
surveys

1. Lathrop Wells 8149 miles (black)
2. Yucca Mt. 1118 miles (blue)
3. Timber Mt. 9614 miles (red)

Digital and hard copies of the following results will be required,
the final scale of the hard copy maps
will be determined by LBNL before the final
results are transmitted to LBNL. The digital versions will be
in a format such that LBNL can plot the results with their
plotting software, i.e., ASCII grid files with X,Y, and Z values,
using Nevada state plane coordinates.
We also require the data points from which the grid files were generated.

The deliverables will be the following:

A final report describing the processing steps and methods used
in sufficient detail such that a person who is knowledgeable in
magnetic methods can reproduce the results if necessary.

The data will be processed to provide the following results:

1- A Total field intensity magnetic map using all three data sets merged
such that the flight elevation of each survey has been properly accounted
for and reduced to a common datum, as well as the diurnal drift being
properly corrected for in each data set.
2-depth to magnetic basement map using at least three differnt
approaches to the the inversion, the final result being a best
fit to the different inversion results.
3-copies of the different profile inversions along all profiles,
and interpretation if possible
4-rtp (reduced to pole) total intensity map
5-map of the near surface faults and intrusions as inferrred from the
magnetic data
6-surface faults and intrusions interpretation
7-horizontal derivative (1st derivative) rtp map
8-rtp high pass 20k ft
9-rtp low pass 20k ft
10- rtp high pass 30k f
11- rtp low pass 30k ft
12-bandpass from 20-30k ft
13- 2nd derivative rtp map

In addition we would also want a presentation of
the results in Berkeley at the end of the work as well
as one trip by LBNL/DOE personnel in the Yucca Mt project to
the vendor to view the progress of the work.

The trip function would be for the work to be seen and reviewed by
oversite specialists, and some of the project management and technical
specialist from the volcanism program. The date and time would be
determined as the data processing and reduction continues.

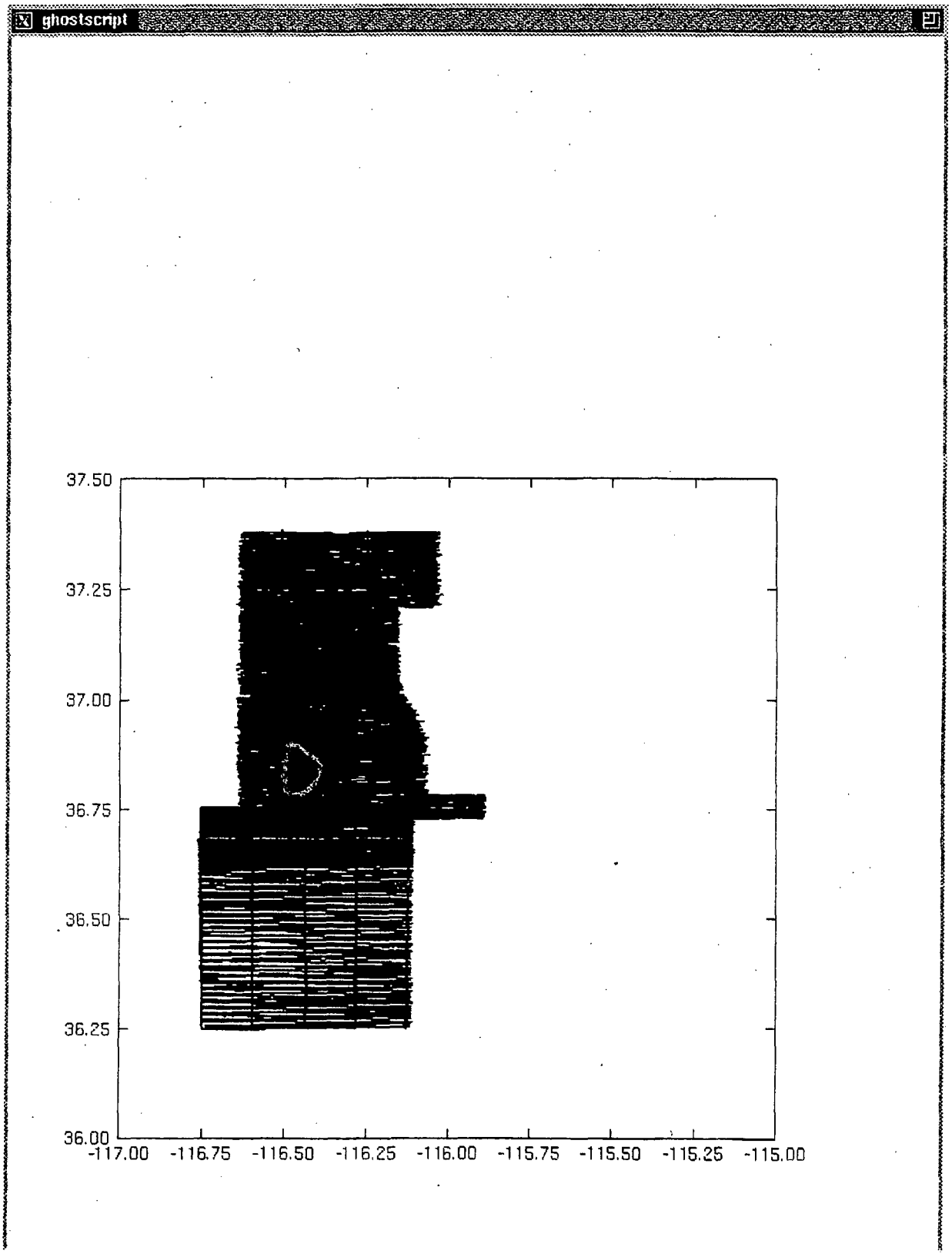
ghostscript
37.50
37.25
37.00
36.75
36.50
36.25
36.00
-117.00
-116.75
-116.50
-116.25
-116.00
-115.75
-115.50
-115.25
-115.00

et earthfield technology

June 18, 1996

Ms. Peggy Jellinghausen
University of California
Ernest Orlando Lawrence
Berkeley National Laboratory
Purchasing 69-201
1 Cyclotron Road
Berkeley, California 74920

RE: PROPOSAL #3655000

Dear Ms. Jellinghausen:

As per your request, Earthfield is pleased to provide you with a quotation for the processing and interpretation of gravity and magnetic data over your project area at Yucca Mountain, Nevada.

The objectives of this study are to:

- map basement depth

- map basement structure

AEROMAGNETIC DATA ANALYSIS

Berkeley National Laboratory will provide all digital aeromagnetic data for this study which are being acquired through the National Geophysical Data Center. As data are acquired they will be reviewed, edited, leveled and merged as necessary at which point analysis may begin.

We would like to state our belief that effective analysis of magnetic data can best be accomplished using a profile by profile approach to evaluate anomalies arising from various depths. There are a variety of automated depth calculation algorithms available, and though your "RFP" requests three profile methods, we prefer, and will only be using the Werner deconvolution method.

650 North Belt East, Suite 410 • Houston, TX 77060 • 713-847-1666 • FAX 713-847-1775

The Werner method of magnetic data interpretation is a widely accepted, profile based, inverse modelling approach. This technique utilizes the raw total intensity data along each flight line and a calculated horizontal derivative of this data to determine the depth of a causative body by assuming two simple geometric configurations of the feature. The two simple geometries used in this technique are the thin dike model, which uses the total intensity data for its calculations, and the infinite block model which uses the horizontal derivative.

By assuming these basic geometries in this fashion the depth, dip and apparent magnetic susceptibility contrast of an anomaly source can then be derived from the data. The Werner algorithm analyzes progressively longer anomaly waveforms in a series of passes along the data with an increasing operator width, thereby calculating depths to progressively deeper sources. In this manner, all types of sources are resolved regardless of the depth.

It is therefore possible to identify cultural, sedimentary, basement structural or intrabasement features on a single profile. The resultant Werner profiles display numerous depth solutions to the various sources which the geophysicist will then interpret to identify the proper depth estimates and to determine from what type of source the solution was produced. This interpretation is critical since the mapping of intrabasement sources as representing basement structure would result in an inaccurate map of the basement surface. Likewise, anomalies arising from sedimentary sources do no want to be confused with those arising from basement sources.

The interpreter will evaluate your data to determine and map sources arising from basement, sedimentary and cultural sources. Depths picks will be posted and contoured producing a structural/depth to basement mylar overlay. The interpretation will then be digitized and mapped in color.

DELIVERABLES

All magnetic maps will be laminated and will consist of the following:

- Total magnetic intensity contours of the merged data set in color with shaded relief
- rtp magnetic contours in color with shaded relief
- rtp high pass 20,000 feet in color with shaded relief
- rtp low pass 20,000 feet in color with shaded relief
- rtp high pass 30,000 feet in color with shaded relief

- rtp low pass 30,000 feet in color with shaded relief

- band-pass residual map from 20,000-30,000

- 1st derivative in color with shaded relief

- 2nd derivative in color with shaded relief

- flightline map

- Werner deconvolution profiles along each flightline *approximately 18,881 line miles (not laminated)*

- depth to basement/structural interpretation overlay from Werner analysis on a clear overlay

- digitized depth to basement in ASCII format

- color version of depth to basement map

- interpretation of near-surface faults derived from magnetics on a clear overlay

- digital version of each map in HPGL format and of basement surface in ASCII format.

- merged TMI in ASCII format

GRAVITY DATA ANALYSIS

Earthfield will produce the following qualitative maps from Bouguer gravity data already on-hand. These maps will be used by the project supervisor as an aid in producing the interpretation overlay listed above.

- Bouguer gravity contours in color with shaded relief

- Residual gravity contours emphasizing long wavelength anomalies

- Residual gravity contours emphasizing intermediate wavelength anomalies

- Residual gravity contours emphasizing short wavelength anomalies

- Euler 3d deconvolution solutions in color

FINAL REPORT

Earthfield will prepare a summary report detailing all work performed

PRESENTATION

This bid allows for a one day visit to Earthfield's office in Houston during the term of the project. Additional visits can be scheduled if necessary.

Upon completion, the project geophysicist will present the results of this study in your office in Berkeley,California. All costs associated with this presentation are covered by this proposal.

TIME FRAME

If project begins no later than July 1, 1996, completion will be on, or before, November 22, 1996.

COST

The cost of the project, as defined above, will be $25,000.00.

If you have any questions regarding this proposal, or if you require any additional information, please let me know and I will respond as soon as possible.

Very truly yours,

David Lane
President

R&D - Expense Type 54

certifier if different from below:

start date:	end date:
9/9/96	11/29/96

Requester:	Bldg. &	Room:	Deliver to::	Bldg.	Room	Notify:	Extension:
Ernie Majer	90	1116	Same			E. Majer	6709

Approved by:	Account no.:	Amount of Transaction:	Stat. Code:	Req. No.	
Andre Bell	8175-41	$ 20,000.00	7112200	194444	

Submit correspondence to Procurement Specialist FAX: (510) 486-4380

DPAS Rating: (15 CFR 700)

From Receipt of goods or invoice whichever is later.

0 - 1/2% 10th & 25th | 3 - 1% 30 Days
1 - 1/2% 10 days | F - 2% 10th & 25th
C - 1% 10th & 25th | 5 - 2% 10 days
2 - 1% 10 days | H - 2% 20 days
9 - 1% 10th prox. | 6 - 2% 30 days
7 - Net 30 days | 8 - As Shown
J - Net 01 | K - Net 10
L - Net 15 | M - Net 20

Procurement Specialist:	Code:	Subcontract No:	Seller Code	Start date:	Terms:
Peggy Jellinghausen Phone:(510) 486-7210	275	6436583		9/3/96	7

To: Earthfield Technology
Attn: David Lane
650 North Belt East, Suite 410
Houston, TX 77060

Ship to: Berkeley National Laboratory
Attn: E. Majer, S/C #6436583
One Cyclotron Road, m/s 90-1116
Berkeley, CA 94720

MAIL INVOICE IN DUPLICATE TO:
University of California Ernest Orlando Lawrence Berkeley National Laboratory
Accounting Office, S/C #6436583
P.O. Box 528, CODE JS
Berkeley, CA 94701

University of California
Ernest Orlando Lawrence
Berkeley National Laboratory
One Cyclotron Rd. m/s 69-201, Berkeley CA 94720

R & D SUBCONTRACT

For Contract No. W-7405-ENG. 48 Or Contract No. DE-AC03-76SF00098 with the Department of Energy

FOR RESALE:-State Sales Tax should not be charged, as the University holds State Sales Tax Permit SR CH 21-835970 for deliveries to University of California Ernest Orlando Lawrence Berkeley National Laboratory and Permit SR-CHA 21-135323 for deliveries to Lawrence Livermore National Laboratory.

Ship Via: (as coded) 0
1. pickup | 2. Parcel Post | 3. UPS | 4. Federal Exp. 1 | 5. Motor Freight | 6. Air Freight | 7. Air Parcel Post | 8. Federal Exp. 2 | 9. Air Frt. Forwarder 0. See Below
Seller's Choice

Transportation Terms (as coded) 2
1. Account of University see Article V. below
2. Account of Subcontractor Prepaid
3. See Body of Order
Shipping Point: Houston, TX

F.O.B. (as coded) 1
1. Destination
2. Shipping Point
3. Shipping Point, Freight Allowed
4. See Body of Order

Earthfield Technology, herein and in attachments hereto called "Seller" or "Subcontractor", agrees to furnish to the University of California Ernest Orlando Lawrence Berkeley National Laboratory, herein and in attachments hereto called "University", "Berkeley Lab", "LBL", and "LBNL", the following in strict accordance with the terms, conditions, and provisions of this Subcontract, herein and in attachments hereto called "Order", or "Subcontract":

I. SCOPE OF WORK

Subcontractor shall furnish the labor necessary to perform the work described under Scope of Work in the attached Appendix A which is hereby made a part of this subcontract.

II. PRICE, ACCEPTANCE AND PAYMENT

Subcontractor shall perform the work described herein for the firm fixed price of $20,000.00

Acceptance of work and payment under this subcontract shall be based on satisfactory compliance with the following:

A. Subcontractor's performance of work as set forth herein in consonance with high professional standards as determined by Berkeley Lab.

B. Compliance with the reporting requirements set forth in the Scope of Work.

III. TERM

Unless completely performed thereto or sooner terminated by either party, the work described herein shall begin September 9, 1996 and be completed by November 29, 1996.

IV. INVOICING

Invoices shall be reviewed, approved and certified for payment by Berkeley Lab's Ernie Majer. Invoices shall be submitted in arrears for work completed to:

University of California, Ernest Orlando
Lawrence Berkeley National Laboratory
Accounting Office, Subcontract #6436583
P.O. Box 528, CODE JS
Berkeley, CA 94701

V. ATTACHMENTS

In addition, the provisions or articles listed below and attached hereto are made a part of this order and are equally binding.

1. Appendix A, Scope of Work
2. Survey Map
3. Addendum to Terms and Conditions of University of California Subcontract.
4. General Provisions for Fixed Price Supplies & Services.

Authorized by: _____

University of California, Ernest Orlando
Lawrence Berkeley National Laboratory
Renee Jewell
Group Leader

ACCEPTED: Earthfield Technology

BY: _____

TITLE: _____

DATE: _____

APPENDIX A - SCOPE OF WORK
Processing and Interpretation of Aeromagnetic Data

I. BACKGROUND

This project is very similar to that performed by subcontractor under Subcontract #4613410. A full set of corrected data will be submitted to subcontractor in addition to the previous maps submitted to Berkeley Lab under the previous subcontract. Subcontractor shall rework the maps and previous findings to incorporate the corrected data. The method to be used on this project is the Werner deconvolution method.

II. SCOPE OF WORK

Subcontractor shall provide processing and interpretation of aeromagnetic data as described below.

Subcontractor shall receive the maps previously submitted by subcontractor to Berkeley Lab under Subcontract #4613410. These shall be used as reference and shall be submitted under separate cover. Additionally, subcontractor shall receive three data sets delivered in ASCII format as obtained from the National Geophysical Data Center. There shall be 1/4 mile spacing on flight lines. See enclosed map for location of surveys with descriptions shown below.

1. Lathrop Wells, 8149 miles (black)
2. Yucca Mt., 1118 miles (blue)
3. Timber Mt., 9614 miles (red)

Please note that in this particular region of Nevada the basement defined by the gravity data is not the same as the basement defined by aeromagnetic data. In interpreting the aeromagnetic data this should be considered. Berkeley Lab will have the basement structure (usually the paleozoic surface) as derived from the gravity values. In addition, Berkeley Lab will supply a regional geologic map showing the location of surface intrusions.

Digital and hard copies of the following results will be required. The final scale of the hard copy maps will be determined by Berkeley Lab before the final results are transmitted to Berkeley Lab. The digital versions will be in a format such that Berkeley Lab can plot the results with their plotting software, i.e., ASCII grid files with X, Y, and Z values, using Nevada state plane coordinates. Berkeley Lab also requires the data points from which the grid files were generated.

III. DELIVERABLES

Subcontractor shall submit a final report describing the processing steps and methods used in sufficient detail such that a person who is knowledgeable in magnetic methods can reproduce the results if necessary.

The data will be processed to provide the following results:

1. Depth to magnetic basement map
2. Digital depth to magnetic basement map
3. Magnetic lineation interpretation map
4. RTP, high pass 20,000 ft, 1st vert. derivative
5. RTP, high pass, 20,000 ft
6. RTP, low pass 30,000 ft
7. RTP
8. Total magnetic intensity

9. RTP horizontal derivative
10. Topographic map
11. Geologic map
12. Digital topography map
13. Magnetic flight path

In addition, Berkeley Lab will also require a presentation of the results in Houston, Texas upon completion of the work. Berkeley Lab also reserves the right to send Berkeley/DOE personnel from the Yucca Mt. project to subcontractor's facility to view the work in progress. The function of the trip would allow for the work to be seen and reviewed by oversite specialists as well as the project management and technical specialist from the volcanism program. The date and time would be determined as the data processing and reduction continues.

A summary report shall be written by the subcontractor summarizing the data results and all relevant information. Two (2) copies of the report shall be submitted to Berkeley Lab by November 29, 1996 to the following address:

University of California, Ernest Orlando
Lawrence Berkeley National Laboratory
Attn: E. Majer, m/s 90-1116
One Cyclotron Road
Berkeley, CA 94720

The Subcontractor shall not distribute reports of work, drawings, specifications, etc., under this Subcontract to any individual or organization other than those indicated above without the prior written approval of the Subcontract Administrator.

IV. OPERATING ASSURANCE

Subcontractor shall bear primary responsibility for the services. Subcontractor shall use its own best ability, skill and care in the performance of work. Specifically, subcontractor will be responsible for the professional quality, technical accuracy and the coordination of all data, reports, documentation and other services furnished by subcontractor. Subcontractor shall without additional compensation correct or revise any errors or deficiencies in its data, reports, documentation, and other services.

V. KEY PERSONNEL

note:

The Principal Investigator at Earthfield Technology is William Cathey, Senior Geophysicist who: (A.) will devote a reasonable amount of time to the work; (B.) be closely involved and continuously responsible for the conduct of the work; (C.) will not be replaced unless approved by the Laboratory; and (D.) will advise the Laboratory if he will devote substantially less effort to the subcontract than anticipated.

It is understood and agreed that any key technical individual(s) assigned to this work shall not be reassigned to other work that will interfere with the research and support activities under this Subcontract without prior Berkeley Laboratory approval, except in circumstances beyond the reasonable control of Earthfield Technology. If such circumstances arise, Earthfield Technology shall inform the Technical Coordinator of such reassignments within (5) working days. A replacement individual shall be assigned by Earthfield Technology and approved by the Berkeley Laboratory Technical Coordinator within ten (10) working days. If an acceptable individual is not identified; Berkeley Laboratory reserves the right to terminate this Subcontract.

VI. SELLER/SUBCONTRACTOR CHANGE(S) TO SCOPE OF WORK

Ernest Orlando Lawrence Berkeley National Laboratory's approval is required to change the phenomenon under study, the stated objectives of the research, or the methodology.

VII. EQUIPMENT AND SUPPLIES

Equipment and supplies acquired with funds provided by this Subcontract is governed under the provisions of the Property Article from the Addendum to Terms and Conditions of University of California Subcontract.

VIII. COORDINATION AND ADMINISTRATION

The Berkeley Laboratory Technical Coordinator under this Subcontract is Ernie Majer, or his designee(s), who shall represent Berkeley Laboratory in matters relating to technical performance of this Subcontract. All other matters relating to the performance of this Subcontract are reserved to the Subcontract Administrator.

Further, any technical direction which will affect the estimated cost or time of performance under this Subcontract shall require prior formal amendment to the subcontract, or prior written direction in accordance with Clause 52, Changes-Fixed Price, of the University of California, Ernest Orlando Lawrence Berkeley National Laboratory, General Provisions for Fixed Price Supplies and Services.

The Laboratory's Subcontract Administrator is Peggy Jellinghausen or her designee. All matters relating to the interpretation and administration of this Subcontract which are not specifically delegated to the Laboratory's Technical Coordinator are reserved for the Subcontractor Administrator. The Subcontractor shall direct all notices and requests for approval to the Subcontractor Administrator, and any notice or approval from Berkeley Lab. to the Subcontractor will be issued by the Subcontract Administrator.

IX. ACCESS TO SUBCONTRACTOR'S FACILITIES

The University of California, the U.S. Department of Energy, and Ernest Orlando Lawrence Berkeley National Laboratory or their designees, shall have the right to inspect the work and activities of Earthfield Technology under this Subcontract at such time and in such manner as they shall deem appropriate.

X. NOTICES-INABILITY TO PERFORM

If, at any time during the performance of this Subcontract, the Subcontractor becomes aware of any circumstances whatsoever which may jeopardize its fulfillment of the agreed performance of all or any portion of the Subcontract, it shall immediately notify the University's Subcontract Administrator in writing of such circumstances, and the Subcontractor shall take whatever action is necessary to cure such defect within the shortest possible time.

Digital aeromagnetic grids for data centered on the Southwestern Nevada Volcanic Field, Nevada and California

by

*A. E. McCafferty

U.S. Geological Survey
P.O.Box 25046, Denver Federal Center, MS 964
Denver, CO 80225

* e-mail: anne@musette.cr.usgs.gov

Introduction

Aeromagnetic data were compiled for an area encompassing the Miocene southwestern Nevada volcanic field as part of a cooperative study between the U.S. Geological Survey (USGS) and the Department of Energy Environmental Restoration (ER) program. The overall objective of this project is to investigate the regional hydrogeologic setting of the Nevada Test Site (NTS) and vicinity and in particular, to define and characterize the ground water-flow pathways around the NTS.

The Environmental Restoration study area is located in the south central part of the northern Basin and Range Province and is centered on the Timber Mountain-Silent Canyon caldera complexes of the southwest Nevada volcanic field (figure 1). The volcanic field is comprised of a number of overlapping calderas and volcanic centers covering an area of approximately 1800 km^2, which represents one of the largest caldera systems in the United States (Snyder and Carr, 1984). Extensional normal faulting has been active previous to, throughout, and after the emplacement of the calderas, but more so during the late stages of volcanism (Christiansen and others, 1977). The region is characterized by surface outcrops of thin, relatively flat-lying deposits of ash-flow tuffs and alluvial deposits associated with the volcanic centers within and surrounding the caldera complexes that have an accumulated thickness of more than 4 km.

The exposed Cenozoic volcanic and sedimentary rocks have been extensively studied as part of the nation's nuclear testing and high-level waste disposal programs. Geologic maps exist that cover part of the ER area (Frizzell and Shulters, 1990) and the remaining areas have been revised and compiled from draft maps by the USGS (Minor and others, 1992, Carr and others, 199_). Although most of the area has been mapped in detail, these studies provide little control on the units most critical to ground water flow. Pre-Tertiary geology, mostly obscured by the volcanic units, consist of an 3.5 km-thick sedimentary package of alternating carbonates and clastic rocks that form the aquifers and aquitards respectively (Winograd and Thordarson, 1975). Additionally, little is known about buried volcanic units and their possible influence on ground water movement. The geometry and depth to buried volcanic and pre-Tertiary geologic units can only be defined by indirect methods such as regional reconnaissance geophysical mapping combined with drilling.

Regional compilations of aeromagnetic data are published that cover a large part of the ER study area (Kirchoff-Stein and others, 1989, Hildenbrand and Kucks, 1988) and were initiated by work concerned particularly with the Nevada Test Site but also included regional state studies. The data used for these previous compilations used older surveys, which have since been replaced with the surveys shown in this report. Additionally, the previously

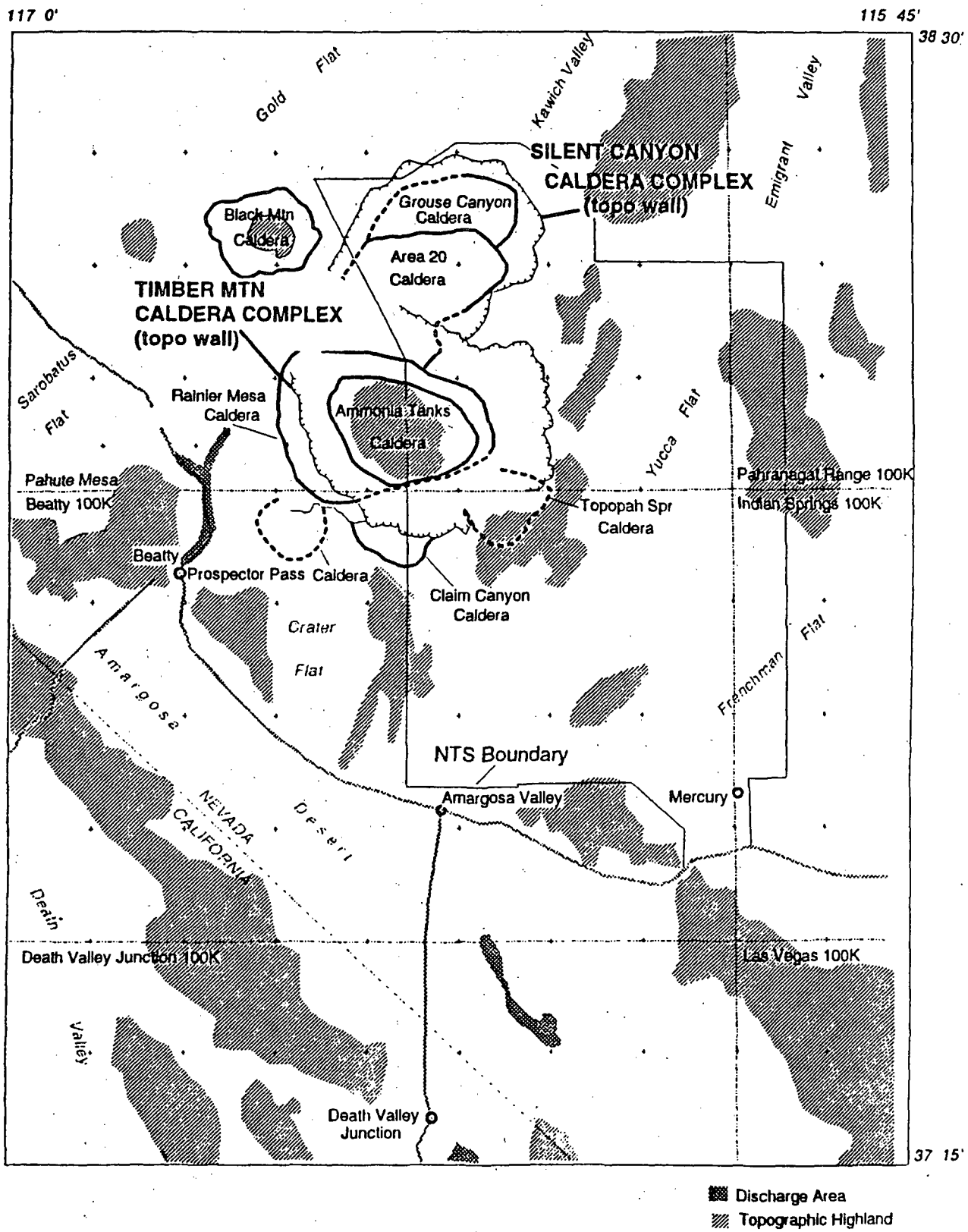

Figure 1 Map showing caldera boundaries and select topographic features modified from Frizzell and Shulters, 1990. Caldera boundaries after Sawyer (U.S. Geological Survey, unpublished data)

published aeromagnetic maps were compiled at a 1 km grid interval, an order of magnitude coarser than the 100 m grid interval used to produce the map in this study. Therefore, much of the high resolution available in the detailed survey areas was lost due to the coarseness of the 1-km grid.

The study area covers a region between lat 36° 15' N. and 37° 30' N., and long 115° 45' W. and 117° 0' W. The maps cover the entire Beatty and Pahute Mesa 30- by 60-minute (1:100,000-scale) quadrangle maps and parts of the Pahranagat Range, Indian Springs, Death Valley Junction, and Las Vegas 1:100,000-scale maps (fig. 1). The aeromagnetic anomaly grids form the basis of the geophysical contribution to this multidisiplinary study.

COMPOSITE AEROMAGNETIC ANOMALY GRID: 'ERJIGSAW.ASC'

Aeromagnetic data exist for the study area in the form of a patchwork of thirteen surveys collected in a piecemeal fashion over a period of two decades. 'ERJIGSAW.ASC' is a gridded mosaic of the surveys and shows the individual surveys in their original form before the data were further processed and merged into one data set. The surveys were flown with varying flight-line spacing, altitudes, and flight specifications. Figure 2 and table 1 outline and describe the flight specifications and detail the manner in which the data were collected.

Most of the NTS and the central part of the Environmental Restoration study area are covered by detailed, high-quality digital data (surveys 6,7,9a-c,10 and 11 in figure 2). The detailed surveys were flown at low altitude with flightline spacing of 800 m or less. The flight-line data for these surveys are archived on 9-track magnetic tapes in retrievable digital form. However, for surveys flown pre-1971, the data are archived as contour maps only and required digitization along contour-line-flight-path intersections before further processing and integration with adjacent surveys.

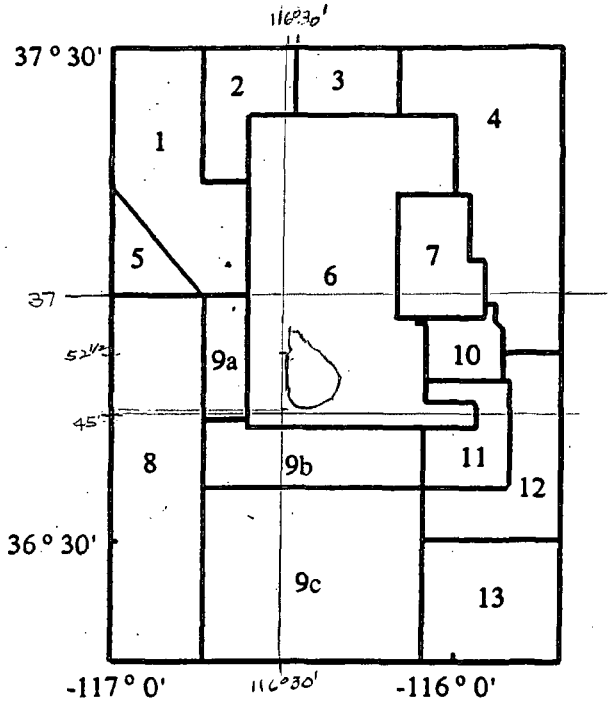

Figure 2-- Index map showing locations of aeromagnetic surveys used for this study. Numbers refer to table 1.

Table 1--Aeromagnetic data specifications for surveys used in the compilation for this study [AG, above ground; B, barometric]

Area	Name	Year Flown	Flight Elevation (m)		Flight Spacing (m)	Flight Direction	Reference
1	Sarcobatus Flat	1963	2440	B	800	E-W	Philbin and White, 1965a
2	Black Mtn	1963	2440	B	1600	E-W	Philbin and White, 1965b
3	Silent Canyon	1963	2440	B	1600	E-W	Philbin and White, 1965c
4	Climax Stock	1980	2286-2440	B	1600	E-W	Bath and others, 1983
5	Bonnie Clair	1967	2740	B	1600	E-W	U.S. Geological Survey, 1967
6	Timber Mtn	1977	122	AG	400	E-W	U.S. Geological Survey, 1977
7	Yucca Flat: Los Alamos	1990	146	AG	400	E-W	Los Alamos unpublished, 1990
8	Death Valley	1979	122	AG	1600	N-S	Geodata International, 1979a
9a	Lathrop Wells	1978	122	AG	800	N-S	Langenheim and others, 1991
9b	" "	" "	122	AG	400	E-W	" "
9c	" "	" "	122	AG	800	E-W	" "
10	Yucca Flat	1971	122	AG	400	E-W	U.S. Geological Survey, 1971
11	Mercury	1982	122	AG	400	E-W	U.S. Geological Survey, 1984
12	Las Vegas	1982	305	AG	1600	E-W	U.S. Geological Survey, 1983
13	S. Nevada	1978	305	AG	1600	E-W	U.S. Geological Survey, 1979b

The data were projected onto a Cartesian coordinate system using a Universal Transverse Mercator (UTM) projection with a central meridian of 117° W. and a base latitude of 36° N. Data from each survey were interpolated to a square grid using a minimum-curvature algorithm (Webring, 1981); grid spacing was typically 1/4 to 1/3 the original flight-line spacing. The magnetic-anomaly grid (total field intensity minus the Definitive Geomagnetic Reference Field: DGRF) was calculated (Sweeney, 1990) for the appropriate time of year and elevation of the original survey. If an obsolete regional field other than the

DGRF had been removed, the outdated geomagnetic reference field was added back and the appropriate DGRF was subtracted from the grid.

The surveys were trimmed to the borders shown on figure 2 (program *JIGSAW*, Cordell and others, 1992). The majority of the surveys in this report have some overlap with adjacent surveys. When surveys overlapped, the survey with the higher quality data (closer spaced flight-lines, digital, low altitude) was chosen to define the trimmed edge. The white areas between surveys are 'dvals' (dummy values or areas of no data); the result of data being removed from around the survey grid periphery before plotting in order to emphasize the aerial extent of each survey used to produce the merged aeromagnetic grid.

MERGED AEROMAGNETIC ANOMALY GRID: 'ERMERGED.ASC'

This is a grid of the merged aeromagnetic anomaly data of the thirteen surveys from 'ERJIGSAW.ASC'. The grid is a representation of the data as if all surveys were flown at a constant altitude (also called draped mode) above topography. Elevations of 122 to 305 m above terrain were selected as the reduction datum levels for the merged grid. The majority of high-quality surveys for this study were flown in a draped mode. Two datum levels were chosen because the differences at the boundaries between surveys flown 122 m and surveys flown 305 m were insignificant. Therefore, the surveys would require no further data processing in order to be merged with adjacent surveys. Filtering of the data can produce distortion of anomalies and amplify the noise content of the data. Whenever possible, it is best to leave data in original form in order to avoid producing unacceptable artifacts in the resulting map. The choice to maintain two datum levels was made for this reason and because the surveys were visually and numerically continuous across the boundaries without filtering. However, some of the older aeromagnetic surveys on the periphery of the study area were flown at level barometric elevations and required filtering (downward continuation) of the data to the draped mode before merging with adjacent surveys.

For surveys flown at a constant barometric elevation, the data were analytically continued to the draped surface of 305 m above ground using the method of Cordell (1985). The method takes the gridded data from the older barometric surveys and calculates an approximation of the magnetic field data as if it had been observed on an irregular surface. The method calculates the magnetic field on a stack of horizontal levels using a fast Fourier transform method (Hildenbrand, 1985). The horizontal levels are defined such that they extend over the elevation range of the irregular surface. The magnetic field is then extrapolated from the intersections of the irregular surface and horizontal levels.

After reducing the data to an irregular surface (if necessary), each data set was regridded to a 100-m interval and compared (either visually or where the survey grid

overlapped) with the Timber Mountain survey (area 6) to determine a constant to add to or subtract from the data. The Timber Mountain survey was chosen to be the baseline survey that all other surveys would be referenced to due to its' central location and the general high quality of the data. The surveys were trimmed to the boundaries shown in Map A and merged to adjacent surveys using a minimum curvature algorithm (program *MEGAPLUG*, Cordell and others, 1992).

DISCUSSION

The merged and mosaic aeromagnetic grids mutually complement each other and should be used together when analyzing and interpreting anomalies. The mosaic grid preserves the original quality of the data and should be referred to when analyzing anomalies of the merged grid that are located at or near survey boundaries. During the merging process, gradients coincident with survey boundaries were avoided whenever possible. This was feasible for the majority of the data in the study area because the surveys were flown with similar specifications. However, the older surveys were difficult to integrate with the detailed surveys and gradients at the survey boundaries between the Timber Mountain survey and the adjacent older surveys to the north and west were unavoidable. In order to preserve the anomaly texture and quality of the Timber Mountain survey data (as well as the data from other detailed surveys), a fine grid interval was chosen, which was not appropriate to the more regional surveys. Rather than degrade the data from the more detailed surveys, the older surveys were originally gridded to an interval appropriate to their flight specifications then regridded and merged at the 100-m grid interval. Gradients are evident at this boundary and the obvious textural changes from the Timber Mountain survey to the older surveys should be noted as artifacts of the merging process and differences in the quality of data and should not be attributed to any change due to different geologic sources or lithologies.

The data from the older aeromagnetic surveys are, in general, of poor quality in comparison with the more recently flown, high resolution surveys, but they do provide a synoptic view of the regional magnetic field over the study area and allow for interpretation of anomalies across survey boundaries. However, the data from the older surveys are of insufficient quality and resolution to provide proper analysis of short wavelength anomalies related to subsurface geologic structures that could have some influence on groundwater movement. The need for high quality data in this region of older surveys is necessary before any detail on the geometry of or depth to hydrologic-related source rock can be determined.

Digital Data Format

The digital data for the 2 grids are available as USGS standard format grids written with FORTRAN format. A 'row' is defined as a series of data positions that extend from west to east along a common north coordinate. The first value in each row contains a "0", which indicates an evenly spaced grid. The first row is the southernmost (see figure below). Dval (dummy values) are used to indicate areas of no data and have a value of 0.1E+31.

Line 1-10: Header record

Line 11: Magnetic values in gammas [5E16.8].

Line 12-* row1, column 1-m; row 2, column 1-n, ect.. Where line 11 contains the first 5 elements of row1, and so on, until all the elements in the grid are exhausted.

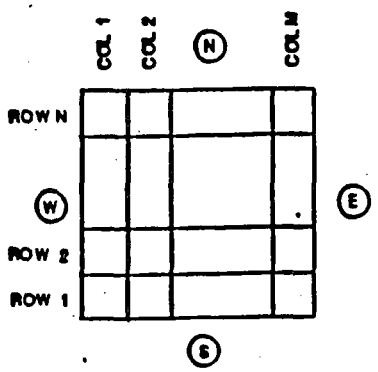

Columns and rows of USGS grids

References

Bath, G.D., Jahren, C.E., Rosenbaum, J.G., and Baldwin, M.J., 1983, Magnetic investigations in Geologic and geophysical investigations of the Climax Stock intrusive, Nevada: U.S. Geological Survey Open-File Report 83-377, p.40-77.

Briggs, I.C., 1974, Machine contouring using minimum curvature: Geophysics, v. 39, no.1, p. 39-48.

Carr, M.D., and others, 199_, (in preparation) Preliminary geologic map of the Beatty 30- by 60-minute quadrangle, Nevada: U.S. Geological Survey Open-File Report-___, scale 1:100,000.

Christiansen, R.L., Lipman, P.W., Carr, W.J., Byers, F.M., Orkild, P.P., and Sargent, K.A., 1977, Timber Mountain-Oasis Valley caldera complex of southern Nevada: Geological Society of America Bulletin, v. 88, p. 943-959.

Cordell, Lindrith, 1985, Techniques, applications, and problems of analytical continuation of New Mexico aeromagnetic data between arbitrary surfaces of very high relief [abs.]: International Meeting of Potential Fields in Rugged Topography, 1985, Proceedings: Lausanne, Switzerland, Institut de Geophysique, Universite de Lausanne, Bulletin no. 7, p. 96-99.

Cordell, Lindrith, Phillips, J.D., and Godson, R.H., 1992, U.S. Geological Survey potential-field geophysical software version 2.0: U.S. Geological Survey Open-File Report 92-18 a-g.

Frizzell, V.A. and Shulters, J., 1990, Geologic map of the Nevada Test Site, southern Nevada: U.S. Geological Survey Miscellaneous Investigations Series Map I-2046, scale 1:100,000.

Geodata International, Inc., 1979 Aerial radiometric and magnetic survey: Death Valley National Topographic Map, Nevada, California: U.S. Department of Energy, Grand Junction Office Report GJBX-164(79), v. 2, scale 1:250,000.

Harris, R.N., Ponce, D.A., Healey, D.L., and Oliver, H.W., 1989, Principal facts for about 16,000 gravity stations in the Nevada Test Site and vicinity: U.S. Geological Survey Open-File report 89-682a-c.

Hildenbrand, T.G. and Kucks, R.P., 1988, Total intensity magnetic anomaly map of Nevada: Nevada Bureau of Mines and Geology Map 93A, scale 1:750,000.

Hildenbrand, T.G., 1985, FFTFIL--A filtering program based on two-dimensional Fourier analysis: U.S. Geological Survey Open-File Report 83-237, 29 p.

Kirchoff-Stein, K.S., Ponce, D.A., and Chuchel, B.A., 1989, Preliminary aeromagnetic map of the Nevada Test Site and Vicinity: U.S. Geological Survey Open-File report 89-446, scale 1:100,000.

Langenheim, V.E., Carle, S.F., Ponce, D.A., and Phillips, J.D., 1990, Revision of an aeromagnetic survey of the Lathrop Wells area, Nevada: U.S. Geological Survey Open-File Report 91-46, in press, scale 1:62,500, 3 sheets.

Minor, S.A., Sawyer, D.A., Wahl, R.R., Frizzell, V.A., Orkild, P.P., Schilling, S.P., Warren, R.G., Swadley, W.C., Coe, J.A., and Cole, J.A., 1992, Preliminary geologic map of the Pahute Mesa 30- by 60-minute quadrangle, Nevada: U.S. Geological Survey Open-File Report-___, scale 1:100,000.

Philbin, P.W. and White, B.L., 1965a, Aeromagnetic map of the Sarcobatus Flat area, Esmeralda and Nye Counties, Nevada: U.S. Geological Survey Geophysical Investigations Map GP-512, scale 1:125,000.

-------- 1965b, Aeromagnetic map of the Black Mountain quadrangle, Nye County, Nevada: U.S. Geological Survey Geophysical Investigations Map GP-519, scale 1:125,000.

-------- 1965c, Aeromagnetic map of the Silent Canyon quadrangle, Nye County, Nevada: U.S. Geological Survey Geophysical Investigations Map GP-520, scale 1:125,000.

Snyder, D.B., and Carr, W.J., 1984, Interpretation of gravity data in a complex volcano-tectonic setting, southwestern Nevada: Journal of Geophysical Research, v. 89, no B12, p. 10,193-10,206.

Sweeney, R.E., 1990, IGRFGRID--A program for creation of a total magnetic field (International Geomagnetic Reference Field) grid representing the earth's main magnetic field: U.S. Geological Survey Open-File Report 90-45a, 37 p.

U.S. Geological Survey, 1967, Aeromagnetic map of Bonnie Claire and parts of Grapevine Canyon and Springdale, Nevada and California: U.S. Geological Survey Open-File Report 67-229.

-------- 1971, Aeromagnetic map of Yucca Flats, Nevada Test Site, Nevada: U.S. Geological Survey unpublished, scale 1:24,000, 2 sheets.

-------- 1979, Aeromagnetic map of the Timber Mountain area, Nevada: U.S. Geological Survey Open-File Report 79-587, scale 1:62,500, 3 sheets.

-------- 1983, Aeromagnetic map of the Las Vegas 1^{o} by 2^{o} quadrangle, Nevada: U.S. Geological Survey Open-File Report 83-729, scale 1:250,000.

-------- 1984 Aeromagnetic map of the Mercury area, Nevada: U.S. Geological Survey Open-File Report 84-209, scale 1:62,500.

Webring, M.W., 1981, MINC--A gridding program based on minimum curvature: U.S. Geological Survey Open-File Report 81-1224, 41 p.

Winograd, I.J., and Thordarson, William, 1975, Hydrogeologic and hydrochemical framework, south-central Great Basin, Nevada-California, with special reference to the Nevada Test Site: U.S. Geological Survey Professional Paper 712-C, 126 p.

USGS-OFR-83-377

United States
Department of the Interior
Geological Survey

GEOLOGIC AND GEOPHYSICAL INVESTIGATIONS OF CLIMAX STOCK INTRUSIVE, NEVADA

Open-File Report 83-377

1983

This report is preliminary and has not been reviewed for conformity with U.S. Geological Survey editorial standards and stratigraphic nomenclature. Company names are for descriptive purposes only and do not constitute endorsement by the U.S. Geological Survey.

Prepared by the U.S. Geological Survey
for the
U.S. Department of Energy
(Interagency Agreement DE-AI08-76DP00474)
and the
Defense Nuclear Agency

MAGNETIC INVESTIGATIONS

G. D. Bath, C. E. Jahren, J. G. Rosenbaum, and M. J. Baldwin

ABSTRACT

Air and ground magnetic anomalies in the Climax stock area of the NTS help define the gross configuration of the stock and detailed configuration of magnetized rocks at the Boundary and Tippinip faults that border the stock. Magnetizations of geologic units were evaluated by measurements of magnetic properties of drill core, minimum estimates of magnetizations from ground magnetic anomalies for near surface rocks, and comparisons of measured anomalies with anomalies computed by a three-dimensional forward program. Alluvial deposits and most sedimentary rocks are nonmagnetic, but drill core measurements reveal large and irregular changes in magnetization for some quartzites and marbles. The magnetizations of quartz monzonite and granodiorite near the stock surface are weak, about 0.15 A/m, and increase at a rate of 0.00196 A/m/m to 1.55 A/m, at depths greater than 700 m (2,300 ft). The volcanic rocks of the area are weakly magnetized. Aeromagnetic anomalies 850 m (2,800 ft) above the stock are explained by a model consisting of five vertical prisms. Prisms 1, 2, and 3 represent the near surface outline of the stock, prism 4 is one of the models developed by Whitehill (1973), and prism 5 is modified from the model developed by Allingham and Zietz (1962). Most of the anomaly comes from unsampled and strongly-magnetized deep sources that could be either granite or metamorphosed sedimentary rocks. A combination of horizontal and vertical prisms was used to relate details of structure at faults to ground magnetic anomalies 1.5 m (5 ft) above the surface. The stock is defined at its southeastern edge by the Boundary fault which has dips of 70 to 80^{o} to the southeast and a displacement of 2,000 m (6,500 ft). The western edge of the stock dips at an angle of 30^{o}, and there is no evidence of displaced granitic rock at the Tippinip fault. A small anomaly west of the fault arises from magnetized sedimentary rocks, and not from displaced granitic rocks. New data from a recent aeromagnetic survey show that the trend of positive magnetic anomalies over the Gold Meadows, Climax, and Twinridge stocks extends to the southeast for more than 65 km (40 miles).

INTRODUCTION

This study is similar to several the USGS has undertaken at the NTS and nearby areas to locate large bodies of buried granitic rock, estimate their depths and shapes, and thus define prospects for further investigations as possible sites for storage of radioactive waste. Measurements of magnetic properties indicate that the total magnetization of a granitic mass usually has a normal polarity in the approximate direction of the Earth's magnetic field, and prominent positive anomalies are often found over large exposures of granitic rock. Examples of normally-magnetized quartz monzonite and granodiorite bodies that produce broad positive anomalies include the Climax stock (Allingham and Zietz, 1962), and satellitic stocks or certain plutons within the Sierra Nevada batholith 250 km (155 mi) to the west (Currie and others, 1963; Gromme and Merrill, 1965; and Oliver, 1977). In the test site region metamorphosed sedimentary rocks, volcanic ash, and rhyolitic lava flows may also be magnetized along the Earth's field. They can occur in large volumes and may cause prominent positive anomalies. Identification of a buried source is thus often difficult.

Within the NTS and nearby areas, a number of positive anomalies are positioned over the relatively few intrusive rocks that have been identified during surface mapping and drill-hole logging. The residual aeromagnetic map of figure 1C shows nine magnetic highs that are associated with areas of known intrusive rock, as indicated by letters A through I. Five of the nine areas of intrusive rock are alined across the northern part of the NTS: (A) Twinridge (Barnes and others, 1965); (B) Climax stock (Houser and Poole, 1960, and Barnes and others, 1963): (C) Gold Meadows stock (Gibbons and others, 1963; (D) northwest Pahute Mesa (Orkild and Jenkins, written commun., 1978); and (E) Black Mountain (Noble and Christiansen, 1968). The remaining four areas are (F) Wahmonie (Ekren and Sargent, 1965); (G) Calico Hills (McKay and Williams, 1964); (H) Timber Mountain (Carr and Quinlivan, 1966); and (I) Quartzite Mountain (Rodgers and others, 1967).

Residual maps were prepared by subtracting the regional field from observed anomalies, a process designed to give a residual datum of about zero over large areas underlain by thick deposits of nonmagnetic alluvium and bedrock. To prepare figure 1C, a least-square procedure was applied to data at 3-km grid intervals to define a planar regional field for an area of 10,000 Km^2 (3,860 mi^2) covered by 14 published aeromagnetic maps that includes the NTS and most of the Nellis Air Force Bombing and Gunnery Range: Boynton and Vargo, 1963a,b; Boynton and others, 1963a,b; and Philbin and White, 1965a-j. A graphical method was then used to remove regional from observed contours.

Most anomalies in the stock region appear to be related to outcrops of granitic or volcanic rocks as indicated by comparing positions of the more detailed aeromagnetic anomalies of figure 2C and the generalized geology of plate 1A. The western third of figure 2C was compiled from the survey data of figure 1C, and the eastern two thirds of figure 2C were taken from the survey data of figure 3C. The aeromagnetic survey and compilation of figure 3C were made in 1980 by the U.S. Naval Oceanographic Office for an area of about 3,800km^2 (1,450 mi^2) in eastern Nye and western Lincoln counties, Nevada. This coverage was not available during the compilation of aeromagnetic maps of Nevada by Zietz and others (1977), and Sweeney and others (1978).

Some of the significant aeromagnetic anomalies of figure 2C have been investigated in recent years and their sources can be stated with confidence, but others have not and their sources must be inferred. From east to west in figure 2C, the positive anomalies arise from the following sources: an inferred stock that is covered by older sedimentary rocks at A in the Papoose Range; a quartz monzonite stock that is mostly covered by alluvium, volcanic rock, and older sedimentary rock at B near Twinridge hill; a body of quartz monzonite and granodiorite C at Climax stock; an inferred stock that is covered by volcanic rock at D northwest of Climax stock; and a body of quartz monzonite E at Gold Meadows stock.

The strongly-magnetized volcanic rocks in the Climax region have reversed magnetic polarities and produce negative anomalies. From east to west in figure 2C, negative anomalies arise from the following sources: the Rainier Mesa Member ash flow (Sargent and Orkild, 1973) at Aqueduct Mesa F and at Rainier Mesa G; and from pre-Ammonia Tanks rhyolite lavas (Byers and others, 1976) buried by alluvium and volcanic flows at H, I, and J in the Timber Mountain caldera, and exposed and penetrated by drilling at K on Pahute Mesa.

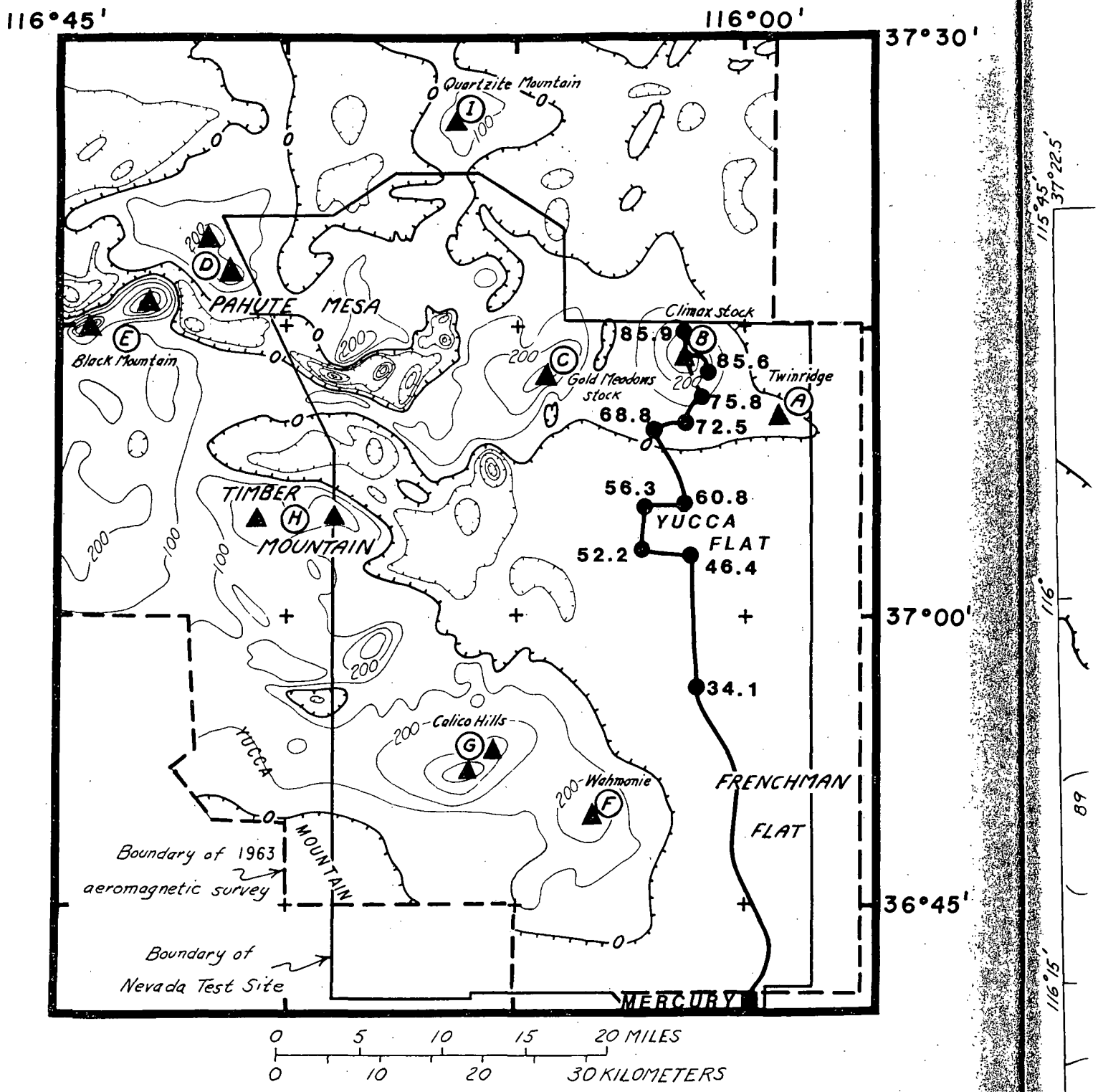

Figure 1C--Residual aeromagnetic map of Nevada Test Site and nearby regions showing nine prominent positive anomalies (lettered A through I), over exposed granitic rock, or over areas where granitic rock is inferred at depth. Measurements were at about 2,450 m (8,000 ft) above sea level, contour interval is 100 nanoteslas, and zero and negative contours are hachured. The bold hashured line represents the zero contour that separates positive from negative residual anomalies. Solid triangles give locations of anomaly maxima, and solid line indicates traverse along which ground magnetic anomalies were measured by a truck-mounted magnetometer from Mercury to Climax stock. Traverse distances are in kilometers.

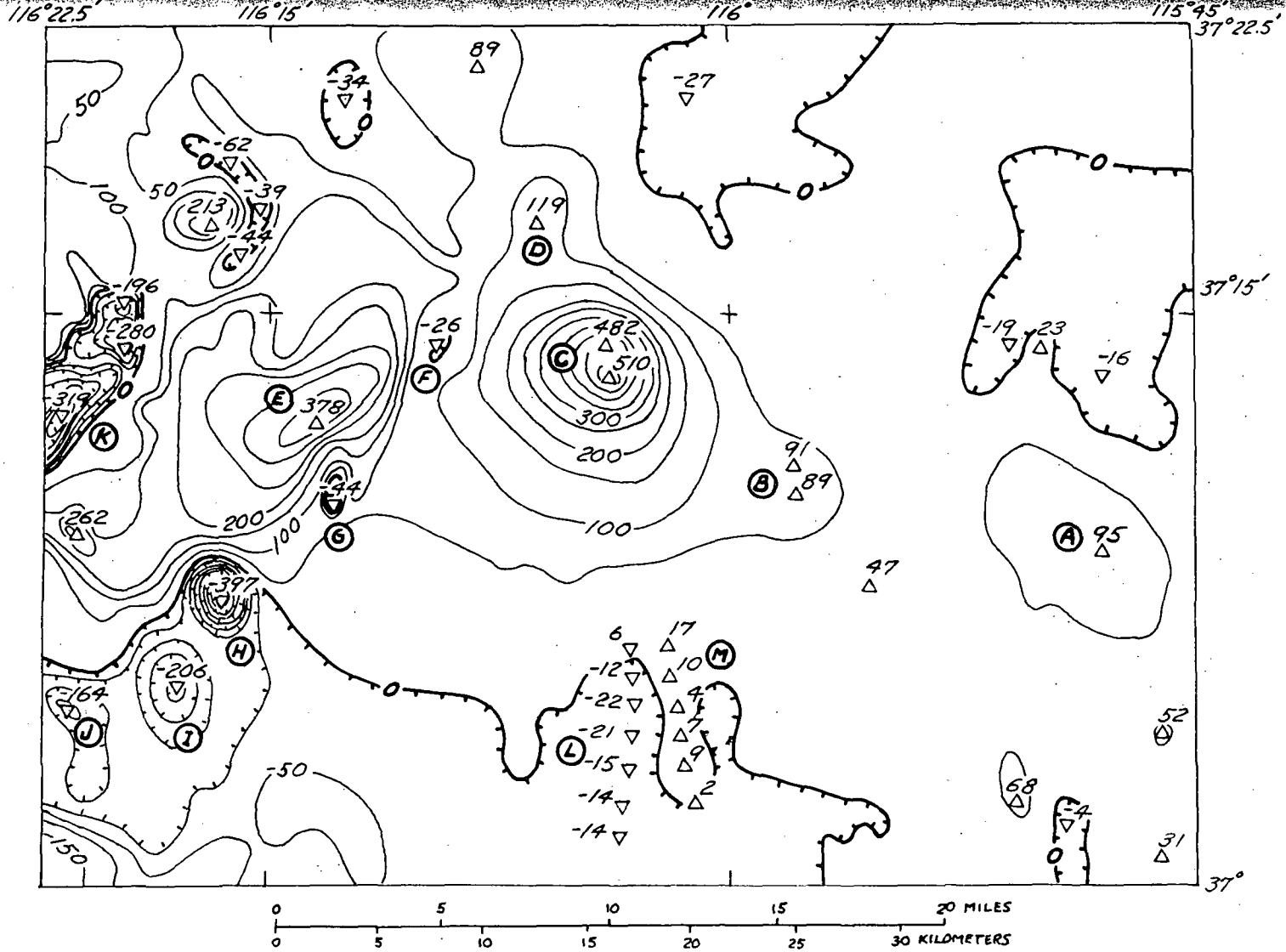

Figure 2C.--Residual aeromagnetic map of Climax stock region showing broad positive anomalies (lettered A through E), over known or inferred granitic rock; narrow negative anomalies (lettered F through K), over known or inferred volcanic rock; and anomaly minima (near L) and maxima (near M), over volcanic rock along the Yucca fault. Measurements were at about 2,480 m (8,000 ft) above sea level for western third of map, and at about 2,130 m (7,000 ft) for eastern two thirds of map. Contour interval is 50 nT, and zero and negative contours are hachured. Triangles give locations of anomaly maxima, and inverted triangles give locations of anomaly minima.

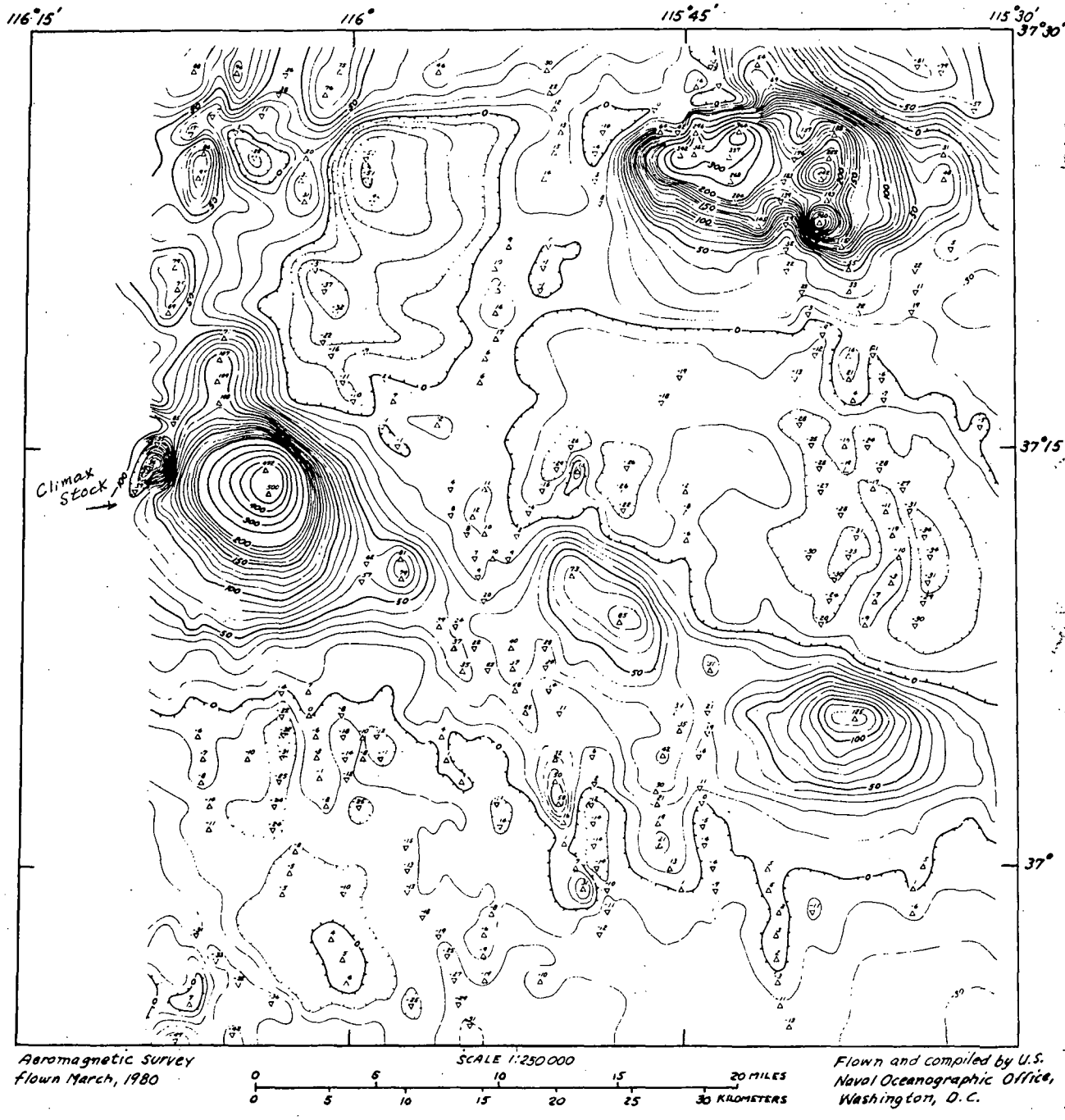

Figure 3C.--Aeromagnetic map of parts of eastern Nye and western Lincoln Counties, Nevada, showing residual anomalies in total magnetic intensity relative to 1980 International Geomagnetic Reference Field. Datum was increased 280 nT to give values near zero over large areas of nonmagnetic rock. Contour intervals are 10 and 50 nT, and zero and negative contours are hachured. Triangles give locations of anomaly maxima, and inverted triangles give locations of anomaly minima. Measurements were at about 2,285 m (7,500 ft) barometric elevation for southern half and about 2,560 m (8,400 ft) for northern half of map.

Also, the Rainier Mesa Member ash flow, which underlies alluvium and a volcanic flow along the Yucca fault, produces a line of negative anomalies L on the high-standing side of the fault, and a positive anomalies M on the low-standing side of the fault.

MAGNETIC PROPERTIES

The average total magnetization of a uniformly magnetized rock mass, denoted as the vector $\vec{J}_t$, is defined as the vector sum of the induced magnetization, $\vec{J}_i$, and remanent magnetization, $\vec{J}_r$:

$$\vec{J}_t = \vec{J}_i + \vec{J}_r.$$

The direction and intensity of induced magnetization is a function of the magnetic susceptibility, k, and field, $\vec{B}_o$:

$$\vec{J}_i = \frac{kB_o}{\mu_o},$$

where $\mu_o = 4\pi x10^{-7}$ henrys/m.

Remanent magnetization, on the other hand, is independent of the external field. The Koenigsberger ratio (1938), $Q = J_r/J_i$, is often used to indicate the relative contribution of the two components to J_t.

Air and ground magnetic surveys will usually detect a geologic unit when its total magnetization is equal to or greater than 0.05 A/m (ampere per meter). Therefore, rocks having average intensities less than 0.05 A/m are designated nonmagnetic; and those having greater intensities are here arbitrarily designated as either weakly, moderately, or strongly magnetized, as defined by the following limits:

nonmagnetic < 0.05 A/m
0.05 A/m < weakly magnetized < 0.50 A/m
0.50 A/m < moderately magnetized < 1.50 A/m
1.50 A/m < strongly magnetized

The magnetic properties of older sedimentary rocks, granitic rocks, volcanic rocks, and alluvial deposits in the Climax region were estimated by collecting and measuring surface and drill core samples, and by relating maximum slopes of ground magnetic anomalies to minimum estimates of magnetization for geologic features close to the surface. Also, general information is available on the magnetic properties of NTS rocks of nearby areas (Bath, 1968, 1976).

Estimate of Magnetization

A minimum estimate of total magnetization, J_t, is given by Smith (1961, equation 2.7) which requires information only on anomaly amplitude and depth to the magnetized body. No assumptions are necessary for body shape or direction of magnetization except that the direction must be uniform throughout the

body. The anomaly amplitude, t, is measured between two points separated by a distance, c. The relation is given by

$$J_t \geq \hat{J}_t = \frac{|t|}{F\left(\frac{h}{c}\right)} \qquad (1)$$

where h is the depth to anomaly source, and $F\left(\frac{h}{c}\right)$ is a function tabulated by Smith.

In our studies, the anomaly amplitude is measured over the slope distance, c, as defined by Vacquier and others, 1951. The distance is designated the maximum slope parameter by Nettleton (1976 p. 395-403), and it is commonly assumed equal to the approximate depths of anomaly-producing bodies. Under this assumption, c = h, and equation 1 reduces to a simple expression,

$$\hat{J}_t = \frac{|t|}{289} \qquad (2)$$

when J_t is expressed in A/m, and t in nanoteslas.

The amplitudes of ground magnetic anomalies can now be employed to designate magnetizations of near surface rocks as follows:

nonmagnetic < 15 nT
15 nT < weakly magnetized < 150 nT
150 nT < moderately magnetized < 450 nT
450 nT < strongly magnetized

Ground magnetic surveys have been used as a convenient and prompt method over large areas of the Test Site and have provided estimates of magnetization for geologic features at or near the surface that compare favorably with magnetic properties determined from surface and drill-core samples in the laboratory. For example, the anomaly profile of traverse B66-B66', located on the west side of the stock (fig. 4C), indicates dolomite and marble are nonmagnetic, and that masses of quartz monzonite within 10 m (32.8 ft) of the surface are only weakly magnetized (fig. 5C). Slope distances and their respective t and c components are shown along the traverse for the three strongest anomalies on the traverse which occur over the quartz monzonite. The amplitudes average 75 nT and yield a minimum estimate for J_t of 0.26 A/m. Elsewhere on the traverse the amplitudes are considerably less, but remain mostly within the weakly-magnetized range.

Older Sedimentary Rocks

Sedimentary rocks of Paleozoic and Precambrian age at the NTS consist mainly of argillite, dolomite, limestone, and quartzite that are usually found to be nonmagnetic. Thick deposits are often present within large areas characterized by a relatively uniform aeromagnetic field. This is illustrated by the thick section of quartzite and marble of the Eleana Formation in the Eleana Range west of Yucca Flat on plate 1A, and the lack of a significant magnetic anomaly over the Eleana Range in the aeromagnetic map of figure 2C. There are, however, notable exceptions to this generalization, as observed in

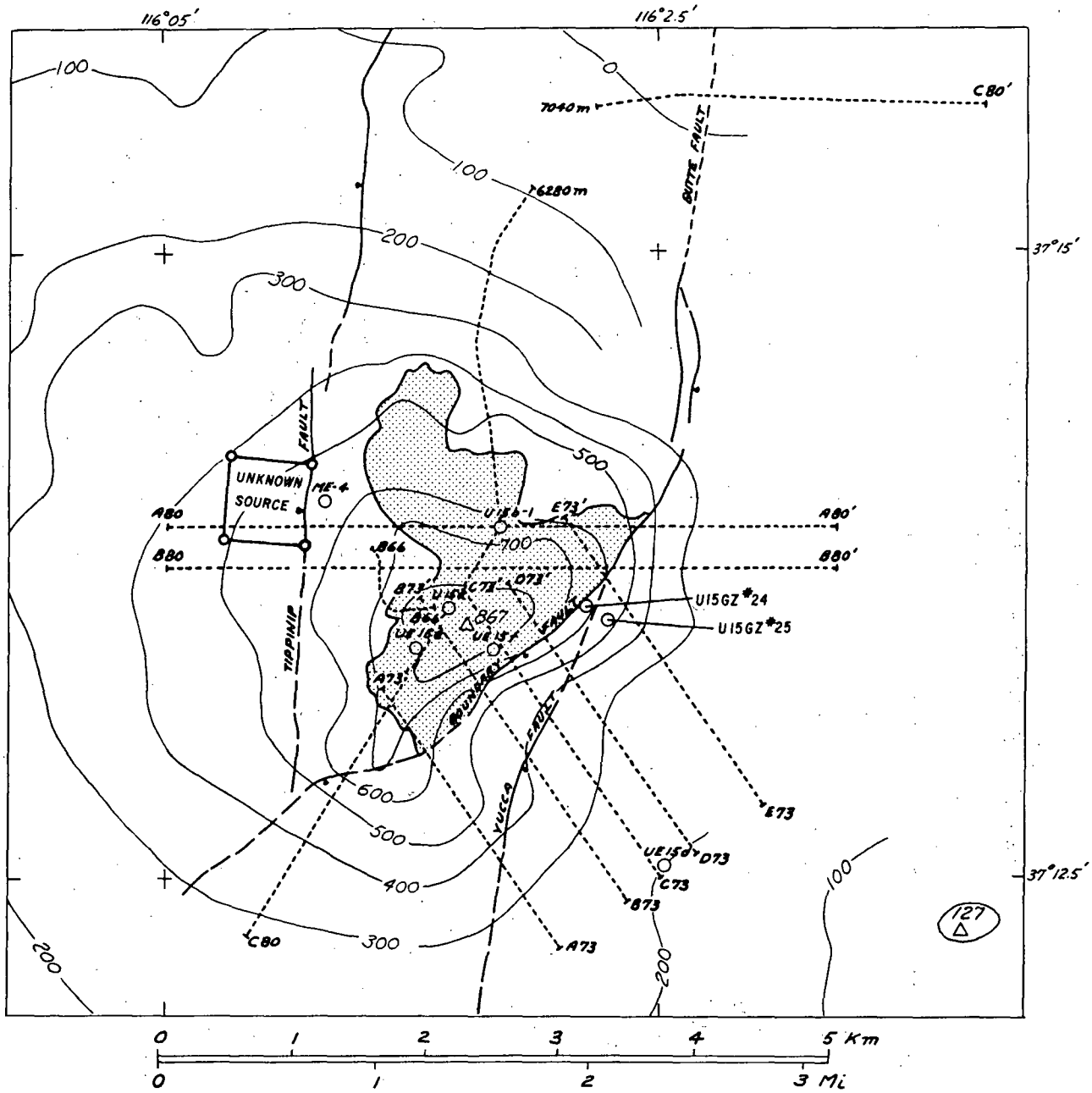

Figure 4C.--Residual aeromagnetic map showing broad positive anomaly over Climax stock (shaded outline of exposed part of stock); major faults bordering the stock; drill holes ME-4, U15b-1, U15a, UE15e, UE15f, U15gz#24, U15gz#25, and UE15d; ground traverses A80-A80', B80-B80', C80-C80', A73-A73', B73-B73', C73-C73', D73-D73', E73-E73', and B66-B66'. Square outline of unknown source was used on figure 20 to model Tippinip fault. Measurements were at about 120 m (394 ft) above the ground surface; contour interval is 100 nT, and triangles give locations of anomaly maxima. Readings were not taken along interval 6,280 to 7,040 m (20,604-23,097 ft) over steep topography of ground traverse C80-C80'.

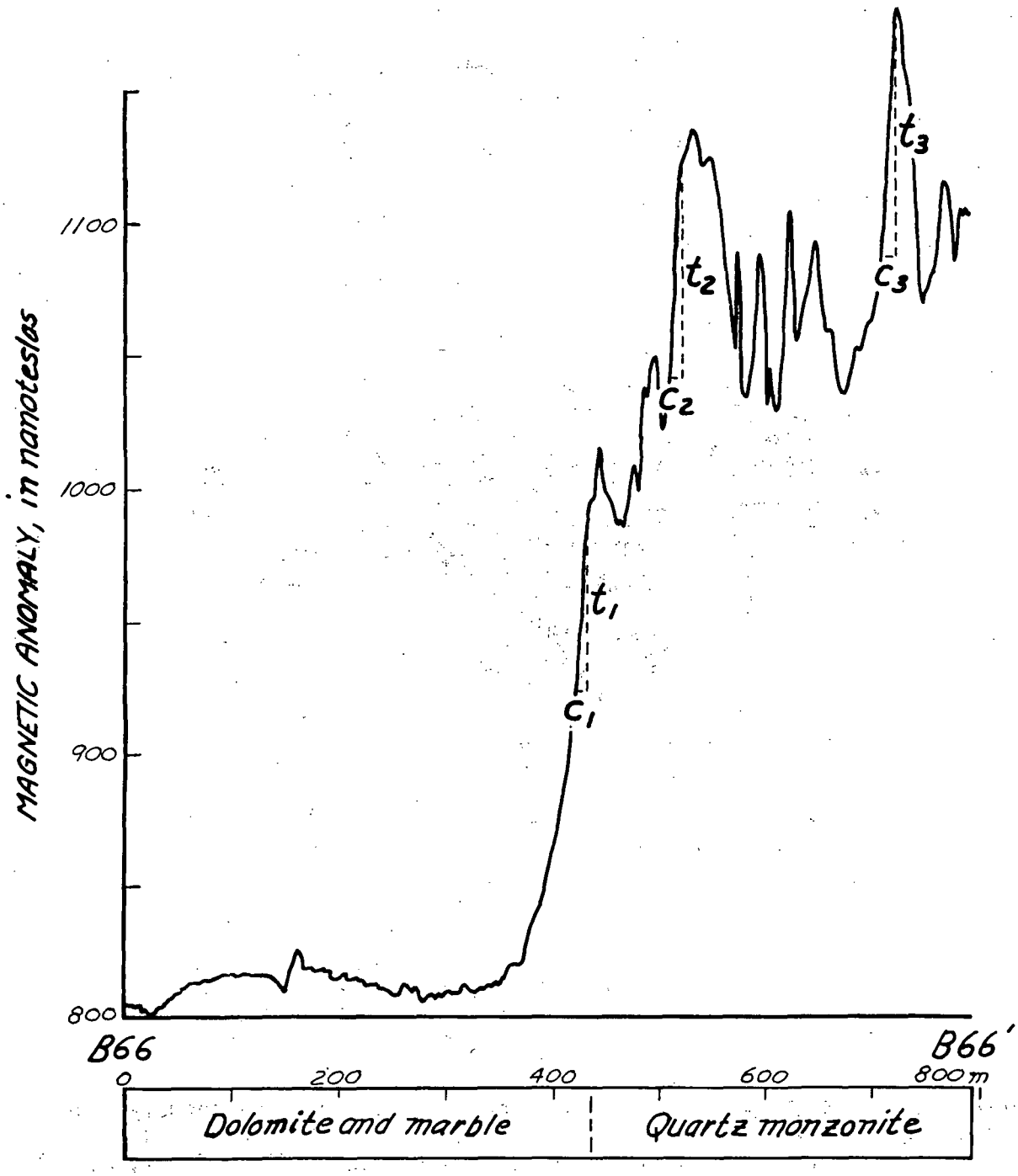

Figure 5C.--Profile of residual ground magnetic anomalies along traverse B66-B66' over dolomite and marble, and quartz monzonite showing distances, c and amplitudes, t, that are used to compute minimum estimates of magnetization. Profile is plotted from 516 rubidium magnetometer measurements 1.5 m (5 ft) above ground surface.

the magnetic properties of surface exposures and drill core from the Calico Hills (Baldwin and Jahren, 1982), and in the core from two holes drilled near the Climax stock. At Calico Hills in the southwestern part of the NTS, the strongly-magnetized argillite of the Eleana Formation appears to be the principal cause of the prominent aeromagnetic anomaly, G of figure 1C. In that region, nonmagnetic argillite has been altered to strongly-magnetized rock, apparently by the conversion of pyrite to magnetite. At the Climax stock, similar high values of magnetic susceptibility were reported by P. H. Cole and W. P. Williams (written commun., 1962) for a 200 m (656 ft) interval of quartzite and siltstone in drill hole UE15d.

Measurements of susceptibility and remanent intensity of core samples from drill holes UE15d and ME-4 fig. 4C supplement the magnetic property data mentioned above. UE15d penetrated 88 m (289 ft) of alluvium, 452 m (1,483 ft) of gently dipping volcanic rocks, and 1,288 m (4,226 ft) of steeply dipping Precambrian metasedimentary rocks (Harley Barnes, written commun., 1962). ME-4 penetrated 350 m (1,148 ft) of marble and 5 m (16 ft) of granite.

Magnetic susceptibilities of core samples were measured by means of a digital susceptibility meter which is available commercially; and induced magnetizations were computed from susceptibilities using the formula

$$J_i = (k_{SI}/4\pi)\ B_{nT} \times 10^{-2}, \text{ where } B_{nT} = 51900 \text{ nT},$$

the strength of the Earth's field in the stock area. Susceptibilities and remanent magnetizations of representative samples were then determined by the method of Jahren and Bath (1967). Koenigsberger ratios were computed from these measurements and average values were assigned to the various rock types. Total magnetizations were computed for all samples by assuming a normal polarity of remanence, and by using the relation

$$Q = \frac{J_r}{k \cdot T}$$

$$J_t = (Q + 1)\ J_i. \qquad \frac{J_t}{J_i} = \frac{J_r}{J_k} + 1$$

Averages of total magnetization vary from nonmagnetic to moderately magnetic for older sedimentary rocks available from the two drill holes, as shown in tables 1C and 2C. Values of Q were based on only 42 samples. The Q values used in the tables, their standard deviations, and the number of samples are 0.5±1.0 for 10 samples of quartzite, 2.0±1.9 for 12 samples of marble, 0.3±0.3 for 5 samples of granite, and 0.9±1.7 for 15 samples of volcanic rock.

A reliable estimate of the magnitude of magnetization for the sedimentary sequence penetrated by drilling could not be determined because of large, apparently unsystematic changes in total magnetization from nonmagnetic to 9.59 A/m in UE15d and 5.81 A/m in ME-4, and insufficient available core. No consistent pattern of magnetization could be determined. The values do not increase with depth, or with relation to known granitic rock at ME-4, or to inferred granitic rock at UE15d. Samples from two zones, 1168-1354 m (3,832-4,442 ft) in UE15d and 335-338 m (1,099-1009 ft) in ME-4 have average total magnetizations of 0.7 A/m and 1.4 A/m respectively (tables 1C and 2C). This result indicates that both the quartzite and the marble may show moderate magnetizations comparable to that of granite. If present in sufficient thicknesses, these magnetized sediments will contribute to the aeromagnetic anomaly, and their effects may be indistinguishable from those of the intrusive.

Table 1C.--Average induced magnetization, J_i, and total magnetization, J_t, of core of irregular shape from drill hole UE15d.

Rock type	Interval sampled: Depth (m)	Thickness (m)	Core available (m)	Number of samples	J_i (A/m)	Assigned Q	J_t (A/m)
Volcanic tuff	228-541	313	295	15	0.16	0.9	0.3
Quartzite	541-1,140	599	285	(1/)	<.05	.5	<.1
Quartzite	1,140-1,168	28	7	25	.08	.5	.1
Quartzite	1,168-1,354	186	35	291	.49	.5	.7
Quartzite	1,354-1,470	116	30	109	.04	.5	.1
Quartzite	1,470-1,615	145	20	(1/)	<.05	.5	<.1
Dolomite	1,615-1,829	214	35	(1/)	<.05	2.0	<.2

1/ Core scanned with digital magnetic susceptibility meter.

Table 2C.--Average induced magnetization, J_i, and total magnetization, J_t, of core of irregular shape from drill hole ME-4.

Rock type	Interval sampled: Depth (m)	Thickness (m)	Number of samples	J_i (A/m)	Assigned Q	J_t (A/m)
Marble	4-266	262	(1/)	<0.05	2.0	<0.2
Marble	266-278	12	105	.10	2.0	.3
Marble	278-293	15	170	.03	2.0	.1
Marble	293-335	42	(1/)	<.05	2.0	<.2
Marble	335-338	3	32	.46	2.0	1.4
Marble	338-357	19	137	.06	2.0	.2
Granite	357-362	5	33	.52	.3	.7

1/ Core scanned with digital magnetic susceptibility meter.

Granitic Rocks

Large changes in total magnetization, varying from nonmagnetic to strongly magnetic, also were found in 676 core samples of quartz monzonite and granodiorite. Almost continuous core was available from four holes shown on figure 4C: U15a drilled to 366 m (1,201 ft) depth in moderately-magnetized quartz monzonite and strongly-magnetized granodiorite, U15b-1 drilled to 549 m (1,801 ft) depth in moderately-magnetized granodiorite, UE15e drilled horizontally for a distance of 183 m (600 ft) into the side of a hill of weakly-magnetized quartz monzonite, and UE15f drilled to 100 m (328 ft) depth in moderately-magnetized quartz monzonite. Average magnetic properties are given in table 3C. Sample volumes were included to indicate sample size, and thus, the type of instrument used for measurements. Measurements on large drill core samples were made with equipment described by Jahren and Bath (1967). For small cores, magnetic susceptibilities were measured with a device similar to that described by Christie and Symons (1969) and calibrated by the method of Rosenbaum and others, 1979. Remanent magnetizations were measured with a spinner magnetometer which is commercially available.

Table 3C.--Average sample volume, induced magnetization, J_i, Koenigsberger ratio, Q, and total magnetization, J_t, of 676 core samples of cylindrical shape from drill holes U15a, U15e, U15f, and U15b-1.

Rock type	Drill hole	Interval sampled (m)	Number of samples	Average sample volume[1/] (cm^3)	Average J_i (A/m)	Average Q	Average J_t (A/m)
Quartz monzonite	U15a	122	5	13	0.76	(2/)	0.84
Quartz monzonite	UE15e	181	121	310	.09	(2/)	.10
Quartz monzonite	UE15f	187	124	425	.67	(2/)	.74
Granodiorite	U15a	244	19	13	1.53	(2/)	1.68
Granodiorite	U15b-1	533	351	535	.67	0.22	.82
Granodiorite	U15b-1	533	56	13	.87	.08	.94

1/ Sample volumes greater than 300 cm^3 indicate pieces of actual drill core sawed to cylinders having lengths about equal to diameters. Samples of 13-cm^3 volume were obtained by drilling 2.54-cm diameter cores from the drill core, and sawing ends off to give about 2.54-cm lengths.

2/ J_r not measured; assume Q = 0.10.

The magnetic properties of drill core indicate magnetizations increase with depth in the quartz monzonite and granodiorite stocks. Allingham and Zietz (1962) report the upper 122 m (400 ft) of quartz monzonite from drill hole U15a is moderately magnetized and the lower 244 m (800 ft) of grandiorite is strongly magnetized. Quartz monzonite from the horizontal hole, UE15e, is within 90 m (295 ft) of the surface and weakly magnetized, while quartz monzonite from the vertical hole, UE15f, is within 187 m (614 ft) of the surface and moderately magnetized. Hole U15b-1 extends to a greater depth, 533 m (1,749 ft) in granodiorite, and it was selected to provide the magnetization data that were used in computing a model for this report. About 350 large samples, averaging 535 cm^3, were collected at approximately 1.5-m (5-ft) intervals. A total of 56 small samples, approximately 13 cm^3 in volume, were collected with groups of 2 to 4 specimens separated by approximately 30 m (98 ft). Average induced magnetizations and Koenigsberger ratios are given in table 3C for the large and small samples, and individual values of induced magnetization for the large samples are plotted versus depth in figure 6C.

The line shown in figure 6C is the result of linear regression having a correlation coefficient of 0.75. The line indicates a weak near surface magnetization of 0.13 A/m and an increase of 0.00196 A/m per meter of depth. Linear regression of the small sample data yields similar results with the near surface magnetization being 0.16 A/m and the increase being 0.00225 A/m per meter of depth (correlation coefficient 0.83). Correlation coefficients for higher polynomials are negligibly larger; a fifth order fit to the large sample data produces a correlation coefficient of 0.75.

Remanent magnetization of samples from U15b-1 are low with respect to the induced component with Q averaging less than 0.25 (table 3C). Therefore, the contribution of remanence may be safely ignored for modeling purposes.

Study of opaque minerals in thirteen polished thin sections from U15b-1 indicates that the increase of induced magnetization with depth is due to an increase in the original magnetite content, and not due to deep weathering effects or to changes in size of magnetite grains. The quantity of magnetite observed ranged from 0.1 to 0.65 percent, and a linear regression of percent magnetite versus magnetic susceptibility yielded a correlation coefficient of .81. The magnetite observed in twelve thin sections collected from depths greater than 30 m (98 ft) is largely unaltered. However, the granodiorite in the remaining thin section, from a depth of 13 m (43 ft) is highly altered and approximately 30 percent of the magnetite has been replaced by hematite.

Volcanic Rocks and Alluvial Deposits

Volcanic rocks of Oligocene and Miocene age in the immediate area of the stock consist of bedded, zeolitized, air-fall, and reworked tuffs that generally have weak magnetizations, as well as ash-flow tuffs that generally have weak to moderate magnetizations. Bath (1968) reported that induced magnetizations of most volcanic units in the Test Site area are weak, and it is the strong remanent magnetizations of welded ash flows and lava flows that are responsible for many prominent aeromagnetic anomalies. No strongly-magnetized ash or lava flows occur over or near the Climax stock.

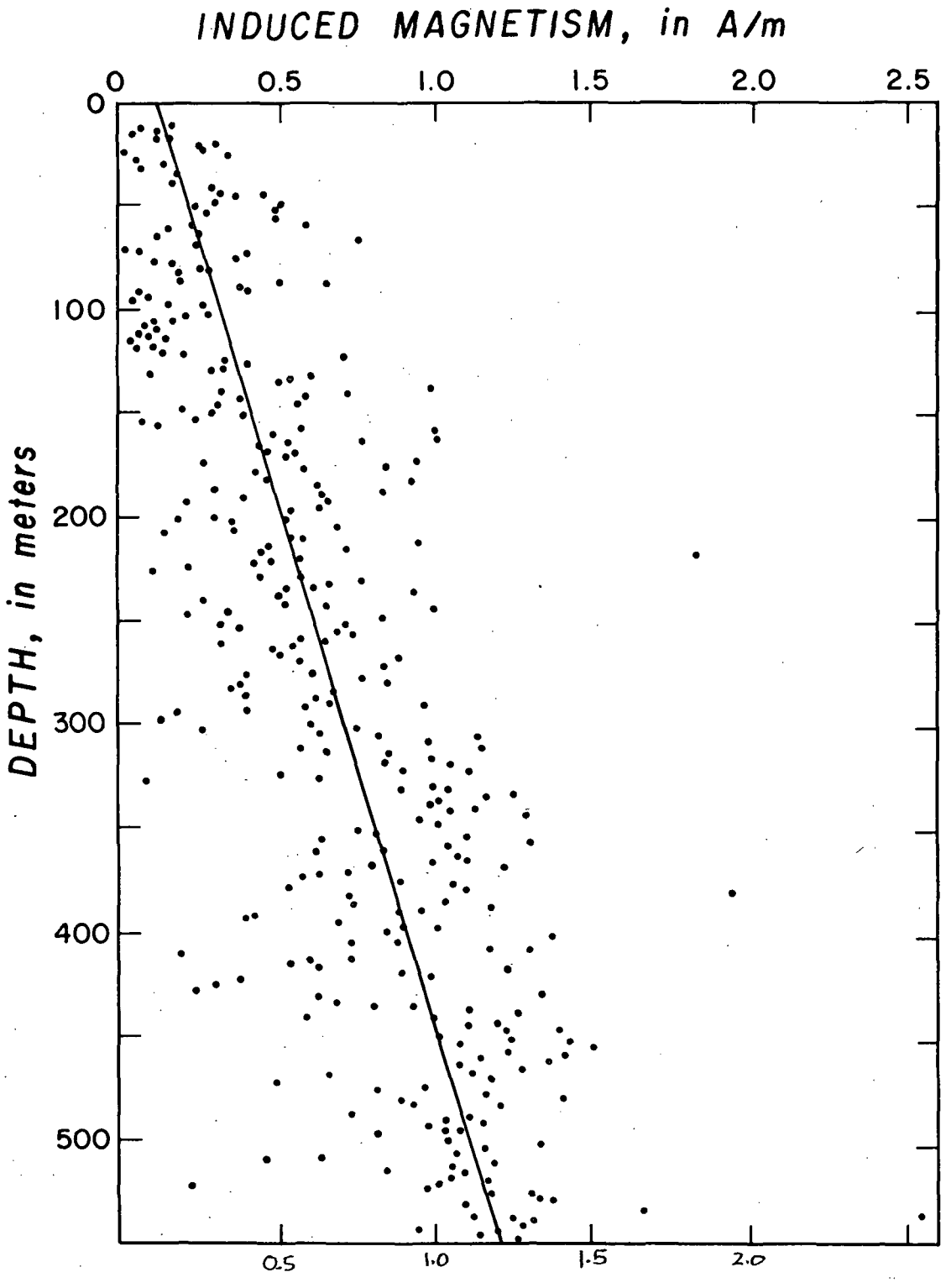

Figure 6C.--Induced magnetization of 351 large core samples of granodiorite with fitted line of linear regression showing an increase in magnetization of 1.05 A/m for a depth interval of 533 m (1,750 ft) in drill hole U15b-1.

Alluvial deposits of Holocene age consist of fragments of reworked granitic, volcanic, and sedimentary rocks. The heterogenous and haphazard manner of deposition results in cancellation of most of the contribution of remanent magnetization. Total magnetizations of alluvium are therefore almost entirely induced magnetizations that are generally categorized as nonmagnetic.

Minimum estimates of magnetization from ground magnetic anomalies indicates most near surface features in the stock area can be designated as either nonmagnetic or weakly magnetized. A 2,100-m (6,900-ft) traverse mostly over alluvium on the southeastern side of the stock illustrates the ambient level of anomaly response that is expected over nonmagnetic rock. Figure 7C shows anomalies measured 1.5 m (5 ft) above the surface along the 80.5 to 82.6 km (50 to 51.3 mi) portion of the long traverse of figure 1C. A rubidium magnetometer was carried 30 m (98 ft) behind the truck in order to eliminate magnetic "noise" caused by the truck. Part A of figure 6C shows residual anomalies that are based on a zero datum over Yucca Flat, and include regional effects of the stock and local effects of the alluvium. Part B shows amplified anomalies after regional effects of the stock have been removed. The anomaly at 80.74 km (50.2 mi) arises from weakly magnetized quartz monzonite at the alluvium-stock contact, and the anomaly at 82.44 km (51.2 mi) arises from a metal sign post. All other anomalies are assumed to be produced by alluvium at or near the surface. Almost all anomaly amplitudes over maximum slope distances are less than 15 nT, the division between nonmagnetic and weakly-magnetized rock.

OBSERVED AND RESIDUAL ANOMALIES

The data recorded by a magnetometer during an aeromagnetic or ground magnetic survey consists of the effects of the geologic feature being studied plus the combined effects of the Earth's magnetic field, and all the magnetized geologic features and man-made objects in a large area near the surface or deeply buried. Several methods have been used to identify and separate these components, and Nettleton (1976, p. 134-187) describes anomaly separation and filtering procedures in detail. In order to isolate the anomaly of interest we first define a reference surface, usually referred to as the regional anomaly, to represent effects from the long wavelength anomalies of the Earth's magnetic field and of geologic features buried at great depth. The regional anomaly then becomes the zero datum upon which residual values are based. An ideal residual anomaly map includes only the short wavelength effects of the feature, or features, under study; but in practice extraneous and overlapping effects are present.

We commonly use two methods to determine regional anomalies for aeromagnetic surveys of large areas. In one method, the regional anomaly consists of a planar surface established by a least-squares fit to data at 3-km (1.86-mi) grid intervals. This method was used in deriving figure 1C and produces contour values that are about zero over large areas of thick, nonmagnetic material. In the second method, the regional anomaly is the International Geomagnetic Reference Field (IGRF) and determined by spherical harmonic analysis of worldwide measurements on a 2^{0} grid (Barraclough and Peddie, 1978). In the area of the NTS, this method produces residual values that are about 280 nT lower than the first method. The IGRF was used in compiling figure 3C and 280nT was added to residual values to make the contours consistent with those of figure 1C.

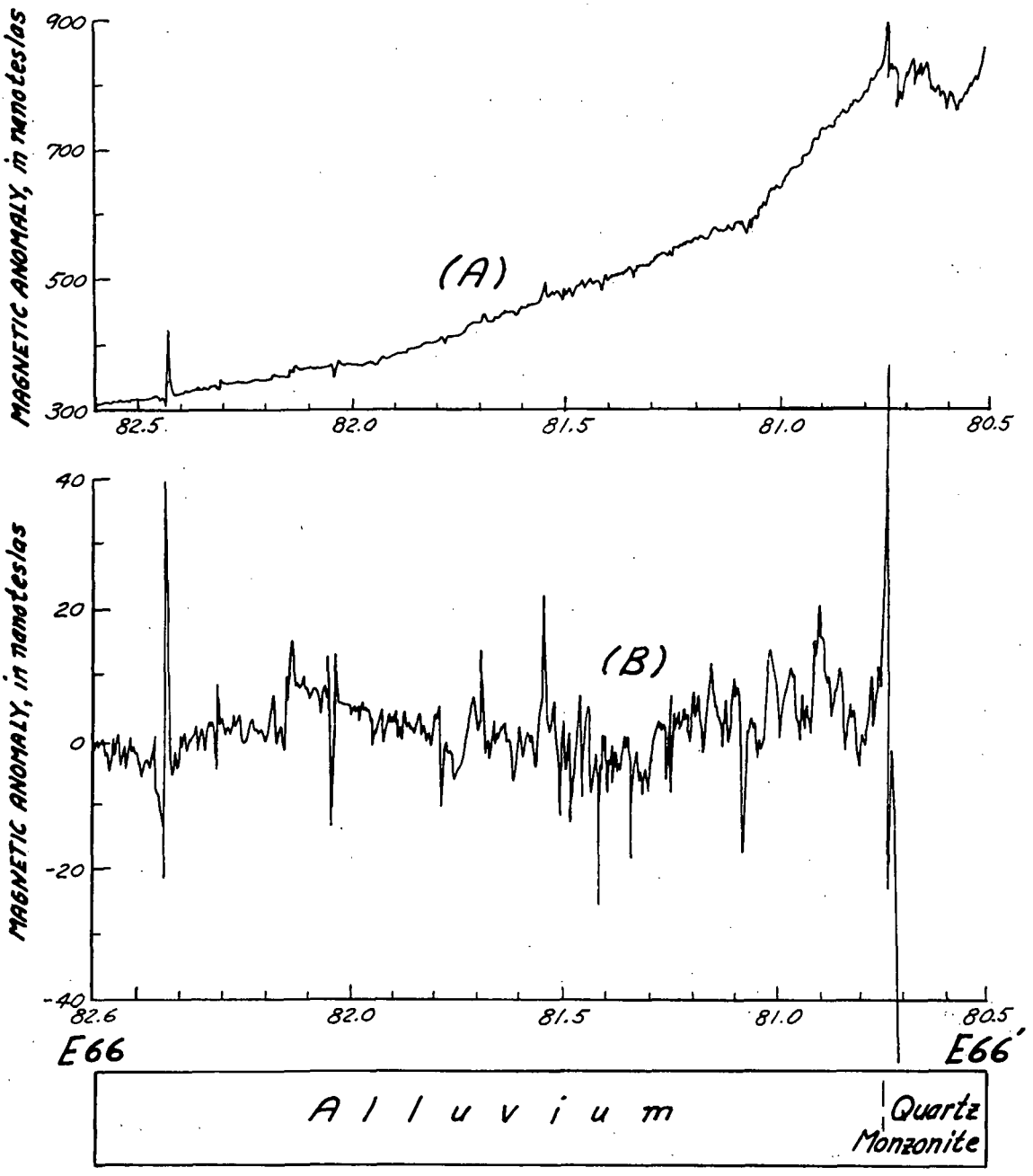

Figure 7C.--Profiles of residual ground magnetic anomalies along the same traverse E66-E66' over alluvium and quartz monzonite showing distances and amplitudes used to compute minimum estimates of magnetization. Profiles are plotted from 1200 rubidium magnetometer measurements 1.5 m (4.9 ft) above ground surface. Profile A is based on zero datum from Yucca Flat, and profile B is based on an average zero datum adjusted to fit the observed data. Distances are in kilometers from Mercury.

For quantitative interpretations of individual anomalies, further adjustment may be required to obtain values closer to zero over nearby deposits of nonmagnetic sedimentary rock. In this report, surfaces are adjusted to an assumed zero field over Yucca Flat where thick deposits of sedimentary rocks underlie relatively thin deposits of alluvium and volcanic rock. For example, a value of 40 nT was added to contours of figure 1C to prepare figure 10C, and 10nT was added to contours of figure 3C to prepare the eastern two thirds of figure 2C.

Measurements were made along a long truck-borne magnetometer traverse to investigate the field over Yucca Flat, and to establish a base station near the Climax stock. The measurement and compilation system was based on work by Kane and others (1971) and Hildenbrand and Sweeney (written commun., 1980). The traverse shown in figure 1C originates at the Mercury base station where investigations during recent years have assigned an Earth's field value of 51550 nT (nanoteslas) and a residual anomaly value of zero. The traverse goes northward on the Mercury highway, along Frenchman Flat, through Yucca Flat, across granitic exposures at Climax stock, and ends at the 85.6-km (53.2-mi) station. Figure 8C shows observed values of the Earth's field along the traverse. The solid line drawn through the anomalies is based on the planar regional anomaly of the NTS region and increases 5.63 nT/km northward and 1.72 nT/km eastward. The line crosses Yucca Flat at about the same average value as the observed anomalies, and at station 75.8 km (47.1 mi) the difference between line and observed value is about 200 nT. The station is therefore assigned a residual value of 200 nT and an Earth's field value of 51880 nT. All ground magnetic traverses measured over the stock were tied to this station.

Figure 9C shows the residual anomalies that result from subtracting regional anomaly values from observed data in part of the profile of figure 8C. The traverse starts at station 34.1 at the south end of Yucca Flat, goes northward across the Flat and stock, and ends at the 85.9 km (53.4 mi) station shown in figure 1C. The residual values were continued upward by the two-dimensional method of Henderson and Zietz (1949) to a level of 2,450 m (8,000 ft) above sea level, the elevation datum of figure 1C. The continuation smoothed and reduced the amplitudes of ground anomalies. Over Yucca Flat the values approach the zero average that has been assumed for both air and ground magnetic anomalies.

REGIONAL INTERPRETATIONS

Recently compiled aeromagnetic data reveal several new anomaly patterns, including a southeastern extension of the belt of positive anomalies that are related to exposures of intrusive rock masses within the NTS. The data are presented on figure 3C at a scale of 1:250,000, the same scale as the geologic map of Lincoln County, Nevada, by Ekren and others (1977).

A trend of positive aeromagnetic anomalies extends from the NTS southeast over known or inferred intrusive bodies for a distance of more than 65 km (40 mi) across eastern Nye and western Lincoln Counties. The anomalies previously shown on figure 2C start at Gold Meadows stock (E) and trend east 20 km (12 mi) to Climax stock (C), southeast 10 km (6 mi) to Twinridge stock (B), and southeast 15 km (9 mi) to the inferred intrusive in the Papoose Range (A).

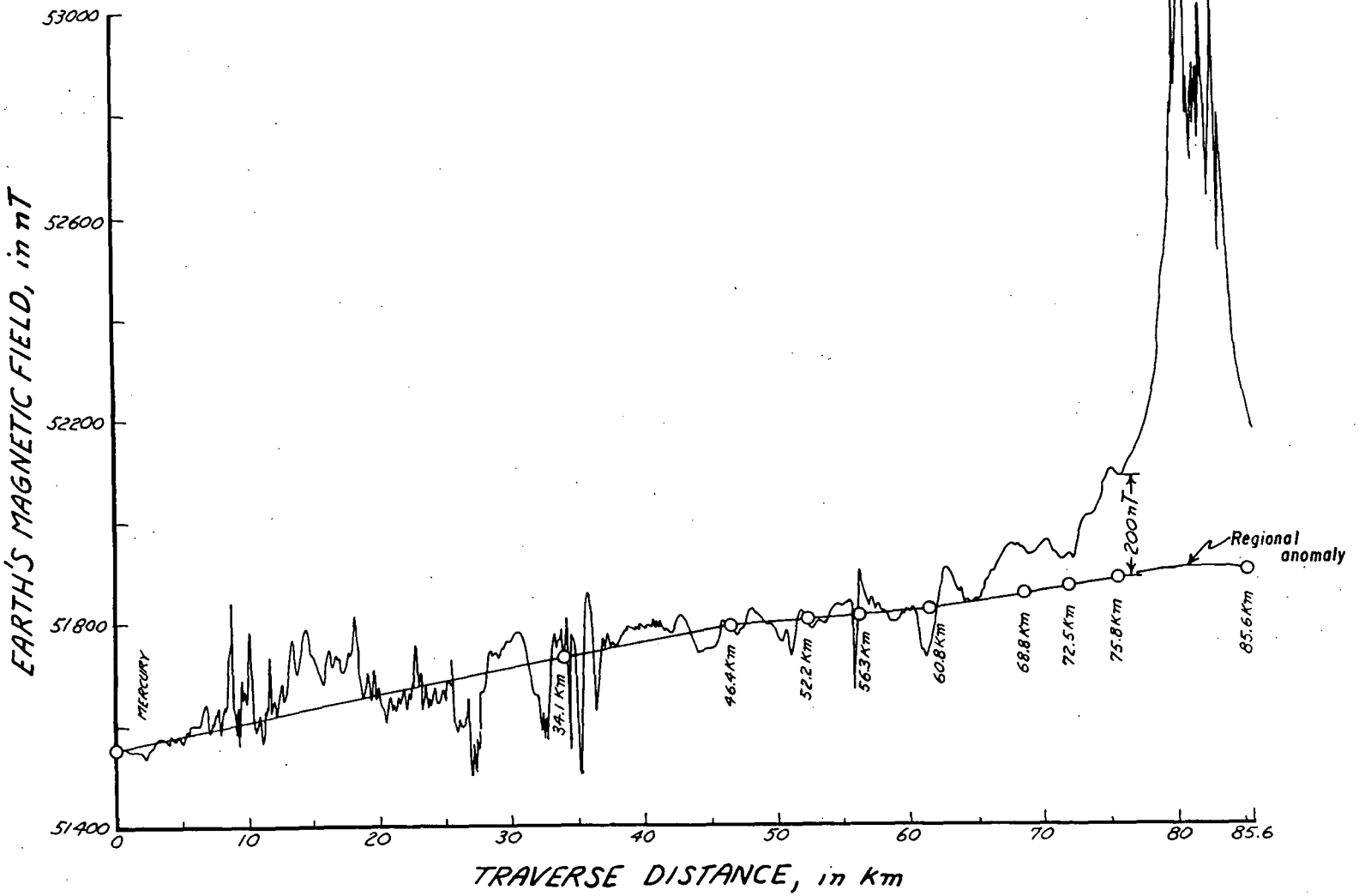

Figure 8C.--Profile of Earth's magnetic field as observed by truck-mounted magnetometer along the traverse of figure 1C extending from base station at Mercury northward 85.6 km (53.2 mi) along west side of Frenchman Flat, 13 to 26 km; through Yucca Flat, 36.6 to 75.8 km; and across granitic exposures at Climax stock, 80 to 83 km. Distances given in figure 1C are shown as circles on the regional line. The profile shows local anomalies arising from geologic features, a gradual northward increase in the Earth's magnetic field, and a line representing the planar regional anomaly of the Test Site region. The residual anomaly, difference between observed and regional anomaly, has a value of 200 nT at the 75.8 km base station.

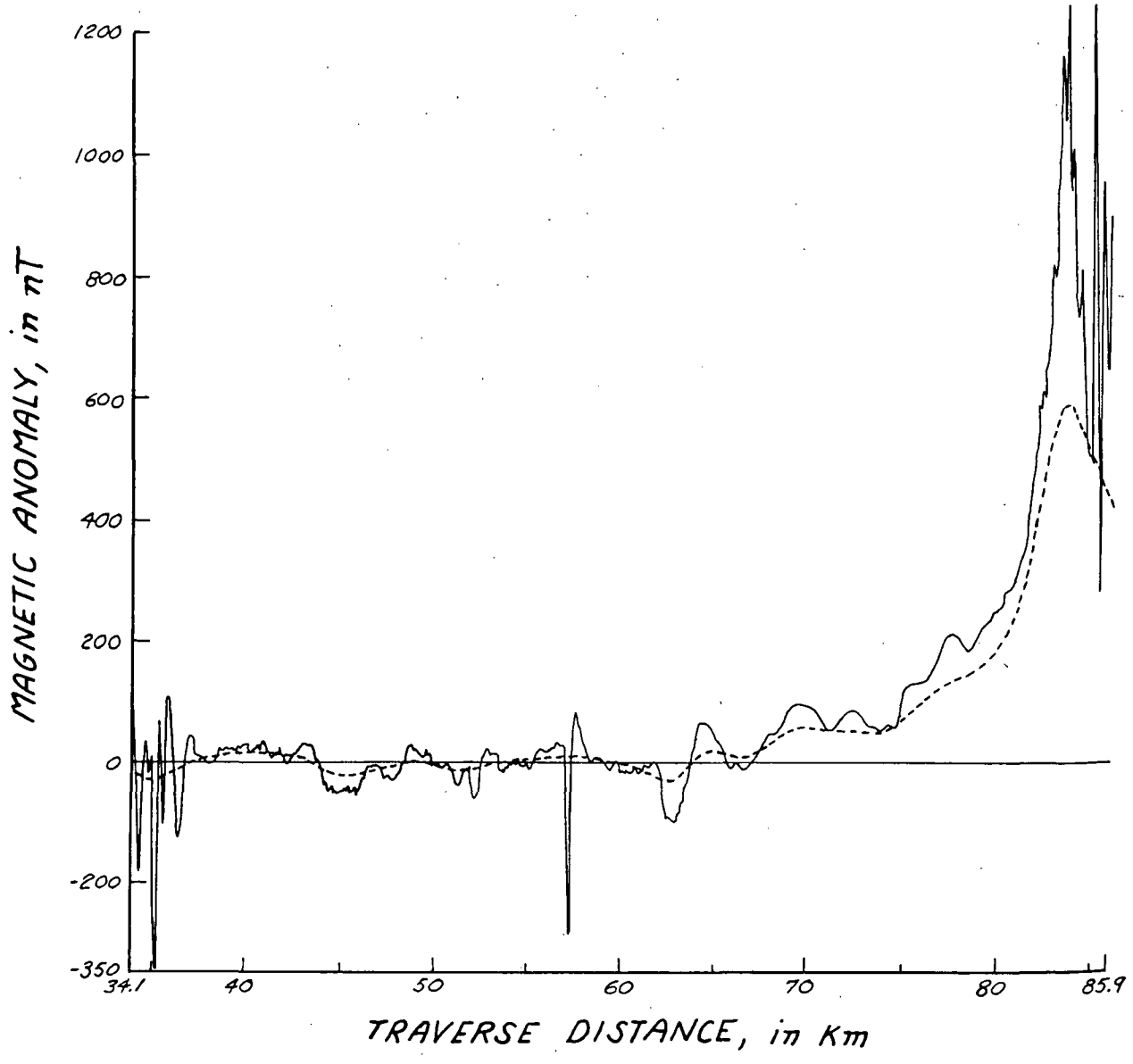

Figure 9C.--Profiles of residual magnetic anomalies, solid line; and data continued upward 914.4 m (3,000 ft), dashed line. Data are from truck-mounted magnetometer traverse of figure 1C extending from 34.1 km (21.2 mi) station northward 51.8 km (32.2 mi) through Yucca Flat, and ending at the 85.9 km (53.4 mi) station on granitic exposures on Climax stock.

The contours of figure 3C extend the trend an additional 20 km (12 mi) southeast to the anomaly maximum of 125 nT over inferred intrusive rock in the northwestern part of the Pintwater Range. The anomalies are interpreted as arising from a belt of magnetized intrusive and associated metamorphosed sedimentary rocks.

The lateral extent of the positive aeromagnetic anomaly in the northeastern corner of figure 4C suggests magnetized intrusives and associated sedimentary rocks are buried beneath the exposures of volcanic rock at the surface. Also, the map shows several belts of alined maxima and minima that strike in a northward direction. The belts are similar to those produced by a faulted volcanic ashflow at the Yucca fault in Yucca Flat (Bath, 1976), and may indicate the presence of buried faults. Data was collected along east-west flight lines, and thus emphasize effects from features that strike north-south.

GROSS CONFIGURATION OF STOCK

Figure 10C is a recompilation of the data of figure 1C at a 20-nT countour interval. The stock anomaly has nearly circular contours over an area of about 200 km^2 (77.3 mi^2), and reaches a maximum of 462 nT at the southwestern edge of the exposed portion of the stock. The compilation is based on measurements 850 m (2,789 ft) above the surface. The effect of the high measurement level is to smooth many of the local anomalies that are found in low-altitude data. Models based on high-altitude data usually represent gross configuration only, and often must be modified in areas where prominent anomalies are present in data measured closer to the ground surface.

Previous Studies

To explain the circular magnetic anomaly, Allingham and Zietz (1962) employed a three-dimensional polar chart method (Henderson, 1960) to produce a model consisting of four cylinders arranged as shown and tabulated on figure 11C. The model represents a gross configuration of the stock that conforms with granitic exposures at the surface, widens and becomes very large at depth, and has steeper slopes on the east and south than to the north and west. The cylinders have a constant magnetization of 1.54 A/m in the direction of the Earth's magnetic field. The magnetization value was determined from core samples in the lower half of drill hole U15a. Figure 11C shows the accepted configuration of the model, and the anomaly that was computed for the model. Subsequently, hole UE15d was drilled to a depth of 1,830 m (6,000 ft) southeast of the stock (fig. 11C). At this location the model of Allingham and Zietz predicts granitic rock at a depth of about 1,400 m (4,600 ft), however, none was encountered in the hole. Possible explanations for failure of the model include (1) the interval of 2,440 m (8,000 ft) from aeromagnetic datum to sea level is too great to give an accurate position for cylinder C, and (2) the granitic rock southeast of the stock is overlain by a thick section of magnetized sedimentary rock.

Whitehill (1973), on the other hand, modeled the circular anomaly with a single rectangular vertical prism. He used a computer to generate anomalies due to a large number of prisims of varying depth, length, width, thickness, and magnetization. Each prism was oriented with its long dimension N. 45° W.

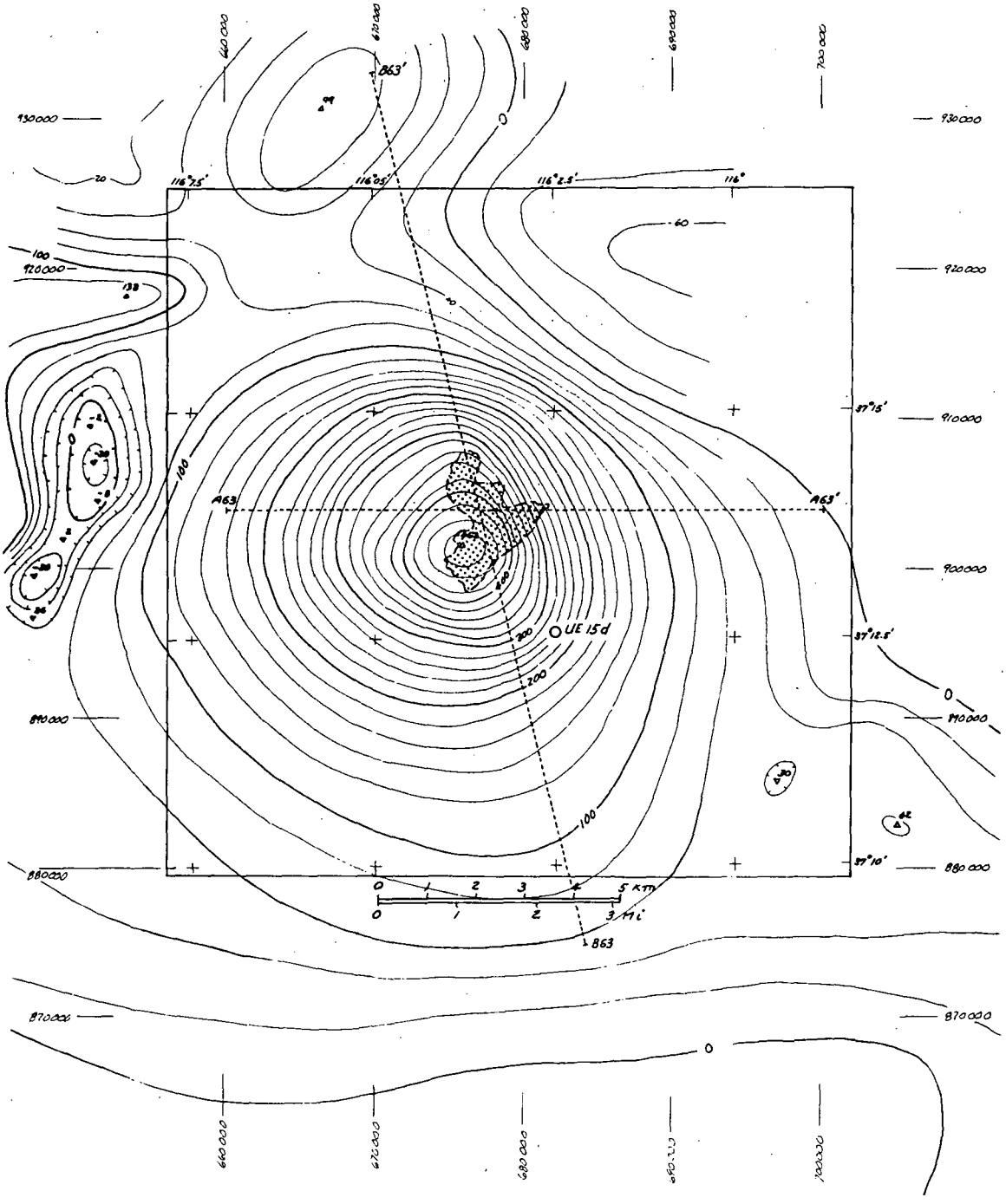

Figure 10C.--Residual aeromagnetic map showing the large circular anomaly that reaches a maximum of 462 nT over shaded outline of exposed part of the stock, and aeromagnetic traverses A63-A63' and B63-B63'. Measurements were at about 2,450 m (8,000 ft) above sea level, and countour interval is 20 nT. Triangles give locations of anomaly maxima, inverted triangles give locations of anamoly minima.

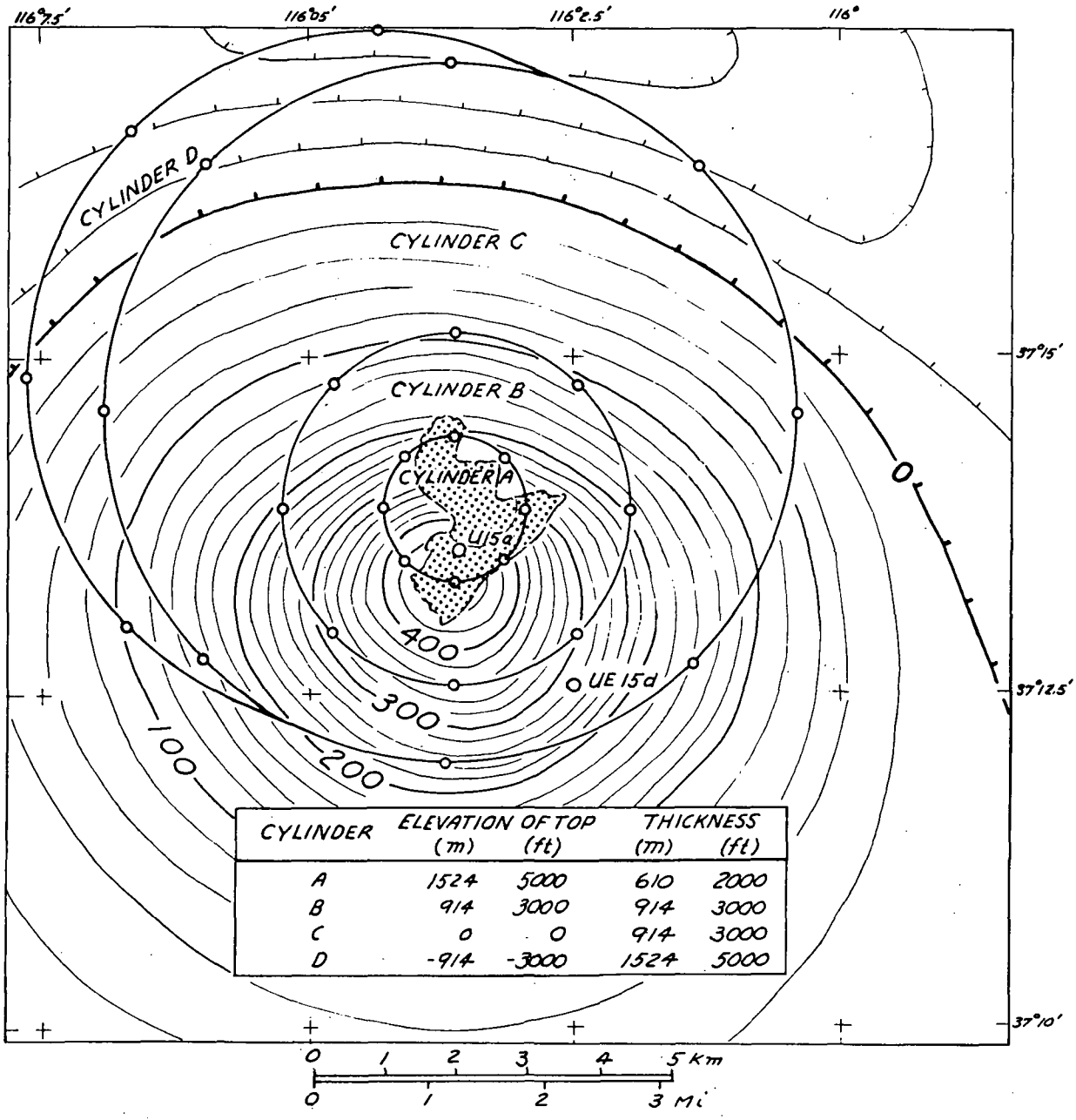

CYLINDER	ELEVATION OF TOP (m)	(ft)	THICKNESS (m)	(ft)
A	1524	5000	610	2000
B	914	3000	914	3000
C	0	0	914	3000
D	-914	-3000	1524	5000

Figure 11C.--Outlines and tabulated dimensions of the four vertical cylinders that Allingham and Zietz (1962) used to represent the stock. Also shown and contoured at 20-nT interval is the anomaly computed from four 8-sided vertical prisms arranged to approximate the circular shapes of the four cylinders. Magnetization of all prisms is along the Earth's field at 1.53 A/m, the average intensity of magnetization for core from drill hole U15a. Drill hole UE15d penetrated volcanic and sedimentary rocks to an elevation of -440 m (-1,445 ft), or 440 m below the top of cylinder C, without entering granitic material. Shaded outline is the exposed part of the stock.

The calculated anomalies that best fit the observed anomaly were for prisms that have tops buried beneath the exposed granitic rock at the stock, and magnetizations greater than the 1.54 A/m used by Allingham and Zietz. Figure 12C shows the prism, which provided the best fit to the observed data and its computed magnetic anomaly. The southeast edge of the prisim is 1,220 m (4,000 ft) northwest of drill hole UE15d, its top is 1,173 m (3,850 ft) below granitic rock at the surface, and its magnetization is 2.27 A/m.

New Model of the Climax Stock

We have developed a new model consisting of five vertical prisms to represent the gross configuration of the Climax stock and to explain anomalies along traverses A63-A63' and B63-B63' of figure 10C. The model resulted from considerations that include the locations of granitic exposures, observed increase in magnetization with depth fig. 6C, depths estimated from slope distances of anomalies, and the model of Allingham and Zietz, and of Whitehill. Outlines and dimensions of the new model are shown in plan view on figure 13C and in section along traverse A63-A63' (fig. 13C) on figure 14C. The upper part of the model consists of three 8-sided vertical prisms, P1, P2, and P3, having outlines that closely approximate granitic exposures in plan view. The low surface magnetization of 0.13 A/m increases to 0.28 A/m in P1, 0.72 A/m in P2, and 1.39 A/m in P3. The remainder of the model consists of rectangular prism, P4, taken from Whitehill, and 8-sided prism, P5, similar to the lowermost cylinder of Allingham and Zietz. Computations with a three-dimensional forward program, and comparisons with anomalies along the two traverses, assigned a magnetization of 1.55 A/m to prisms P4 and P5. Computed anomalies for the model closely resemble the observed residual anomalies along traverse A63-A63' as shown in figure 14C (A).

Model computations and depth estimates from slope distances indicate that most of the stock anomaly arises from rocks at depths greater than 810 m (2,657 ft), the depth to the top of P4. The contribution of each of the five prisms to the 408 nT maximum on traverse A63-A63' is 5 nT from P1, 17 nT from P2, 24 nT from P3, 205 nT from P4, and 157 nT from P5. Most of the anomaly, therefore, comes from unsampled deep sources that could include strongly magnetized sedimentary rocks, as well as strongly magnetized granitic rocks.

FAULT INTERPRETATIONS

Interpretations of magnetic anomalies measured closer to the ground surface indicate major displacements of magnetized rock near the faults along the eastern and southeastern borders of stock exposures. The aeromagnetic map of figure 4C shows the circular stock anomaly 120 m (394 ft) above the surface, the mapped locations of major faults, and the positions of nine ground traverses. The residual anomalies of the map were compiled from aeromagnetic surveys flown about 120 m (394 ft) above the surface (Bath, 1976, and USGS, 1979). Unfortunately, the low-level aeromagentic data are incomplete in important areas along the eastern and southeastern sides of the stock.

The ground data were measured at 3-m (10-ft) intervals 1.5 m (5 ft) above the surface with a proton magnetometer. The ground magnetic anomalies over the stock and bordering faults are shown in east-west traverse A80-A80'

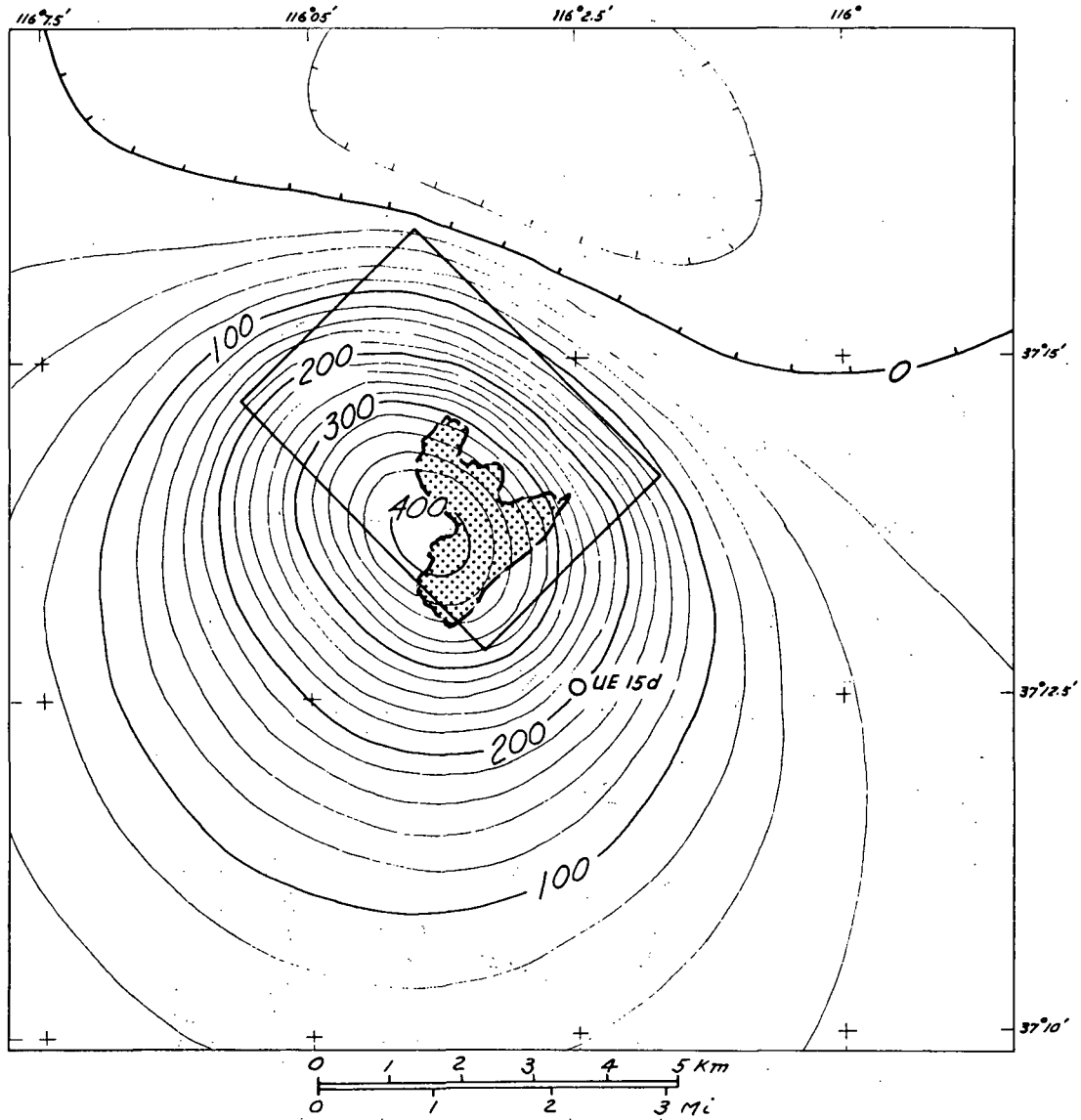

Figure 12C.--Rectangular outline of the vertical prism of Whitehill (1973) giving a computed anomaly that best fits the observed anomaly. Also shown and contoured at 20-nT interval is the anomaly computed for the prism which has a magnetization along the Earth's field at an intensity of 2.27 A/m. The prism is 4,840 m (15,900 ft) long, 3,430 m (11,250 ft) wide, and 17,200 m (56,400 ft) thick. The top of the prism has an elevation of 427 m (1,400 ft) which is 1,160 m (3,800 ft) below the elevation of the shaded outline of exposed granitic rocks. Drill hole UE15d is 1,250 m (4,100 ft) southeast of the prism.

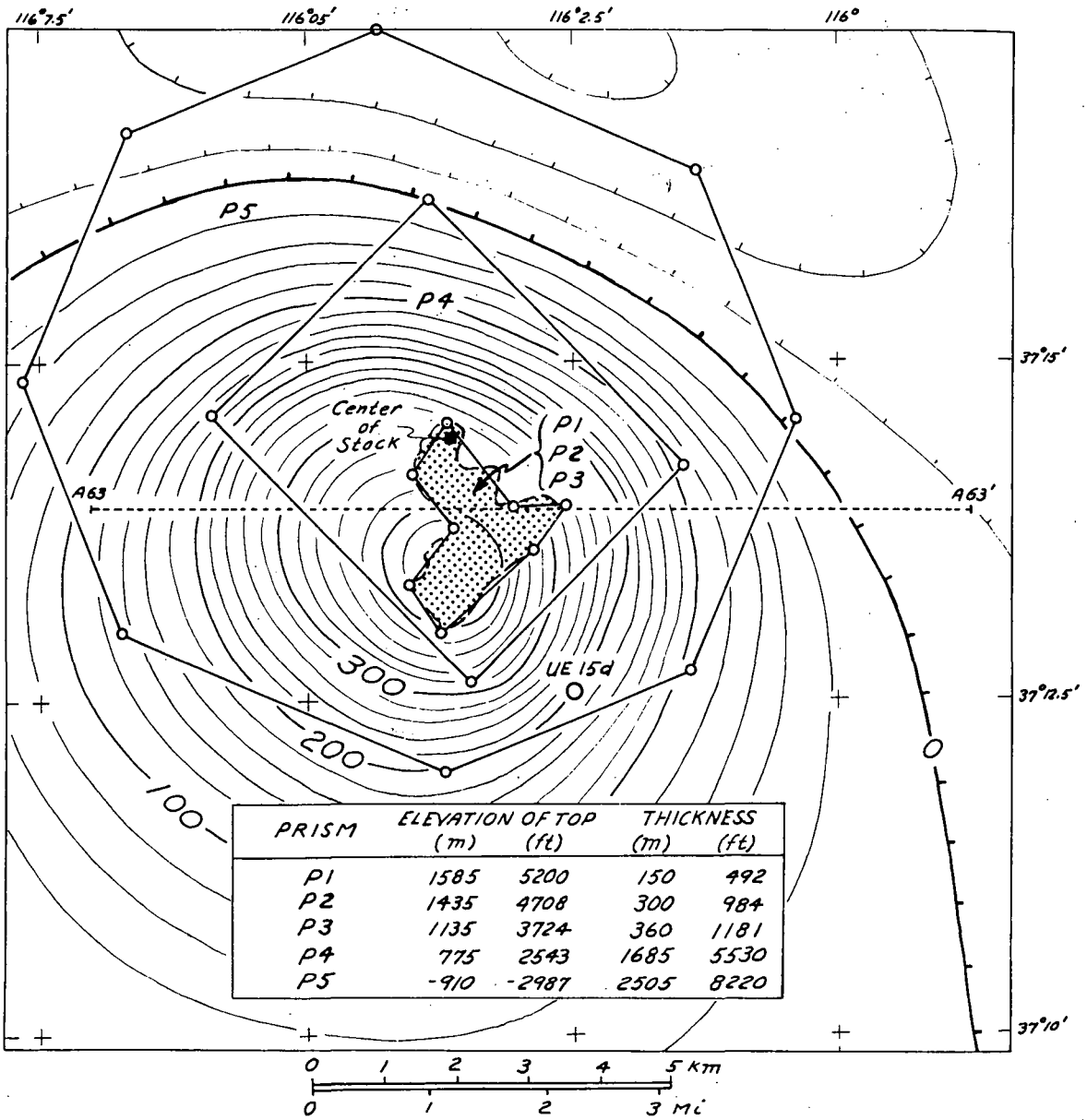

PRISM	ELEVATION OF TOP (m)	(ft)	THICKNESS (m)	(ft)
P1	1585	5200	150	492
P2	1435	4708	300	984
P3	1135	3724	360	1181
P4	775	2543	1685	5530
P5	-910	-2987	2505	8220

Figure 13C.--Outlines and tabulated dimensions of the five vertical prisms used to explain the anomaly of figure 10C, and to represent the gross configuration of the stock. Also shown and contoured at 20-nT interval is anomaly computed for the prisms when magnetized along the Earth's field at an intensity that increases from 0.28 A/m for prism 1 to 1.55 A/m for prisms 4 and 5. Also shown are shaded outline of the exposed part of the stock, approximate center of the stock model, and air traverse A63-A63'.

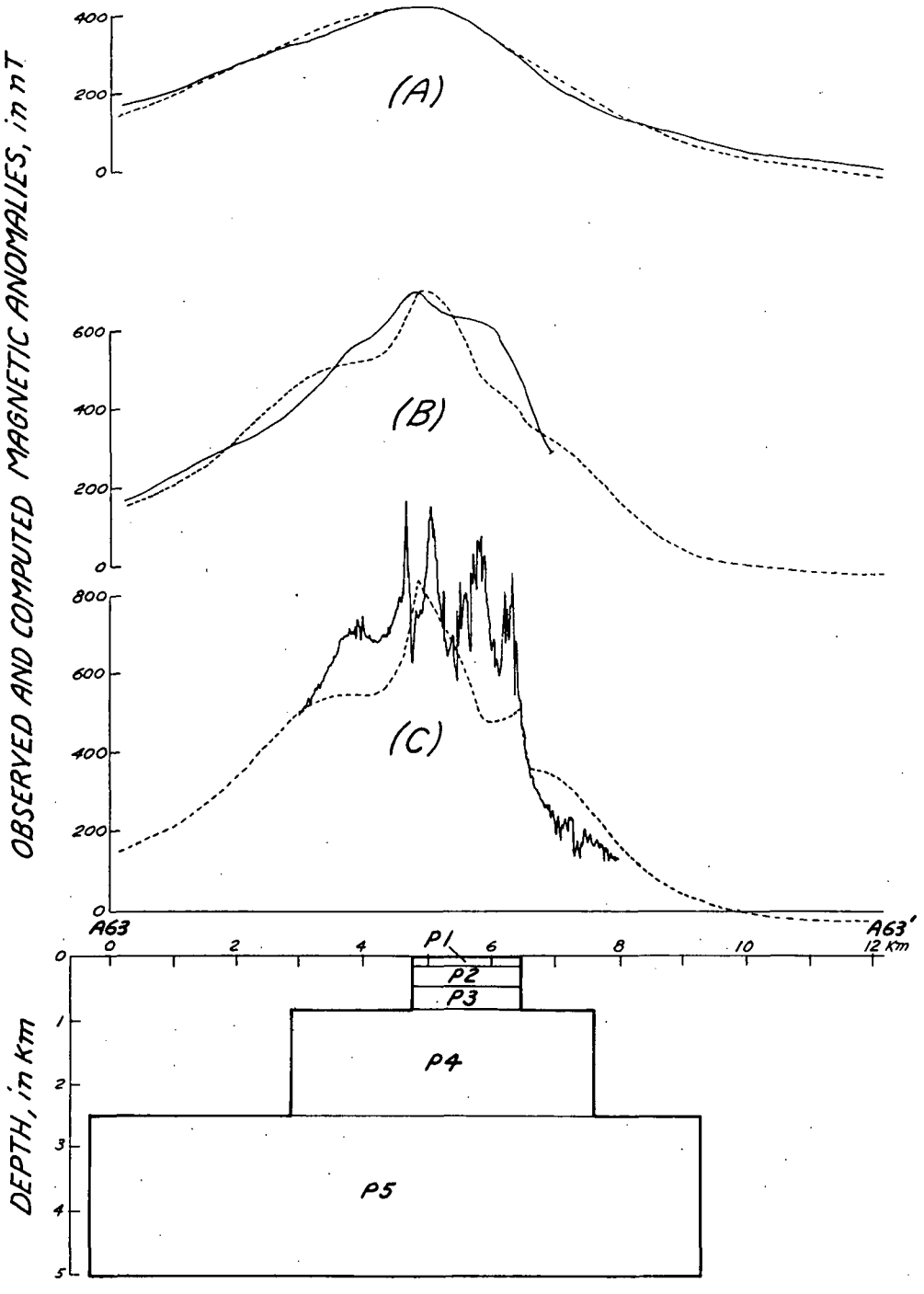

Figure 14C.--Section through the five prisms of figure 13C showing residual and computed anomalies along traverse A63-A63' at (A) 850 m (2,789 ft), (B) 120 m (394 ft), and (C) 1.5 m (5 ft) above the stock. Solid lines are residual anomalies, and dashed lines are computed anomalies.

positioned beneath air traverse A63-A63' (fig. 15C); B80-B80' parallel to and 305 m (1,000 ft) south of A80-A80' (fig. 15C); and C80-C80' to the northeast over the high topography to the north (fig. 16C). Five parallel traverses, A73-A73', B73-B73', C73-C73', D73-D73', and E73-E73', oriented N. 35° W. pass over the southeastern edge of the stock and the Boundary and Yucca faults (fig. 17C). In order to facilitate positional correlations, the ground anomalies are plotted above elevations of the topographic surface and a schematic representation of known faults and geologic units.

Slope distances and anomaly amplitudes provide a basis for estimates of magnetization, and thus for relating ground anomaly patterns to areal distributions of geologic units. Estimates are generally consistent with values from samples listed in tables 1, 2, and 3. Anomaly amplitudes are low, and application of equation (2) usually reveals nonmagnetic or weakly magnetic rocks. The only strongly magnetized rocks are in a granodiorite feature that is 200 m (656 ft) wide at the 85.0-km (52.8-mi) station on the truck-mounted magnetometer traverse shown on figure 9C. The prominent anomaly of more than 1,800 nT at the 2,900-m (9,514-ft) station of traverse C80-C80' (fig. 16C) is assumed to arise from concentrations of iron and steel objects in underground workings. Alluvium and most older sedimentary rocks are nonmagnetic, and most intrusive and all volcanic units are weakly magnetized. There are, however, local occurrences of moderately magnetized quartz monzonite, granodiorite, and sedimentary rocks.

Change of anomaly pattern, as well as distinctive anomalies are present near several faults and contacts, but many amplitudes are small because of weak magnetizations of near-surface rocks. There are minor changes over the Tippinip fault on traverses A80-A80' and B80-B80'; and over the Boundary and Butte faults on traverses A80-A80' and B80-B80'; and over the Boundary and Butte faults on traverse C80-C80'. A local positive anomaly of less than 100 nT is shown west of the Tippinip fault near station 4.0 km (2.5 mi) on traverse A63-A63' (C) of figure 14C, and near station 800 m on traverse A80-A80' of figure 15C. Also six traverses over the eastern and southeastern parts of the stock show the abrupt reductions in anomaly amplitude that are expected at stock edges or displaced magnetized rock. Anomaly decreases are present east of the Boundary fault (fig. 4C) on ground traverses A80-A80' and B80-B80' of figure 16C., and southeast of the Boundary fault (fig. 4C) on ground traverses B73-B73', C73-C73', D73-D73', and E73-E73' of figure 18C.

The computed contours and profiles of figures 13C and 14C illustrate the anomalies expected over the Climax stock, assuming it is bordered by fault-like vertical sides. Computations are for the gross configuration model of figure 13C, and the vertical sides extend to a depth of 810 m (2,658 ft), the combined thickness of prisms P1, P2, and P3. Data are computed at 850 m (2,789 ft), 120 m (394 ft), and 1.5 m (5 ft) above P1.

Boundary and Tippinip Faults

Structures near the Boundary and Tippinip faults were investigated by modifying the configuration and magnetization of the stock model (fig. 13C) in order to explain the local anomalies in ground magnetic traverses over edges of the stock. The stock model is constructed of vertical prisms that have polygonal outlines in plan view. The vertical prisms near the surface were replaced with horizontal prisms that have polygonal outlines in section view.

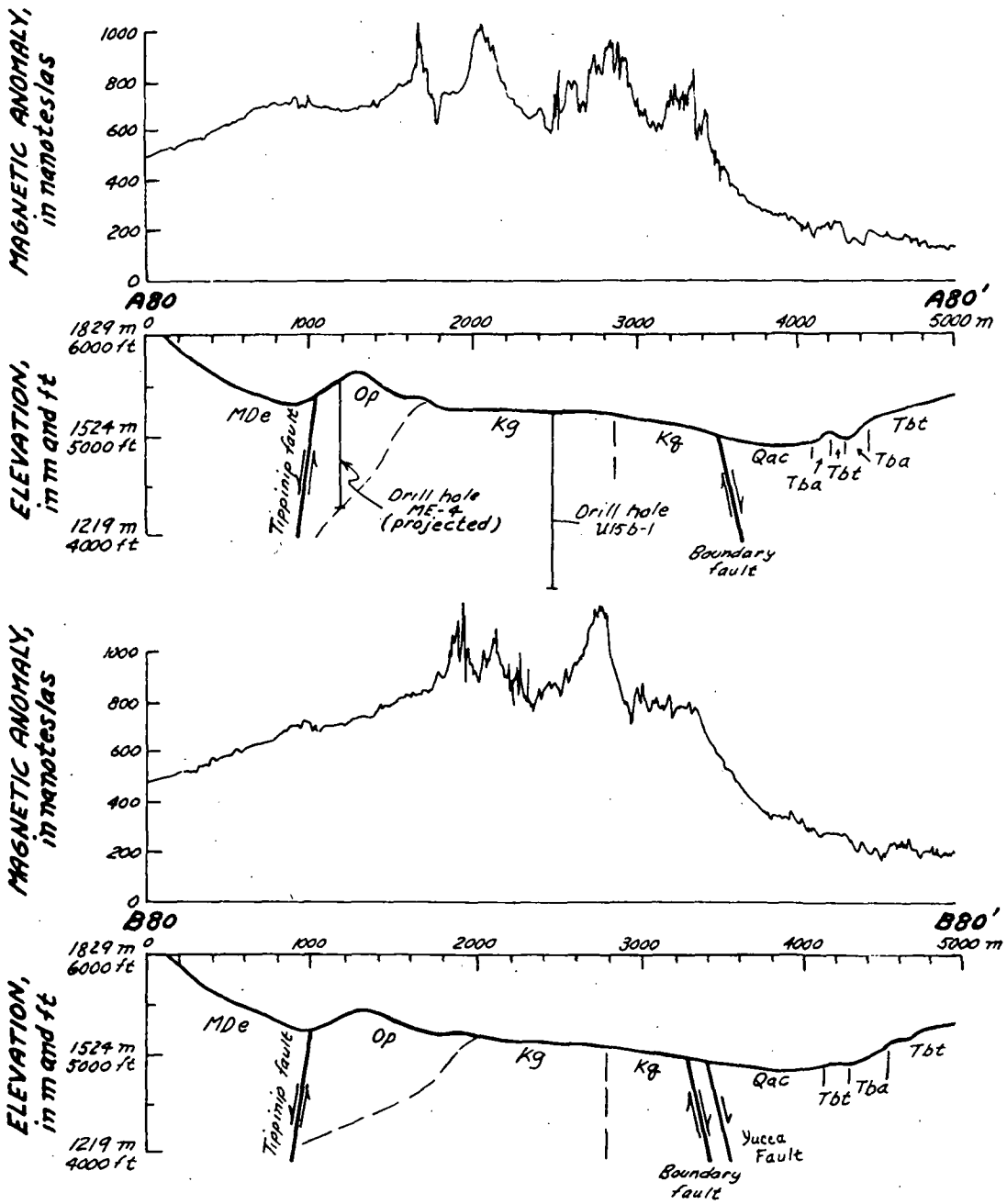

Figure 15C.--Profiles of residual ground magnetic anomalies along traverses A80-A80' and B80-B80' over Eleana Formation, MDe; Pogonip Group, Op; granodiorite stock, Kg; quartz monzonite stock, Kq; alluvium and colluvium, Qac; Tub Spring Member of the Belted Range Tuff, Tbt; air-fall, bedded, and zeolitized tuff, Tba; and Tippinip and Boundary faults. Each profile was plotted from 1,700 proton magnetometer measurements 1.8 m (6 ft) above ground surface.

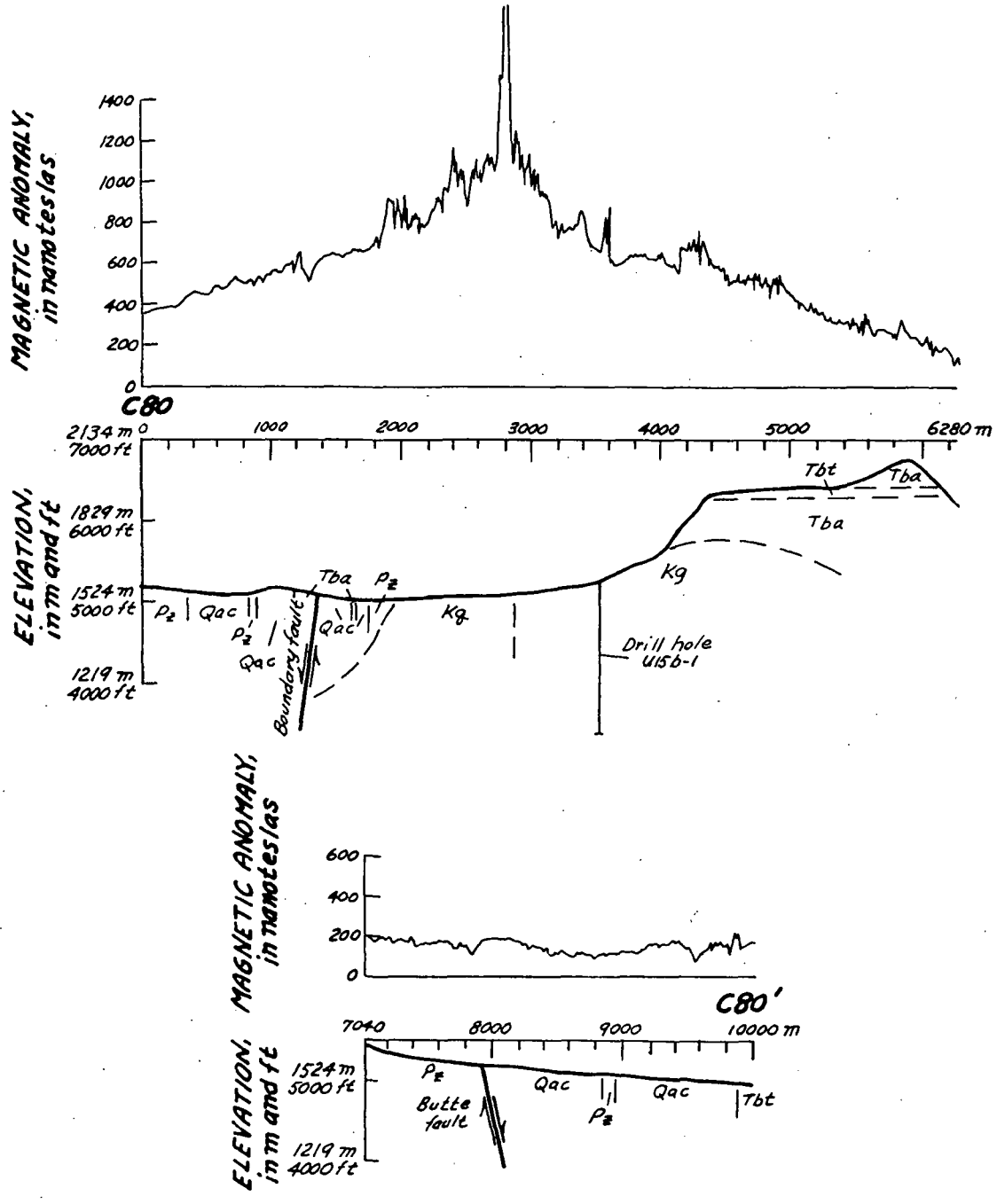

Figure 16C.--Profile of residual ground magnetic anomalies along traverse C80-C80' over Paleozoic sedimentary rocks, Pz; granodiorite stock, Kg; quartz monzonite stock, Kq; Tub Spring Member of the Belted Range Tuff, Tbt; air-fall, bedded, and zeolitized tuff, Tba; alluvium and colluvium, Qac; and Boundary and Butte faults. Profile was plotted from 3,000 proton magnetometer measurements 1.8 m (6 ft) above ground surface. No measurements were made over steep slope in interval 6,280 to 7,040 m (20,603-23,087 ft).

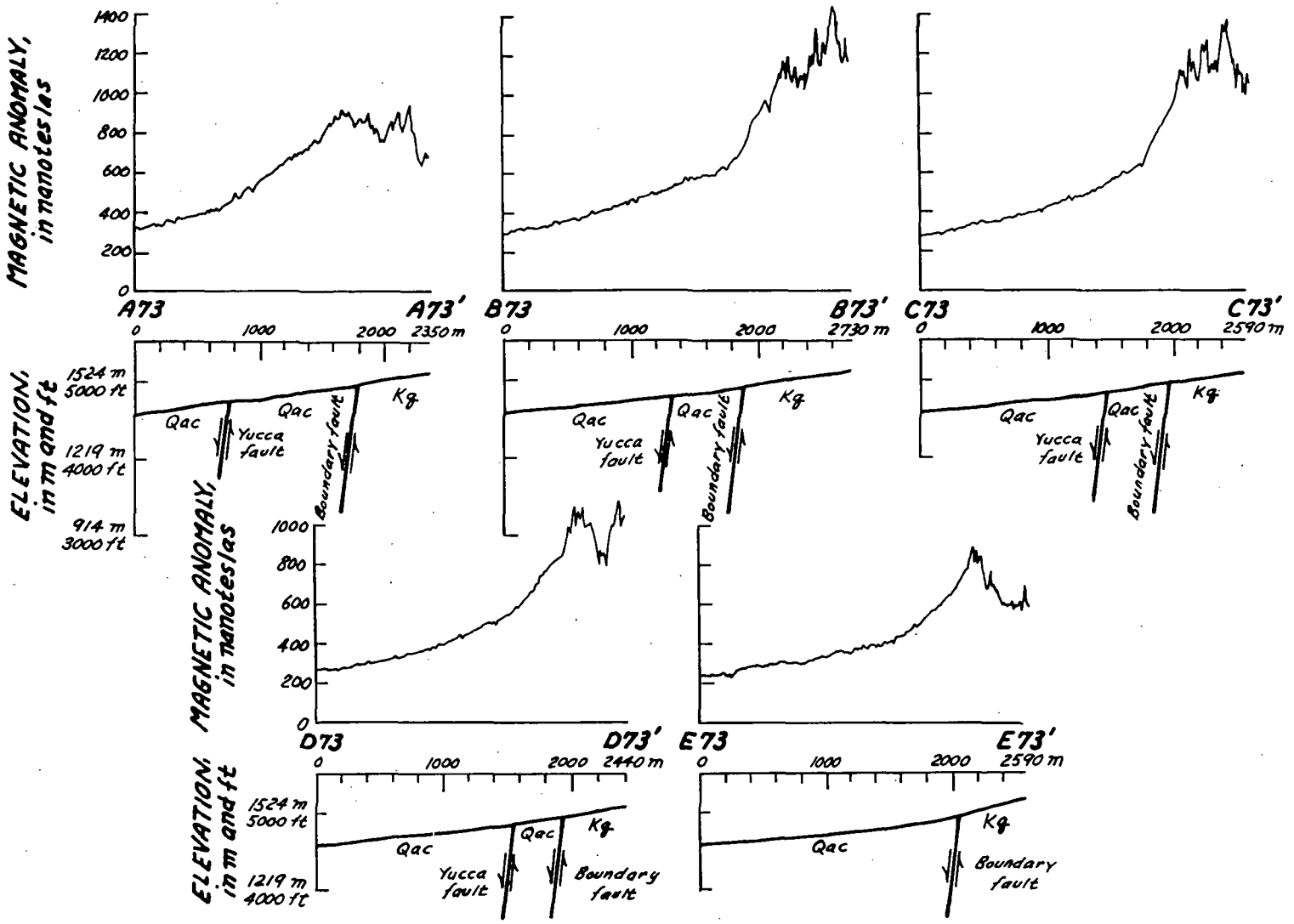

Figure 17C.--Profiles of residual ground magnetic anomalies along traverses A73-A73', B73-B73', C73-C73', D73-D73', and E73-E73' over quartz monzonite stock, Kq; alluvium and colluvium, Qac; and Yucca and Boundary faults. Profiles were plotted from 1,666 proton magnetometer measurements 1.4 m (4.6 ft) above ground surface.

This permitted use of several horizontal prisms of irregular outline to represent the relatively complex configurations of known and inferred geologic structure in section view. The cumulative effects of all vertical and horizontal prisms were then computed with a three-dimensional forward program and compared with the ground magnetic anomalies. Finally, several arrangements of prisms having different outlines and magnetizations were investigated to find the model judged most reasonable in terms of (1) comparisons of computed and measured anomalies, (2) surface and drill-hole geology, and (3) magnetic properties of core samples from nearby drill holes and magnetization estimates from ground magnetic anomalies.

The modified model of Climax stock at its southeastern edge is given on figure 18C along ground traverse C73-C73' (fig. 4C). The stock is represented by five prisms: horizontal prism P_H1 having J_t = 0.74 A/m, the average magnetization of quartz monzonite core from drill hole UE15f (table 3C); horizontal prisms P_H2, P_H3, and P_H4 having assigned magnetization of 1.55 A/m; and vertical prism P_V5 having assigned magnetization of 1.80 A/m. Southeast of the stock, alluvium is represented by horizontal prism Qac having a magnetization of 0 A/m indicated by estimates from the ground anomalies of figure 7C; volcanic rocks by horizontal prisms Tv having J_t = 0.30 A/m, the average of core from drill hole UE15d (table 1C); and metamorphosed sedimentary rocks of Precambrian age by horizontal prisms pCs having J_t = 0.10 A/m, a rough estimate from the limited core of drill hole UE15d (table 1C).

Almost all of the stock is terminated by the Boundary fault. This fault has high-angle southeastern dips of 80° to a depth of 750 m (2,461 ft) and 70° to a depth of 2,000 m (6,562 ft). A possible extension of the stock beyond the fault was investigated by replacing metamorphosed sedimentary rocks with granite in the wedge between the Boundary and Yucca faults. As shown on figure 18C, this resulted in poor comparison between residual and computed anomaly, and thus reduces the possibility of a significant extension to the southeast.

The modified model of Climax stock at its western edge is given in figure 19C along ground traverse A80-A80'. The stock is represented by five prisms: horizontal prism P_H1 having J_t = 0.85 A/m, the average magnetization of granite core from drill hole ME-4 (table 2C) plus the increase of 0.00196 A/m per meter of depth found in core from drill hole U15b-1 (fig. 6C); horizontal prism P_H2 having J_t = 1.30 A/m, resulting from continuing the increase of magnetization with depth; and horizontal prism P_H3, and vertical prisms P_V4 and P5, each having an assigned magnetization of 1.47 A/m. West of the stock, two groups of metamorphosed sedimentary rocks of Paleozoic age are present. The larger is represented by horizontal prism Pzs having J_t = 0.10 A/m, a rough estimate from variable core values of drill hole ME-4 (table 2C). The smaller group of unknown buried rocks is represented by the horizontal prism having an assigned J_t = 0.50 A/m and is defined by the dimensions given on figures 4C and 19C. The prism of unknown rock is required to explain the local magnetic high west of the fault.

The west edge of the stock dips 30° westward. The distinctive anomaly near the Tippinip fault is a local high, and not the reduction in anomaly amplitude expected west of a fault having its low-standing side to the west.

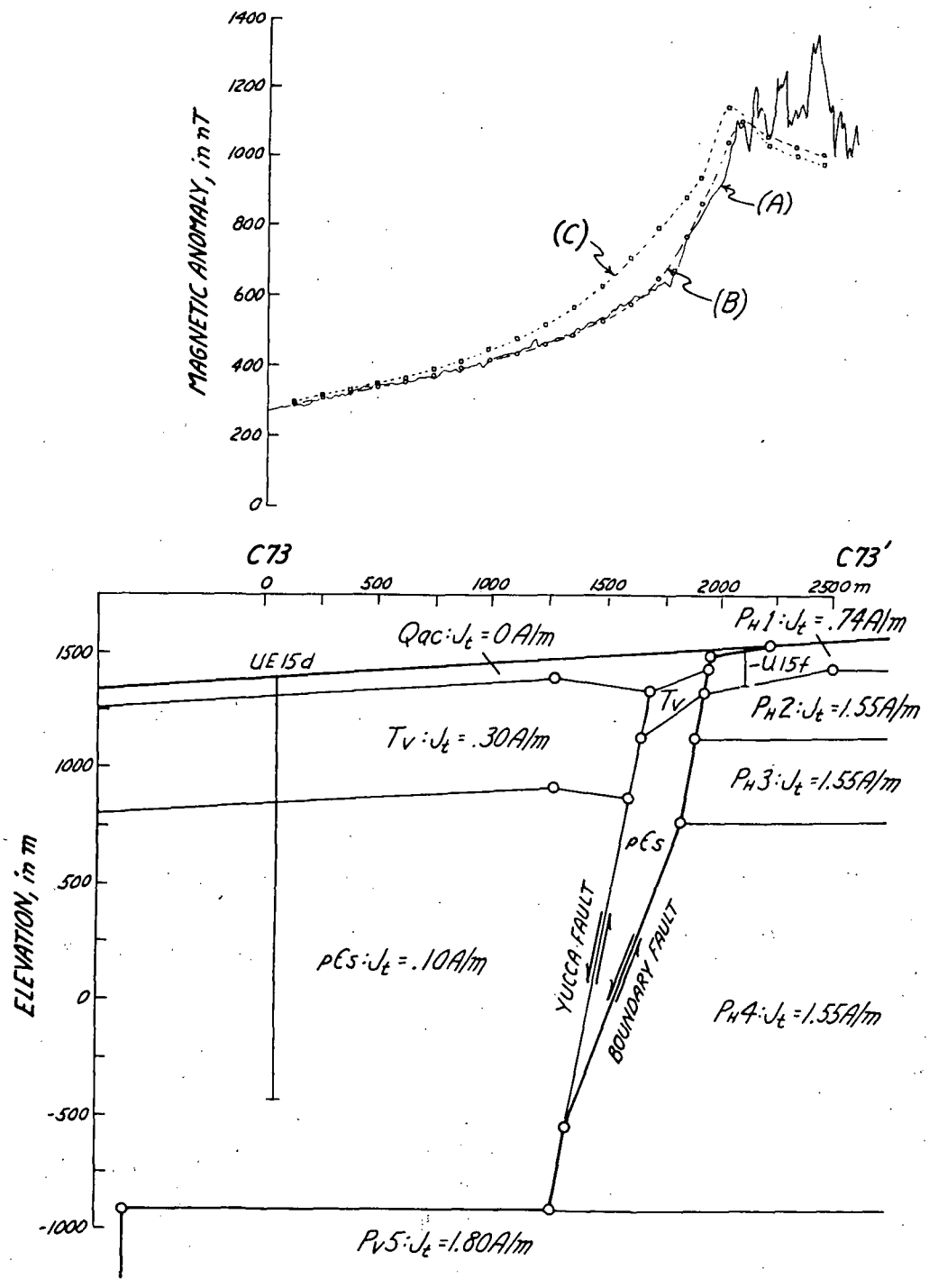

Figure 18C.--Section along ground traverse C73-C73' showing model selected to portray the southeastern edge of the stock. The stock is represented by prisms P_H1, P_H2, P_H3, P_H4, and P_V5; the Quaternary alluvium by prism Qac; the Tertiary volcanic rocks by prism Tv; and the Precambrian metasedimentary rocks by prism pCs. Also shown are Boundary and Yucca faults, and the rocks penetrated by drill holes UE15d and UE15f. Anomalies shown along the traverse are (A) measured residuals, (B) computed effects of the model, and (C) computed effects of the model with the modification of replacing metasedimentary rocks having J_t = 0.10 A/m with granitic rocks having J_t = 1.55 A/m in the wedge between Yucca and Boundary faults.

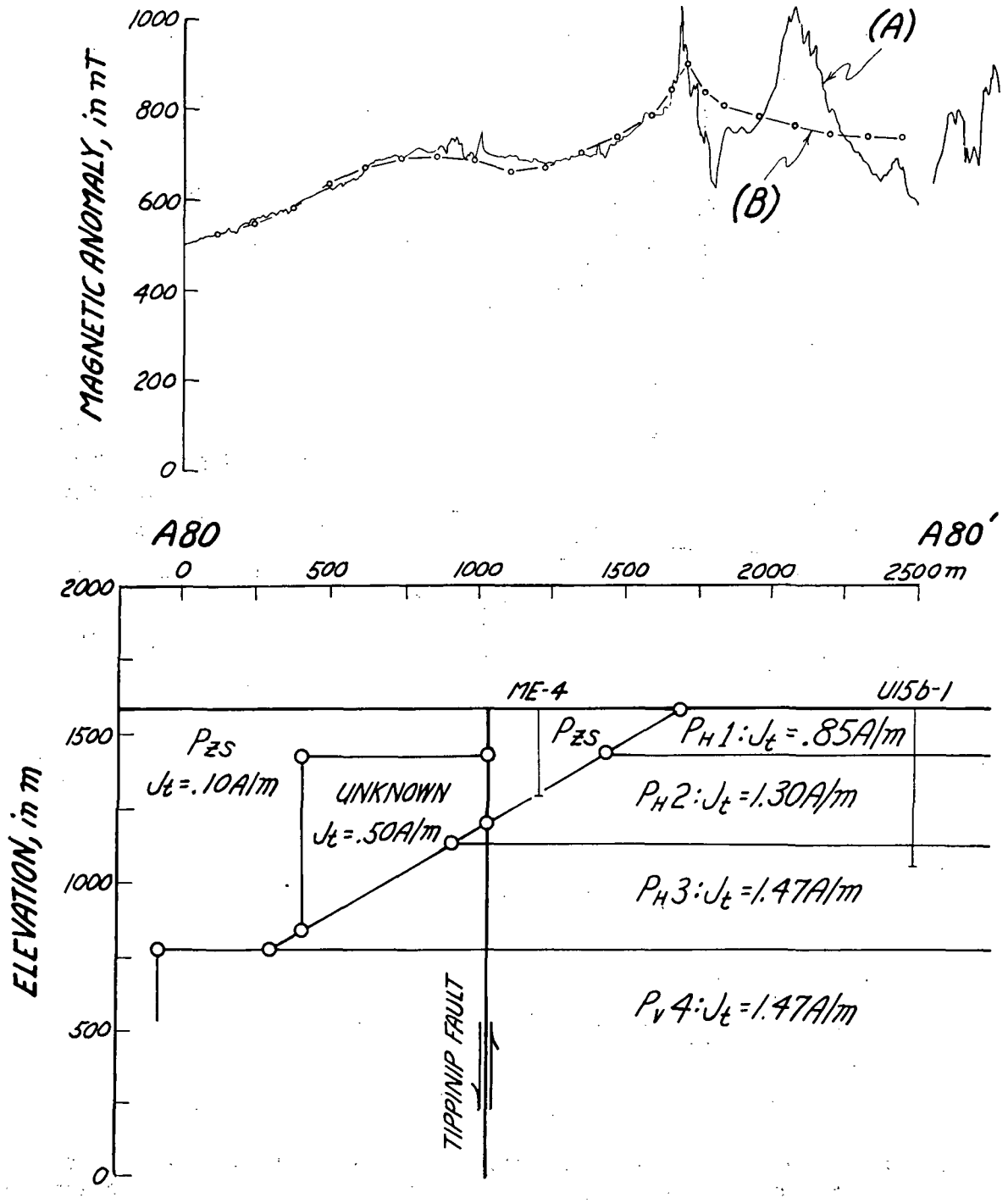

Figure 19C.--Section along ground traverse A80-A80' showing model selected to portray the western edge of the stock. The stock is represented by prisms P_H1, P_H2, P_H3, P_V4, and P5 (fig. 13C); the metasedimentary rocks by prism Pzs; and the unknown buried rocks by the prism having J_t = 0.50 A/m. Also shown is the Tippinip fault, and the rocks penetrated by drill holes ME-4 and U15b-1. Anomalies shown along the traverse are (A) measured residuals, and (B) computed effects of the model.

The unknown buried rocks may be Eleana Formation with an increased magnetite content similar to that observed near Calico Hills (Baldwin and Jahren, 1982), rather than magnetized granitic rock, and we are, therefore, unable to provide an interpretation of displaced granitic rock at the fault. The evidence for identifying the buried rock comes from amplified residual anomalies shown along traverses A80-A80' and B80-B80' on figure 20C. Slope distances indicate that near-surface Eleana Formation is magnetized just west of the Tippinip fault. Thus the Tippinip fault does not appear to bound the west edge or the stock in a fashion similar to the Boundary fault.

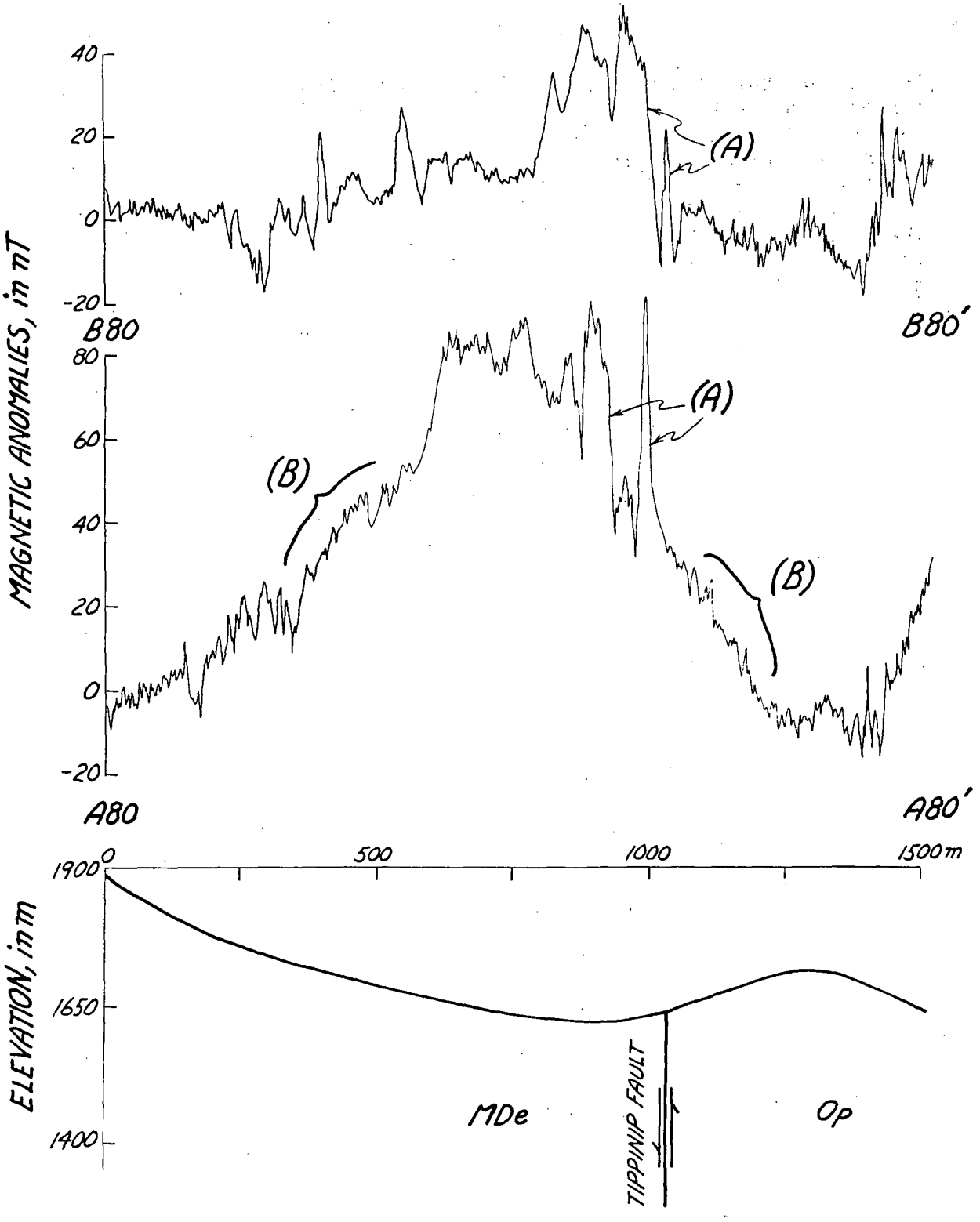

Figure 20C.--The amplified residual anomalies along traverses A80-A80' and B80-B80' showing slope distances that designate sources within 20 m (65 ft) (A) and 150 m (490 ft) (B) of the surface. Also shown are Tippinip fault, metamorphosed sedimentary rocks of the Eleana Formation, MDe, and metamorphosed sedimentary rocks of the Pogonip Group, Op. The shallow sources are just west of the Tippinip fault in the Eleana Formation, MDe.

REFERENCES CITED

Allingham, J. W., and Zietz, Isidore, 1962, Geophysical data on the Climax stock, Nevada Test Site, Nye County, Nevada: Geophysics, v. 27, p. 599-610.

Baldwin, M. J., and Jahren, C. E., 1982, Magnetic properties of drill core and surface samples from the Calico Hills area, Nye County, Nevada: U.S. Geological Survey Open-File Report 82-536, 27 p.

Barnes, Harley, Christiansen, R. L., and Byers, F. M., Jr., 1965, Geologic map of the Jangle Ridge quadrangle, Nye and Lincoln Counties, Nevada: U.S. Geological Survey Geologic Quadrangle Map GQ-363, scale 1:24,000.

Barnes, Harley, Houser, F. N., and Poole, F. G., 1963, Geology of the Oak Spring quadrangle, Nye County, Nevada: U.S. Geological Survey Geologic Quadrangle Map GQ-214, scale 1:24,000.

Barraclough, D. R., and Fabiano, E. B., 1978, Grid values and charts for the International Geomagnetic Reference Field 1975: U.S. Geological Survey Report PB-276 630, 139 p.; available only from U.S. Department of Commerce, National Technical Information Service, Springfield, VA 22161.

Bath, G. D., 1968, Aeromagnetic anomalies related to remanent magnetism in volcanic rock, Nevada Test Site, Nevada, in Nevada Test Site: Geological Society of America Memoir 110, p. 135-146.

_____1976, Interpretation of magnetic surveys in intermontane valleys at Nevada and southern New Mexico: U.S. Geological Survey Open-File Report 76-440, 36 p.

Boynton, G. R., Meuschke, J. L., and Vargo, J. L., 1963a, Aeromagnetic map of the Timber Mountain Quadrangle and part of the Silent Canyon Quadrangle, Nye County, Nevada: U.S. Geological Survey Geophysical Investigations Map GP-443, scale 1:62,500.

_____1963b, Aeromagnetic map of the Tippipah Spring Quadrangle and parts of the Papoose Lake and Wheelbarrow Peak Quadrangles, Nye County, Nevada: U.S. Geological Survey Geophysical Investigations Map GP-441, scale 1:62,500.

Boynton, G. R., and Vargo, J. L., 1963a, Aeromagnetic map of the Cane Spring Quadrangle and parts of Frenchman Lake, Specter Range, and Mercury Quadrangles, Nye County, Nevada: U.S. Geological Survey Geophysical Investigations Map GP-442, scale 1:62,500.

_____1963b, Aeromagnetic map of the Topopah Spring Quadrangle and part of the Bare Mountain Quadrangle, Nye County, Nevada: U.S. Geological Survey Geophysical Investigations Map GP-440, scale 1:62,500.

Byers, F. M., Jr., Carr, W. J., Orkild, P. P., Quinlivan, W. D., and Sargent, K. A., 1976, Volcanic suites and related cauldrons of Timber Mountain-Oasis Valley caldera complex, southern Nevada: U.S. Geological Survey Professional Paper 919, 70 p.

Carr, W. J., and Quinlivan, W. D., 1966, Geologic map of the Timber Mountain quadrangle, Nye County, Nevada: U.S. Geological Survey Quadrangle Map GQ-503, scale 1:24,000.

Christie, K. W., and Symons, D. T. A., 1969, Apparatus for measuring magnetic susceptibility and its anisotropy: Geological Survey of Canada, Paper 69-41, 10 p.

Currie, R. G., Gromme, C. S., and Verhoogan, Jean, 1963, Remanent magnetization of some Upper Cretaceous granitic plutons in the Sierra Nevada, California: Journal of Geophysical Research, v. 68, p. 2263-2279.

Ekren, E. B., and Sargent, K. A., 1965, Geologic map of the Skull Mountain quadrangle, Nye County, Nevada: U.S. Geological Survey Geologic Quadrangle Map GQ-387, scale 1:24,000.
Ekren, E. B., Orkild, P. P., Sargent, K. A., and Dixon, G. L., 1977, Geologic map of Tertiary rocks, Lincoln County, Nevada: U.S. Geological Survey Miscellaneous Geologic Investigations Map I-1041, scale 1:250,000.
Gibbons, A. B., Hinrichs, E. N., Hansen, W. R., and Lemke, R. W., 1963, Geology of the Rainier Mesa quadrangle, Nye County, Nevada: U.S. Geological Survey Geologic Quadrangle Map GQ-215, scale 1:24,000.
Gromme, C. S., and Merrill, R. T., 1965, Paleomagnetism of Late Cretaceous granitic plutons in the Sierra Nevada, California: Further results: Journal of Geophysical Research, v. 70, p. 3407-3420.
Henderson, R. G., and Zietz, Isidore, 1949, The upward continuation of anomalies in total magnetic intensity fields: Geophysics, v. 14, no. 4, p. 517-534.
Henderson, R. G., 1960, Polar charts for evaluating magnetic anomalies of three-dimensional bodies, in U.S. Geological Survey Short Papers in Geological Sciences: U.S. Geological Survey Professioanl Paper 400-B, p. B112-B114.
Houser, F. N., and Poole, F. G., 1960, Preliminary geologic map of the Climax stock and vicinity, Nye County, Nevada: U.S. Geological Survey Miscellaneous Investigations Map I-328, scale 1:4,800.
Jahren, C. E., and Bath, G. D., 1967, Rapid estimation of induced and remanent magnetization of rock samples, Nevada Test Site: U.S. Geological Survey Open-File Report, 29 p.
Kane, M. F., Harwood, D. S., and Hatch, N. L., Jr., 1971, Continuous magnetic profiles near ground level as a means of discriminating and correlating rock units: Geological Society of America Bulletin, v. 82, p. 2449-2456.
Koenigsberger, J. G., 1938, Natural residual magnetism of eruptive rocks: Terrestrial Magnetism and Atmospheric Electricity, v. 43, p. 119-299.
McKay, E. J., and Williams, W. P., 1964, Geology of the Jackass Flats quadrangle, Nye County, Nevada: U.S. Geological Survey Quadrangle Map GQ-368, scale 1:24,000.
Nettleton, L. L., 1976, Gravity and magnetics in oil prospecting, in International series in the Earth and planetary sciences: McGraw-Hill, New York, 464 p.
Noble, D. C., and Christiansen, R. L., 1968, Geologic map of the southwest quarter of the Black Mountain quadrangle, Nye County, Nevada: U.S. Geological Survey Miscellaneous Geologic Investigations Map I-562, scale 1:24,000.
Oliver, H. W., 1977, Gravity and magnetic investigations of the Sierra Nevada batholith, California: Geological Society of America Bulletin, v. 88, p. 445-461.
Philbin, P. W., and White, B. L., Jr., 1965a, Aeromagnetic map of parts of the Cactus Peak and Stinking Spring quadrangles, Nye County, Nevada: U.S. Geological Survey Geophysical Investigations Map GP-517, scale 1:62,500.
_____1965b, Aeromagnetic map of parts of the Kawich Peak and Reveille Peak quadrangles, Nye County, Nevada: U.S. Geological Survey Geophysical Investigations Map GP-516, scale 1:62,500.
Philbin, P. W., and White, B. L., Jr., 1965c, Aeromagnetic map of the Cactus Spring quadrangle and part of the Goldfield quadrangle, Esmeralda and Nye Counties, Nevada: U.S. Geological Survey Geophysical Investigations Map GP-511, scale 1:62,500.

_____1965d, Aeromagnetic map of the Mellan quadrangle, Nye County, Nevada: U.S. Geological Survey Geophysical Investigations Map GP-518, scale 1:62,500.
_____1965e, Aeromagnetic map of the Quartzite Mountain quadrangle, Nye County, Nevada: U.S. Geological Survey Geophysical Investigations Map GP-515, scale 1:62,500.
_____1965f, Aeromagnetic map of the Belted Peak quadrangle and part of White Blotch Springs quadrangle, Nye County, Nevada: U.S. Geological Survey Geophysical Investigations Map GP-514, scale 1:62,500.
_____1965g, Aeromagnetic map of the Sarcobatus Flat area, Esmeralda and Nye Counties, Nevada: U.S. Geological Survey Geophysical Investigations Map GP-512, scale 1:125,000.
_____1965h, Aeromagnetic map of the Black Mountain quadrangle, Nye County, Nevada: U.S. Geological Survey Geophysical Investigations Map GP-519, scale 1:62,500.
_____1965i, Aeromagnetic map of the Silent Canyon quadrangle, Nye County, Nevada: U.S. Geological Survey Geophysical Investigations Map GP-520, scale 1:62,500.
_____1965j, Aeromagnetic map of the Wheelbarrow Peak quadrangle and part of the Groom Mine quadrangle, Nye and Lincoln Counties, Nevada: U.S. Geological Survey Geophysical Investigations Map GP-513, scale 1:62,500.

Rodgers, C. L., Anderson, R., E., Ekren, E. B., and O'Connor, J. T., 1967, Geologic map of the Quartzite Mountain quadrangle, Nye County, Nevada: U.S. Geological Survey Geologic Quadrangle Map GQ-672, scale 1:24,000.

Rosenbaum, J. G., Larson, E. E., Hoblitt, R. P., and Fickett, F. R., 1979, A convenient standard for low field susceptibility calibration: Review of Scientific Instruments, v. 50, p. 1027-1029.

Sargent, K. A., and Orkild, P. P., 1973, Geologic map of the Wheelbarrow Peak-Rainier Mesa area, Nye County, Nevada: U.S. Geological Survey Miscellaneous Geologic Investigations Map I-754, scale 1:48,000.

Smith, R. A., 1961, Some theorems concerning local magnetic anomalies: Geophysical Prospecting, v. 9, p. 399-410.

Sweeney, R. E., Godson, R. H., Hassemer, J. H., Dansereau, D. A., and Bhattacharyya, B. K., 1978, Composite aeromagnetic map of Nevada: U.S. Geological Survey Open-File Report 78-695, scale 1:500,000.

U.S. Geological Survey, 1979, Aeromagnetic map of the Timber Mountain area, Nevada: U.S. Geological Survey Open-File Report 79-587, scale 1:62,500.

Vacquier, Victor, Steenland, N. C., Henderson, R. G., and Zietz, Isidore, 1951, Interpretation of aeromagnetic maps: Geological Society of America Memoir 47, 151 p.

Whitehill, D. E., 1973, Automated interpretation of magnetic anomalies using the vertical prism model: Geophysics, v. 38, p. 1070-1087.

Zietz, Isidore, Stewart, J. H., Gilbert, F. P., and Kirby, J. R., 1977, Aeromagnetic map of Nevada: U.S. Geological Survey Miscellaneous Field Investigations Map MF-902, scale 1:500,000.

SUMMARY OF GEOLOGIC AND GEOPHYSICAL INVESTIGATIONS

By
Paul P. Orkild

The focus of integrated geologic and geophysical studies at the Climax stock was to define the stock boundaries and examine the geologic features pertaining to containment. The three faults (Tippinip, Boundary-Yucca, and Butte) defining the area structurally were examined in detail.

The nature of the Tippinip fault (the attitude and strike) has a little bearing on the geometry of the granite in the subsurface to the west. Surface geology (trenching) and the interpretation of magnetic data indicate that it is a benign feature which, at depth, does not affect the geometry of the granite sloping to the west. The lack of density contrast precludes the usefulness of gravity to define this fault. Field evidence indicates that the Tippinip fault had a fault motion component down to the east before the intrusion of the stock. This motion has since been reversed by the intrusion of the stock. The fault was undoubtedly a plane of weakness along which the stock was emplaced.

The Boundary fault defines the extent of granite outcrops to the southeast and east of the stock. The Yucca fault is projected to join the Boundary fault near trench 5. North of trench 5, the Boundary-Yucca faults are collectively called the Butte fault. The nature and dip of the fault planes are important in defining the boundary of the stock. These planes have been documented in seven trenches along the Boundary fault.

Initial geologic mapping was done by Houser and Poole, 1960; only minor differences were observed during recent field studies. One major difference was shallower dips on the Boundary fault, 43^{o}-59^{o}, with an average dip of 52^{o} SE instead of the recorded 75^{o} by Houser and Poole. However, it is interesting to note that the 75^{o} dip gives a better "fit" in 3-D analysis of the gravity and magnetic data.

Further examination of the Boundary fault structure in trench 5 and north of the confluence of the Boundary and Yucca faults and south in the Smokey Hills region indicates that 75^{o} to 77^{o} is a valid dip for these structures; this, combined with the magnetic and gravity interpretations, has led me to hypothesize that the faults mapped in USGS and LLNL trenches are slump features or low-angle faults of the Boundary fault system which dip into the main Boundary fault. The main trace of the Boundary fault is buried beneath young alluvium (figs. 2A and 1D). Figure 2A shows the inferred trace of the Boundary fault beneath the alluvium; this fits well with an inferred fault on 3-D gravity profile lines N899,000, N901,000, and N903,000. Figure 1D is a diagrammatic cross section of the Boundary fault system. Showing the main trace of the Boundary fault beneath alluvium, offsetting tuff and alluvium down to the east against tuffs and granite. On the footwall of the main trace of Boundary fault, outcrops of tuff were stranded on the irregular granite surface when the fault moved and, subsequently, these tuff deposits were slumped and developed the low-angle faults as seen in the USGS, LLNL, and DNA trenches.

The amount of offset on the Boundary fault, based on the stratigraphic offset of volcanic rocks which occur just beneath the Tub Spring Member on the shoulder of Oak spring Butte to the same stratigraphic horizon in and just

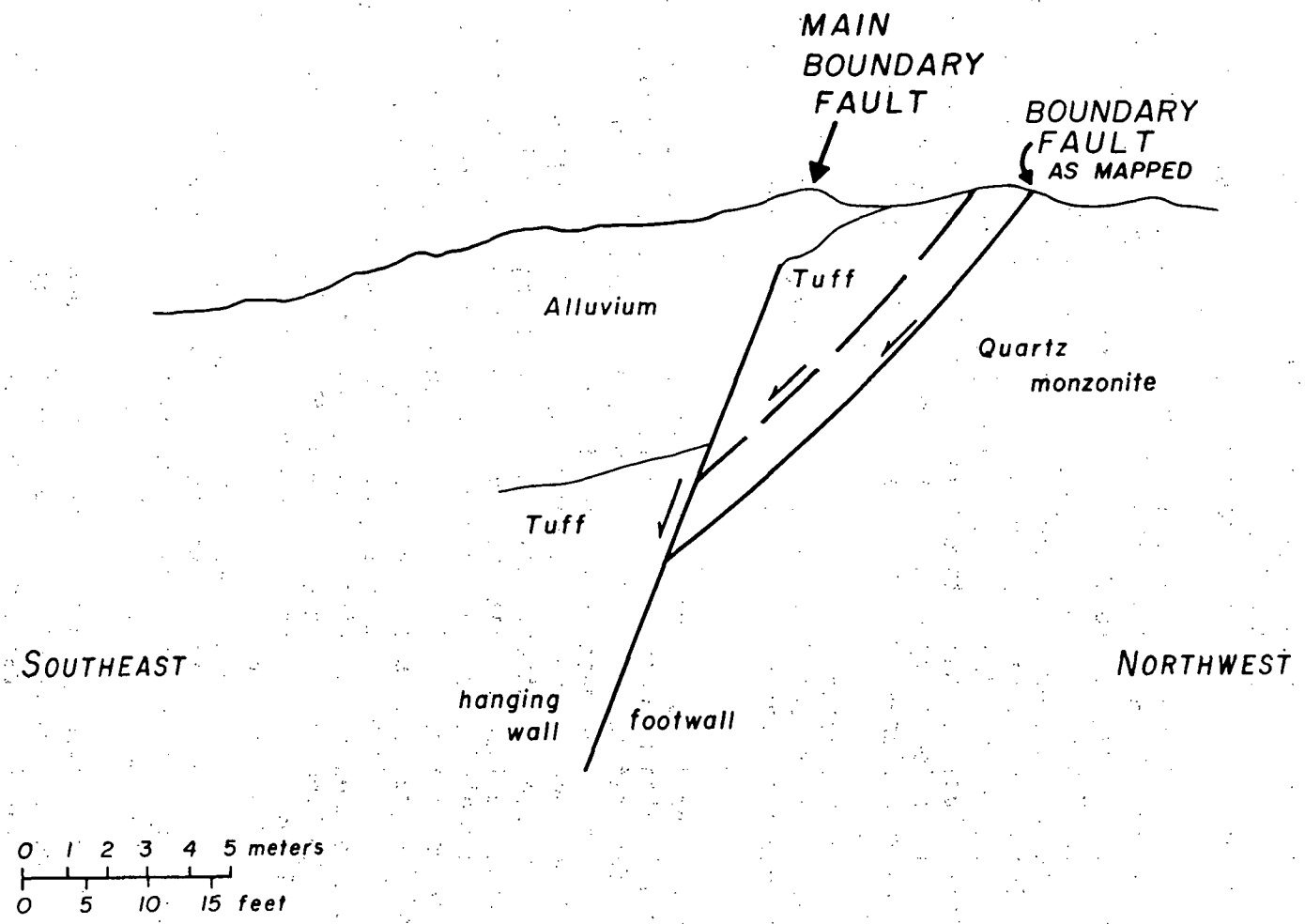

Figure 1D.--Diagrammatic cross section of Boundary fault system.

southeast of trench 5, and interpretations of gravity data, is approximately 213-243 m (700-800 ft). North of trench 5, where the Yucca and Boundary faults join, the Butte fault has a vertical post-tuff movement of 427 m (1,400 ft). A similar displacement is inferred from gravity data. The Butte fault displacement has been measured from two prominent ash-flow tuffs (Grouse Canyon and Tub Spring Members of the Belted Range Tuff), which form the cap and shoulder of Oak Spring Butte, to their down dropped counter parts east of the fault.

The amount of offset on the Boundary fault pre-volcanic rock is unknown, however, it is possible that the large displacement documented is totally post-volcanic and is related to the structural deformation of Yucca Flat basin in post-Miocene. The Yucca/Butte fault system, based on stratigraphic and drill-hole data, existed prior to the deposition of volcanic rock in the test site area. The amount of displacement had to be in excess of 610 m (2,000 ft) and possibly as much as 2,438 m (8,000 ft) based on the juxtaposition of the upper and lower plates of major thrust faults in Climax stock area. The displacement on the Boundary/Yucca fault system is further complicated by the fact that they were planes of weakness along which the stock was emplaced.

Estimates of the depth and width of buried portions of the granitic rocks of the Climax stock are based on geologic data, gravity data obtained by D. L. Healey, and interpretation of aeromagnetic and ground magnetic anomalies by G. D. Bath.

The gravity profiles define the near-surface configuration, but are unable to distinguish between the Paleozoic rocks and granitic rock at depth. The magnetic data defines the width, depth, and the gross subsurface configuration of the intrusive mass, but there is difficulty in approximating the boundaries from high-altitude aeromagnetic data. Geology defines the surface and near surface configuration. Limitations of geology, gravity, and magnetic methods prevent a unique solution by any one method, but, by combining the three, it is possible to obtain a reasonable model of the stock. This configuration is shown in figures 2D and 3D. The stock is elongated parallel to the long axis of the granitic outcrop and has steep southeast slope and moderately steep north slope. Interpretations indicate the Boundary/Yucca fault system truncates the southeast side with a displacement of approximately 2,000 m (6,500 ft). The Tippinip fault on the west flank of the stock shows no significant displacement. The model, as shown, has a total depth extent of about 4.8 km (3 mi), with the upper part of the model being approximately 6x4 km and the lower part enlarging to a diameter of at least 10 km (6 mi). The depth is a minimum estimate because it is assumed that the curie temperature occurs at about 3.4 km (2 mi) below sea level. Nonmagnetic rock probably extends to greater depths than shown on figures 2D and 3D.

Minor differences exist between geologic data and magnetic interpretations. The absence of granitic rocks between the Boundary and Yucca faults along line C73-C73' is at variance with geologic evidence to the northeast between magnetic lines D and E. Granitic rocks were penetrated at approximately 229 m (750 ft) in drill hole U15gz#24, however, to the south in the C73-C73' profile, if granitic rocks are extended southeastward into the wedge between the Boundary and Yucca faults this results in poor agreement between residual and computed anomaly as shown on figure 19C. One possibility is that U15gz#24 is located to the northwest of the concealed main trace of Boundary fault and was drilled into the footwall of the fault.

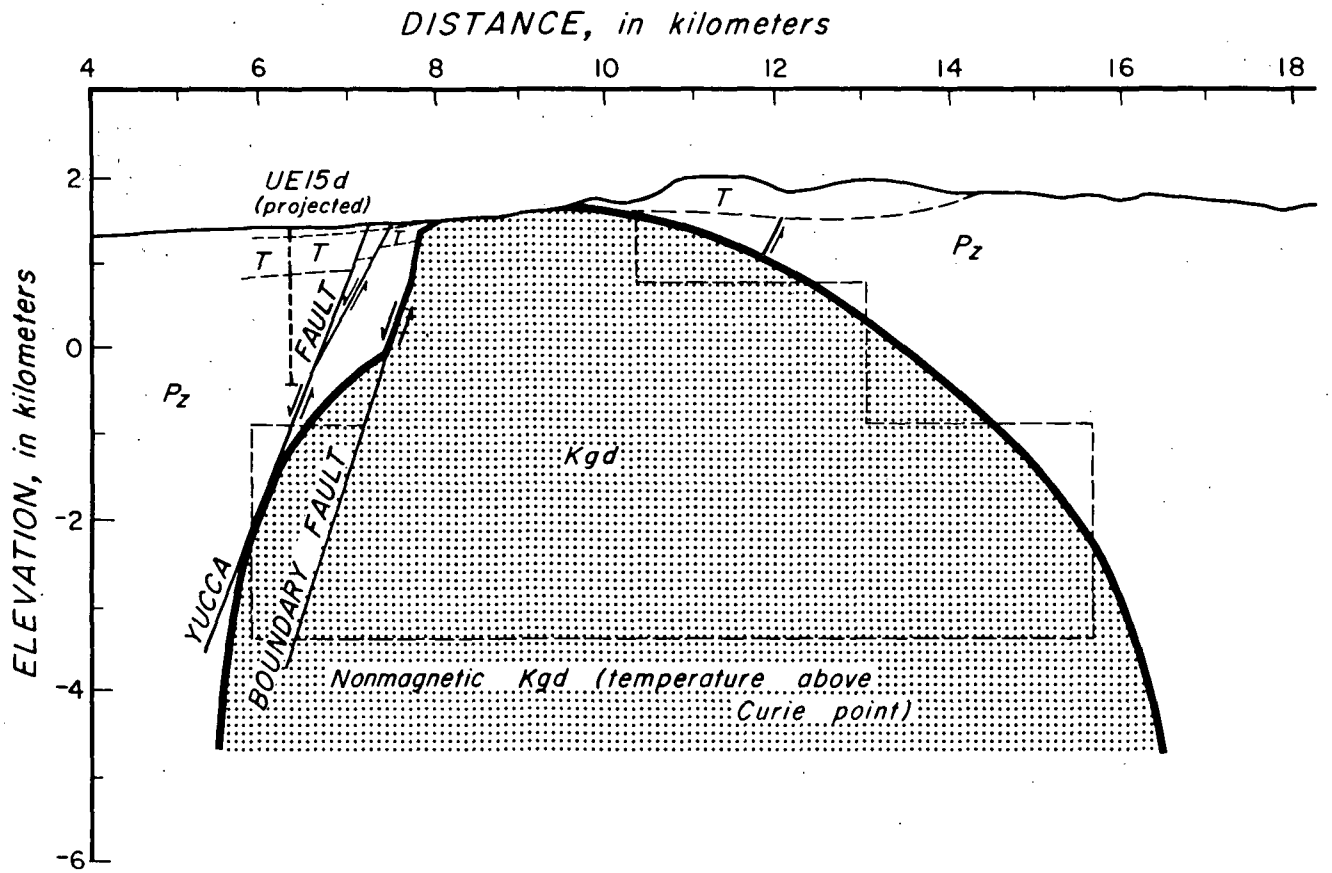

Figure 2D.--North-south section along traverse B63-B63' of figure 10C. Distance of traverse = 18.28 km (60,000 ft), but only 3.0 km to 18.28 km shown. Horizontal and vertical scale: 1" = 5,000 ft. (See plate 1A for explanation of geologic symbols.)

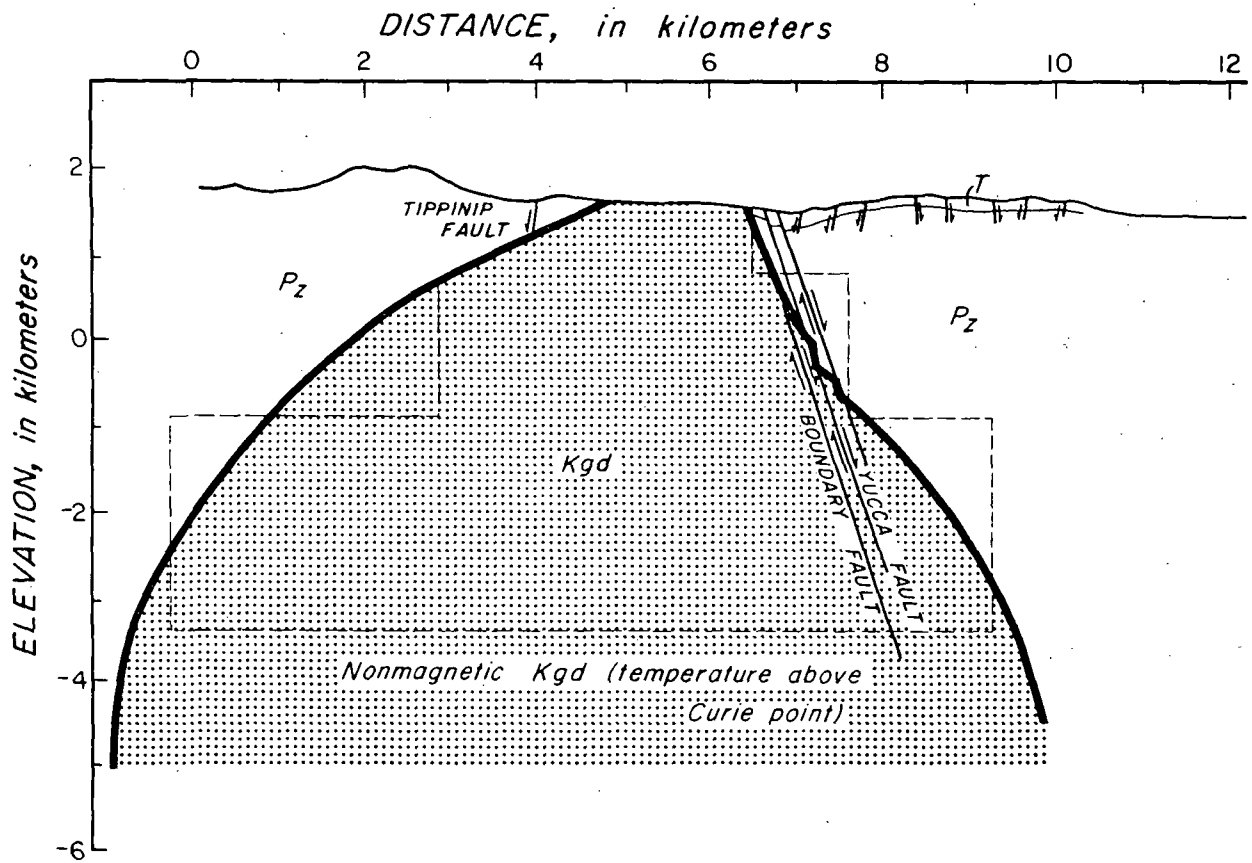

Figure 3D.--East-west section along traverse A63-A63' of figures 10C and 13C. Horizontal and vertical scale: 1" = 5,000 ft. (See plate 1A for explanation of geologic symbols.)

GPO 839-689

Open-File Report 82-536

Steve -
① Geochem on Eleana of DH UE 25a-3
② Geol review of alteration?

UNITED STATES
DEPARTMENT OF THE INTERIOR
GEOLOGICAL SURVEY

MAGNETIC PROPERTIES OF DRILL CORE AND SURFACE SAMPLES FROM THE CALICO HILLS AREA, NYE COUNTY, NEVADA

Open-File Report 82-536
1982

M. J. Baldwin and C. E. Jahren

Prepared by the U.S. Geological Survey

for the

Nevada Operations Office
U.S. Department of Energy
(Interagency Agreement DE-AI08-78ET44802)

Open-File Report 82-536

UNITED STATES
DEPARTMENT OF THE INTERIOR
GEOLOGICAL SURVEY

MAGNETIC PROPERTIES OF DRILL CORE AND SURFACE SAMPLES FROM THE CALICO HILLS AREA, NYE COUNTY, NEVADA

By

Margaret J. Baldwin[1] and Charles E. Jahren[2]

---

[1]Fenix & Scisson, Inc., Mercury, Nev.

[2]U.S. Geological Survey

CONTENTS

ILLUSTRATIONS

TABLES

MAGNETIC PROPERTIES OF DRILL CORE AND SURFACE SAMPLES FROM THE CALICO HILLS AREA, NYE COUNTY, NEVADA

By

Margaret J. Baldwin and Charles E. Jahren

ABSTRACT

The interpretation of the aeromagnetic survey of the Calico Hills area of the Nevada Test Site, Nye County, Nevada, required the determination of magnetic properties of rocks exposed in the region. Eighty-two samples representing a variety of units found at the surface show that most rocks in the Calico Hills, other than parts of the Eleana Formation, are relatively nonmagnetic. The magnetic vector of the Eleana Formation at the surface was found to point northward and downward. Remanence directions were scattered, but a remanence azimuth of 16° east of north was assigned on the basis of present-day declination. Measurements of 123 samples of the Eleana Formation from the exploratory drill hole UE25a-3 indicate that some facies are strongly magnetic. The average total magnetization of the argillite samples is 3.89 A/m (0.00389 emu). These samples have an average natural remanent inclination of 76°. Results of demagnetization demonstrated that this relatively high inclination is due, at least in part, to a soft vertical component of remanent magnetization. The magnitude of the component could not be determined. Further tests showed that the tendency to pick up a soft component of magnetism may be a function of rock type. Inhomogeneity of the Eleana argillite was probably the cause of some differences in remanence values between large and small samples from the same depth.

INTRODUCTION

The Calico Hills area, Nevada, has been the site of geologic and geophysical investigations in support of the U.S. Department of Energy NNWSI (Nevada Nuclear Waste Storage Investigations) program (Maldonado and others, 1979; Daniels and Scott, 1980; Snyder and Oliver, 1981). Magnetic-properties data were collected to aid in the interpretation of aeromagnetic and ground magnetic traverses of the region. In particular, laboratory determination of the total magnetization of rocks from the Calico Hills is vital for interpreting magnetic surveys and correlating magnetic anomalies with specific geologic features.

System of Magnetic Units

In this paper we use the mks or International System (SI) of units. The following table will help readers familiar with the cgs system to understand our use of the International System. See Sheriff (1973) for a more detailed list of terms.

Term	SI (mks) units	Symbol	cgs equivalent	Symbol	
Magnetization or magnetic intensity (magnetic dipole moment per unit volume)	ampere/meter	A/m	10^{-3} emu	emu	
	nanotesla	nT	gamma	gamma	
Magnetic field strength (tesla)		T	(10^9 gamma) (10^4 gauss)		
Magnetic susceptibility (dimensionless)		K_{SI}	K_{SI}	$4\pi k$	k

The gauss, originally a cgs unit, is often used informally in the SI for 10^{-4} tesla.

Acknowledgments

We would like to thank G. D. Bath, USGS (U.S. Geological Survey), for providing information about aeromagnetic anomalies and for his valuable discussions on the content of this report. We gratefully acknowledge the expert advice of J. G. Rosenbaum, USGS, on rock magnetism. Ray Martinson, USGS, drilled small cores of the Eleana Formation in the field and measured their magnetic properties. D. R. Townsend, F&S (Fenix & Scisson, Inc.), gave helpful advice and support, and lent his drafting expertise to many figures in the report. D. Watson and R. Reynolds of the USGS Rock Magnetism Laboratory gave freely of their advice and allowed unlimited use of their facilities. F. Maldonado, USGS, read this report critically and made many helpful suggestions.

AREAL GEOLOGY

The Calico Hills area of the NTS (Nevada Test Site) is geologically complex (McKay and Williams, 1964; Orkild and O'Connor, 1970) (figs. 1, 2). Field data indicate that there have been episodes of regional thrust faulting and doming. The Calico Hills comprise Paleozoic carbonate and clastic rocks, surrounded by Tertiary volcanic rocks (fig. 3). Parts of several Paleozoic units have been thrust over younger volcanic rocks.

The Eleana Formation is a widespread, thick sequence of Devonian-Mississippian marine sediments. It is thought to have been laid down as a flysch deposit, in response to the Antler Orogeny (Poole, 1974). Parts of Units J and I, an argillite and a carbonate, respectively, are present at the Calico Hills. At other localities, Unit J is at least 1,067 m (3,500 ft) thick, and Unit I, at least 152 m (500 ft) thick (Poole and others, 1961).

High-angle faulting and extensive hydrothermal activity in the region may be related to doming and an inferred intrusive body (Maldonado and others, 1979). Much of the Eleana Formation in the Calico Hills area has been hydrothermally altered from the shale and limestone composing this formation elsewhere. In drill hole UE25a-3, the argillite shows a mottled hornfelslike texture, and the carbonate has been altered to marble.

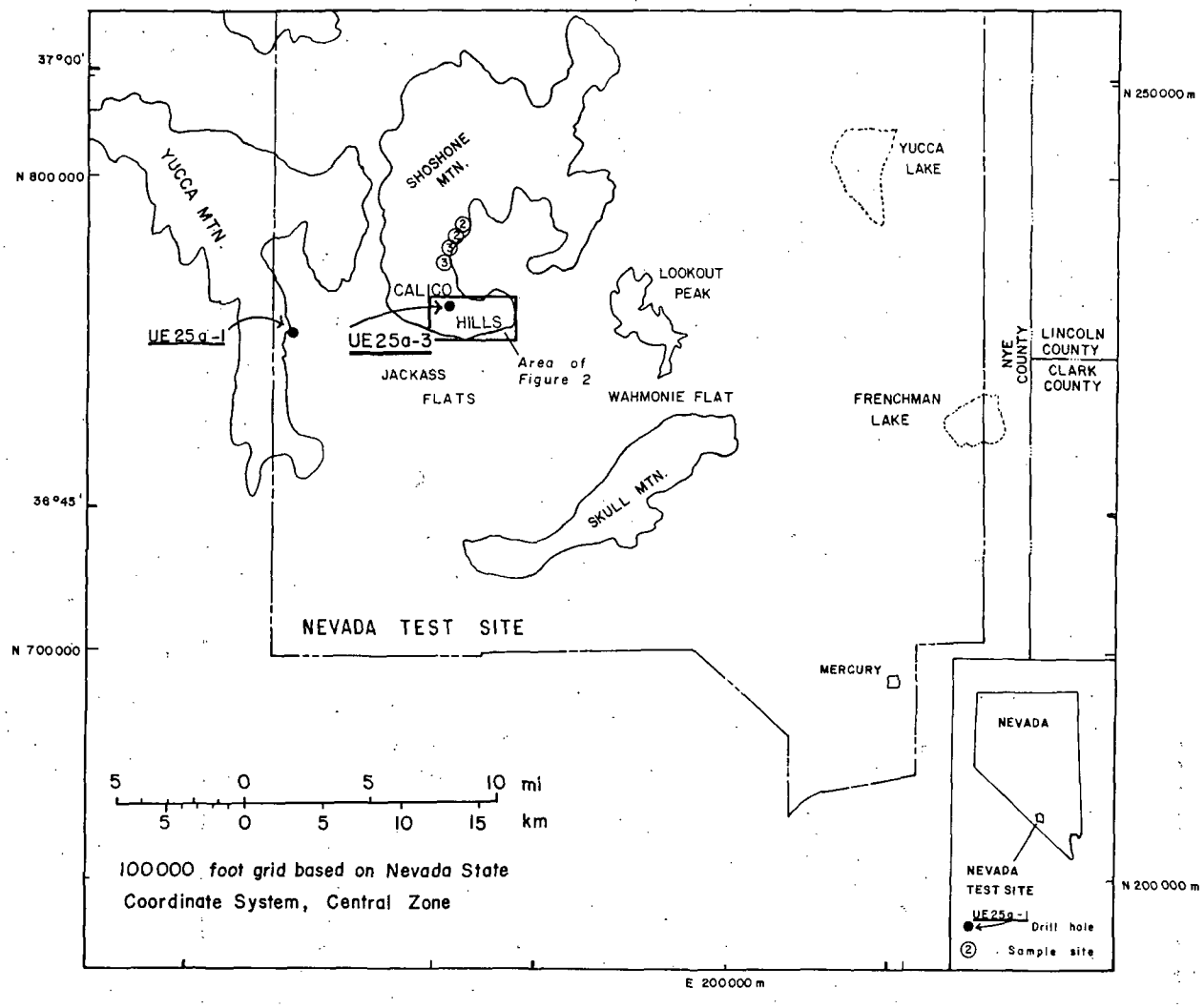

Figure 1.--Reference map showing the Calico Hills area and surface sample sites.

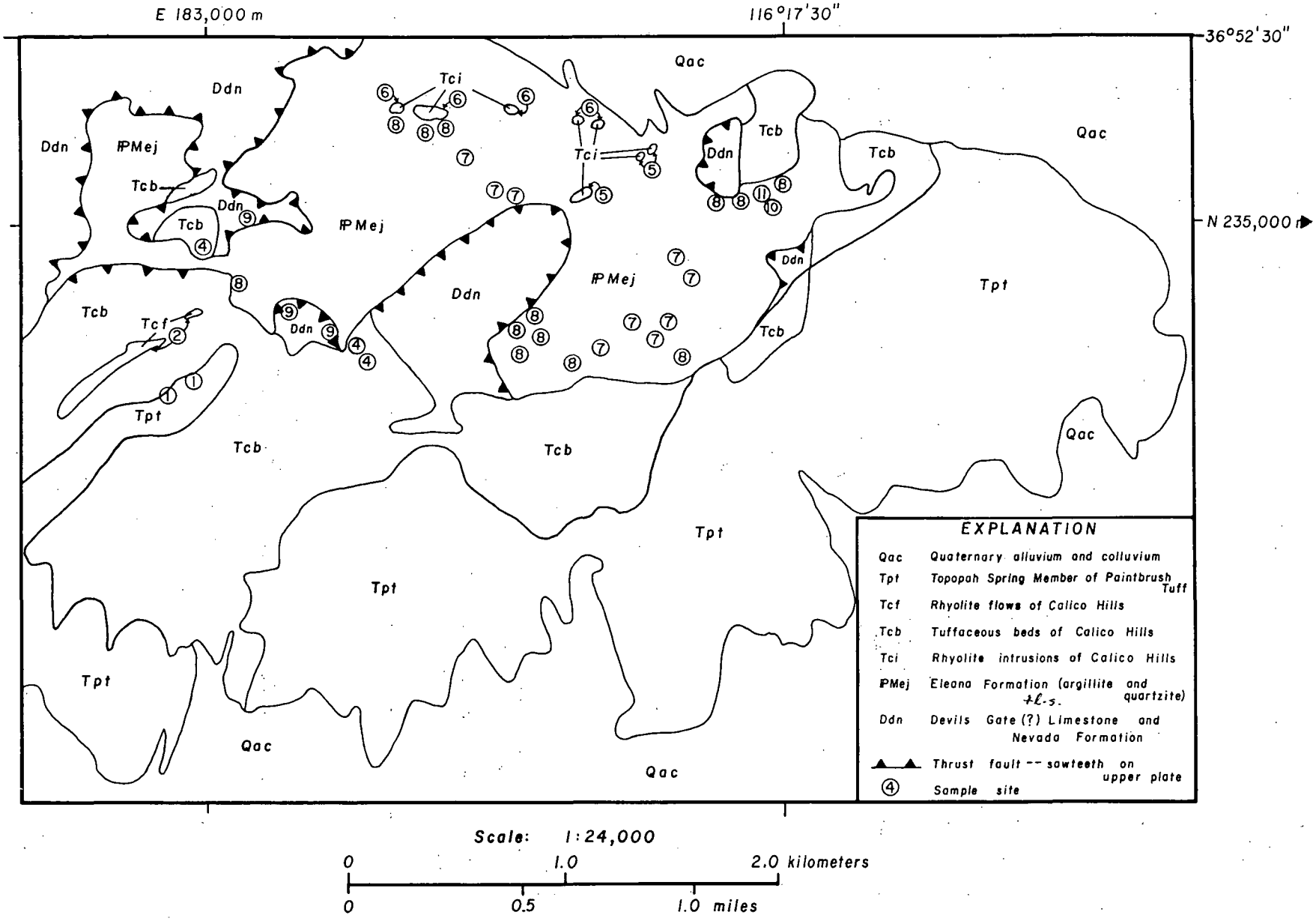

Figure 2.--Generalized geologic map of southern Calico Hills showing surface sample sites.

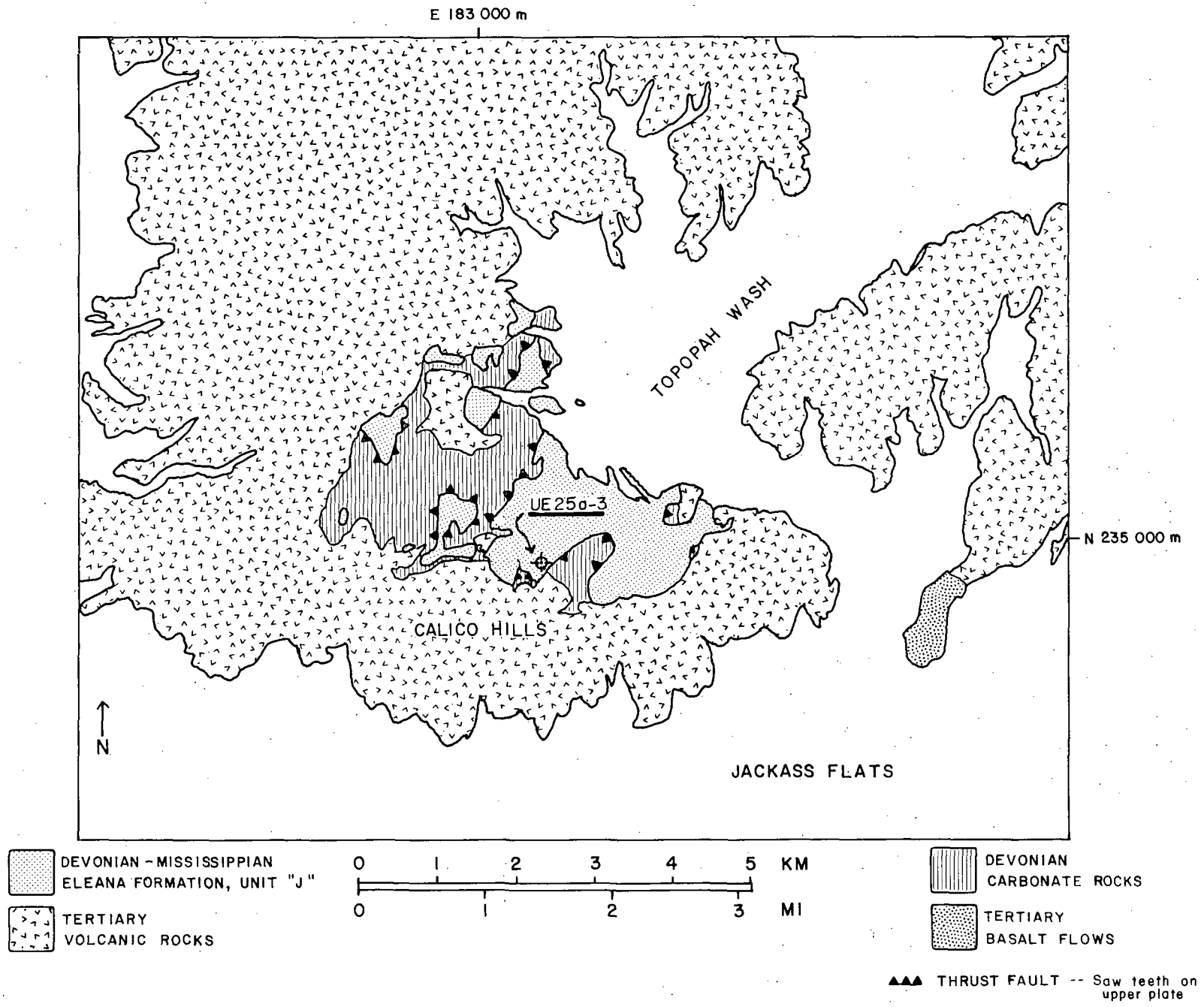

Figure 3.--Generalized geologic map of bedrock outcrop in the Calico Hills area.

An intrusive crystalline body has been hypothesized from aeromagnetic data as shown on figure 4 (G. D. Bath, oral commun., 1978; U.S. Geological Survey, 1979). Figure 4 shows the strong positive anomalies that reach a maximum of 2,343 nT over the Eleana Formation. Measurements were at about 120 m (400 ft) above ground surface along east-west flight lines about 400 m (1,312 ft) apart. Values were corrected for the International Geomagnetic Reference Field plus a 300 nT regional correction. Exploratory hole UE25a-3 was drilled in an effort to determine the depth to this body, but at 771.2 m (2,530.1 ft), the TD (total depth) of the drill hole, no crystalline rocks had been penetrated. Alteration of the rocks did, however, increase with depth (Maldonado and others, 1979).

MAGNETIC SURVEY

A magnetic survey detects geologic features that have magnetic properties causing a disturbance, or an anomaly, in the Earth's magnetic field. The anomaly arises when a feature has an intensity of total magnetization that differs by at least 0.05 A/m from intensities of adjacent features (G. D. Bath and others, written commun., 1981). Features with total magnetizations less than 0.05 A/m are designated nonmagnetic. Those features having greater intensities are designated as either weakly, moderately, or strongly magnetized, as defined by the following limits:

nonmagnetic <0.05 A/m
0.05 A/m < weakly magnetized <0.50 A/m
0.50 A/m < moderately magnetized <1.50 A/m
1.50 A/m < strongly magnetized

Total magnetization of a sample is the vector sum of its remanent and induced components. Remanent magnetism can be measured with a variety of instruments. Induced magnetization is determined from measurements of susceptibility.

Various problems may arise in assigning a magnetization to a particular rock unit. Inhomogeneity of the rocks may make it difficult to obtain values that are representative of a given unit, as is the case with the Eleana Formation. The magnetic properties of surface samples may be altered as a result of lightning strikes or weathering. Rocks collected underground, from tunnels or drill holes, should be free of these problems. However, sampling or laboratory techniques such as drilling may sometimes disrupt in situ magnetic properties.

SURFACE SAMPLES

Rocks exposed at the surface within the Calico Hills aeromagnetic anomaly were sampled to determine their magnetic properties. The formations sampled include the Devils Gate(?) Limestone and Nevada Formation, the Eleana Formation, rhyolite lava flows and tuffaceous beds of the Calico Hills, the Topopah Spring Member of the Paintbrush Tuff, and various small rhyolite intrusions. Oriented, roughhewn samples of each unit were collected in 1978-79 (figs. 1, 2). Analysis of these samples and core from UE25a-3 showed the Eleana Formation to have some magnetized facies. Small oriented cores of Eleana rocks were drilled in 1979 to investigate this phenomenon further.

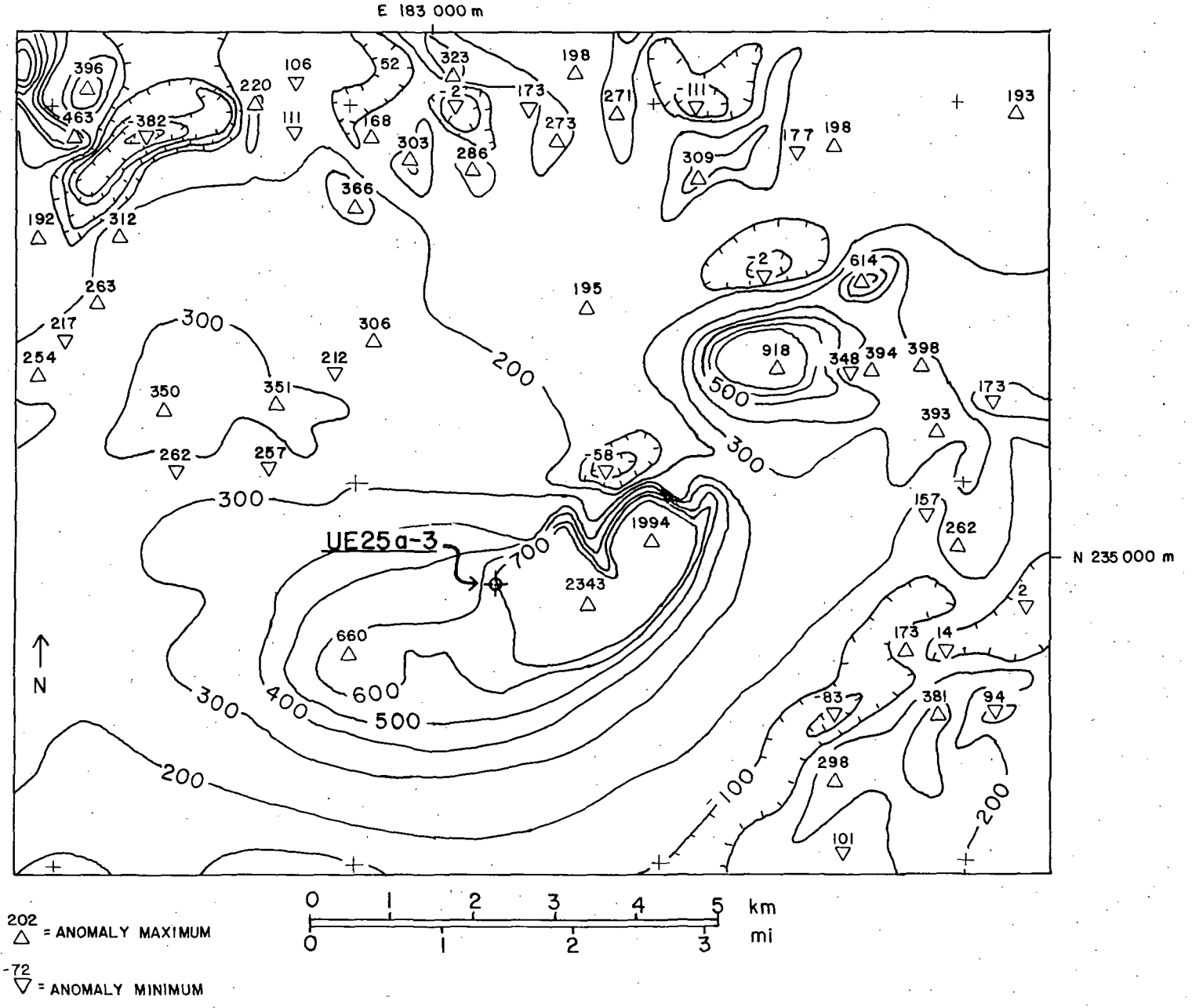

Figure 4.--Residual aeromagnetic map of the Calico Hills area.

Table 1 gives a summary of the magnetic properties of the roughhewn surface samples measured using the method of Jahren and Bath (1967). Limestones, quartzites, and some of the volcanic rocks showed no measureable magnetism. Other volcanic units were moderately magnetic, while the argillite of the Eleana Formation was strongly magnetic. The remanent magnetic vector was normal (pointing northward and downward) for all measureable samples.

A summary of the magnetic properties of field-drilled oriented cores of surface rocks is presented in table 2. All samples are from the argillite of the Eleana Formation, and all but three show moderate to strong magnetization in a normal direction. After measurement of remanent magnetization on a Schonstedt spinner magnetometer, model SSM-1A, five of these samples were subjected to alternating field demagnetization, using a Schonstedt model DSM-1. Remanences were then remeasured. Values after demagnetization are shown in table 2 in parentheses.

The results of these studies indicate that certain facies of the Eleana Formation at this locality are moderately to strongly magnetic, while most of the other units are nonmagnetic. Although remanent directions determined for samples of the Eleana are scattered, they are mostly northward. For purposes of anomaly calculations, the remanences can therefore be considered parallel to the present-day magnetic field, 16° east of north.

DRILL HOLE UE25a-3

Vertical drill hole UE25a-3 was drilled in September 1978 (fig. 1). Core taken was 63 mm (2.48 in.) in diameter to a depth of 598.5 m (1,963.5 ft), where core size was changed because of operational problems to 47 mm (1.85 in.) to a TD of 771.2 m (2,530.2 ft). A suite of logs was run in the drill hole by Birdwell, Inc., and the USGS, which included a magnetic-susceptibility log (Daniels and Scott, 1980).

Several subunits of the Eleana Formation were penetrated in the drill hole. These included argillite of Unit J, altered argillite of Unit J, an altered sequence of thin intercalated marble beds and calcareous argillite of Unit J, and marble of Unit I (Maldonado and others, 1979). No intrusive rocks were penetrated by the drill hole. See figure 5 for the stratigraphy and generalized lithology of UE25a-3.

Magnetic Properties of Core

The magnetic susceptibility log for UE25a-3 (Daniels and Scott, 1980) presented on figure 5 shows two main zones of high-susceptibility rocks, from approximately 290 to 405 m (951-1,329 ft), and from 430 to 680 m (1,411-2,231 ft). We chose samples of core from within these magnetic intervals and from the lower nonmagnetic interval of core. Samples were taken approximately every 3 m (10 ft) in the intervals 278.0 to 406 m (915-1,332 ft) and 438.9 to 771.2 m (1,440-2,530.2 ft TD), and were cut to lengths of nine-tenths the core diameter. The downhole direction was marked on each sample. After measurement, 20 of these samples were re-cored, with a new axis parallel to the original hole axis, to a diameter of 2.5 cm (1 in.), and cut to a length of 2.5 cm.

Table 1.--Magnetic properties of oriented roughhewn surface samples from the Calico Hills area

[Properties measured at the NTS; see figs. 1 and 2 for maps showing sample locations; J_T=total magnetic intensity (averaged vectorially), in amperes/meter; direction of J_T, "normal" direction indicates that vector representing magnetic intensity points northward and downward; leaders (---) indicate direction of magnetization cannot be determined for weakly magnetic samples]

Map reference number	Rock unit	Rock type	Map symbol[1]	J_T (A/m)	Direction of J_T	Number of samples
1	Topopah Spring Member of Paintbrush Tuff	Welded tuff	Tpt	<0.05	---	2
2	Calico Hills	Rhyolite lava flows	Tcf	1.1	Normal	11
3	Do.	Tuffaceous beds	Tct	1.9	Normal	4
4	Do.	Tuffaceous beds	Tcb	< .05	---	3
5	Do.	Rhyolite intrusions	Tci	2.6	Normal	3
6	Do.	Rhyolite intrusions	Tci	< .05	---	7
7	Eleana Formation	Argillite	Mej	4.6	Normal	29
8	Do.	Quartzite	Mej	< .05	---	10
9	Devils Gate(?)	Limestone	Ddn	< .05	---	4

[1]McKay and Williams, 1964; Orkild and O'Connor, 1970.

Table 2.--Magnetic-properties data from Eleana Formation argillite surface samples drilled in the field

[J_I, intensity of induced magnetization, which equals 0.53 X ($k_{SI}/4\pi$)X 10^3 where k_{SI} is susceptibility; J_R, intensity of natural remanent magnetization; A_R, azimuth of natural remanent magnetization; IR, inclination of natural remanent magnetization; J_T, intensity of total magnetization; AZT, total magnetic azimuth; I_T, total magnetic inclination. Values in parentheses were measured after alternating-field demagnetization at a peak of 200 gauss]

Samples[1]	J_I (A/m)	J_R (A/m)	A_R (degrees)	I_R (degrees)	J_T (A/m)	AZT (degrees)	I_T (degrees)
2a	0.66	0.82	23 (30)	59 (54)	1.48	20	61
2b	.51	.28	3 (44)	70 (59)	.79	12	66
2c	.30	.21	15	47	.51	15	56
6a	.04	.37	313 (320)	59 (45)	.40	318	60
6b	.04	2.84	324 (334)	39 (30)	1.87	325	39
6d	.80	1.31	20	53	2.14	18	57
6e	.10	.11	28	44	.20	24	53
6f	.02	.02	11	-12	.03	13	29
6g	.70	2.95	321 (7)	- 5 (15)	3.16	326	7

[1]Map reference numbers (see fig. 2)--samples 2a-c denoted on map by 10; samples 6a-g denoted on map by 11.

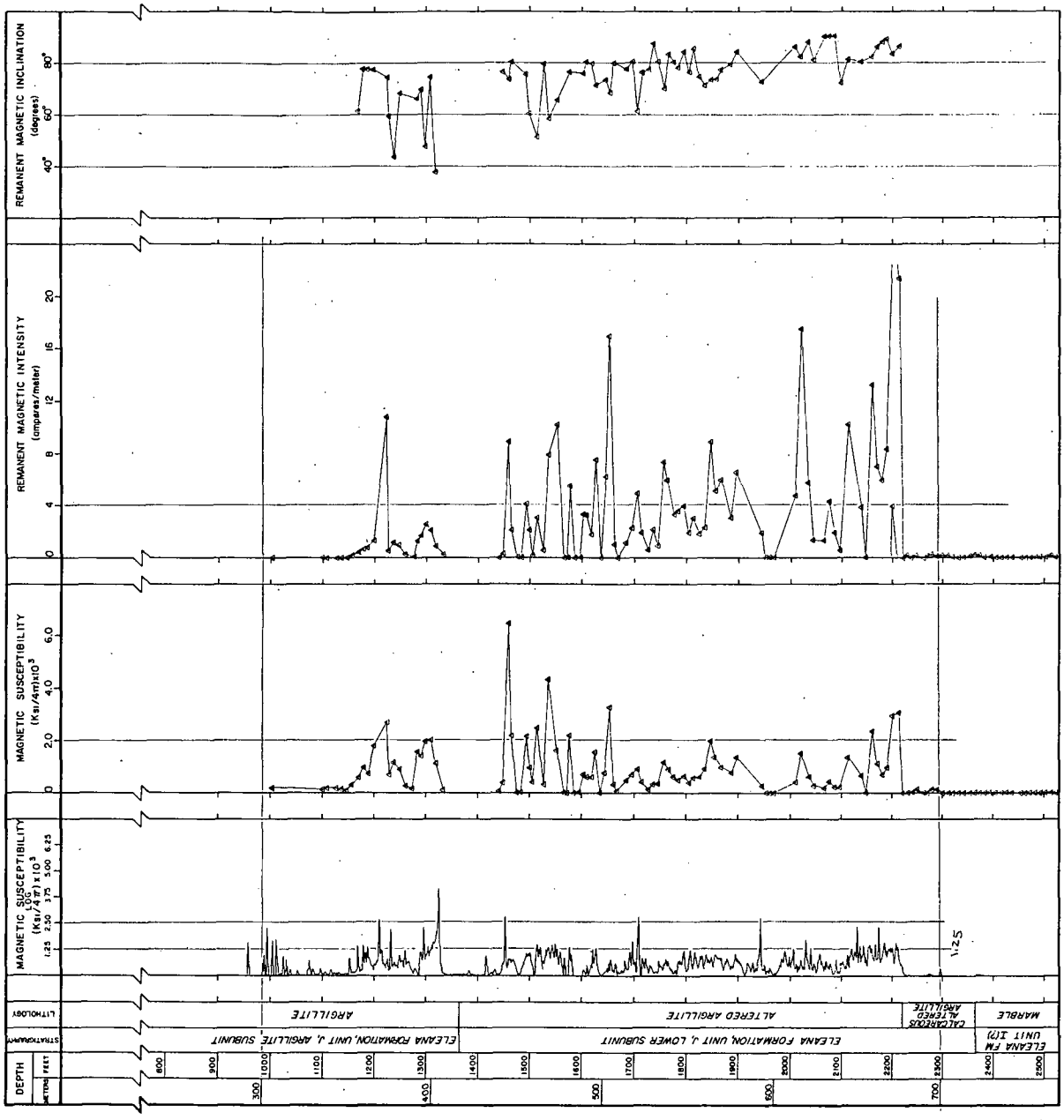

Figure 5.--Magnetic properties of rock from drill hole UE25a-3, before demagnetization, showing lithology, in-hole susceptibility log, sample susceptibility, natural magnetic remanent intensity, and remanent inclination.

Measurements of susceptibility and remanent magnetization were made using the method of Jahren and Bath (1967). The smaller size core samples were taken to Denver for demagnetization and measurement with the spinner magnetometer. The remanent magnetization of each sample was remeasured on the spinner magnetometer, and then 10 samples were progressively demagnetized in an alternating field at peak fields of 50, 100, 150, and 200 gauss. Four samples were demagnetized in 25-gauss steps, and six others were demagnetized in 100-gauss intervals. Data for both large and small core samples are given in tables 3 and 4.

Large Core Samples

Susceptibility values for large core samples are quite variable within magnetized zones penetrated by the drill hole. This is probably due to the stratified nature of the rock and the large number of filled fractures. Layers of argillite alternate with thin quartz-rich, carbonate-rich, or magnetite(?)-rich layers. Fractures and veinlets may be filled with calcite, chlorite, pyrite, or magnetite(?).

Remanent magnetic intensity varies from sample to sample, also reflecting the layered aspect of the argillite. Values as high as 26.6 A/m and as low as 0.0001 A/m were measured in "magnetic" facies of core. The remanent inclination of the core samples is normal in every case. The inclinations, however, are quite high in most cases, averaging 74° for the argillite units and 81° for the carbonate unit.

The arithmetic average of the total intensities of 93 large samples from the depth intervals 278.9 to 406 m (915-1,332 ft) and 438.9 to 677.3 m (1,440-2,222 ft) is 3.89 A/m. The average for 30 samples from the interval 677.3 to 771.2 m (2,222-2,530.1 ft) is 0.0587 A/m.

Small Core Samples

The results of demagnetization on 20 small cores drilled from UE25a-3 core are presented on figure 6 and in table 3. Stereo plots of the remanence vectors of four samples are presented on figure 7, and show the original direction and direction after demagnetization at 50, 100, 150, and 200 gauss. Because these samples are from unoriented core, azimuths shown are arbitrary. "Up" was known on the core, however, so the inclinations shown are real. Plots for 1440 and 1886 (lower diagram on fig. 7) show no directional change. The plots for 2009 and 2160 indicate a high-angle soft component of remanent magnetization removed by the demagnetization process. All samples are normally magnetized. Demagnetization removed a steep component from 13 samples, so that their average remanent inclinations were reduced from 74.6°±8.6° to 54.8°±7.4° (fig. 5).

Seven large-core samples whose remanent inclination angles were high seemed to lose the component responsible for the high inclination sometime before remeasurement on the spinner magnetometer (see sample nos. 1489, 1626, 1660, 1694, 1795, 1886, and 2064 in table 4. Two other samples showed an increase in remanent inclination (samples 2096 and 2160).

Table 3.--Magnetic properties of drill core samples from UE25a-3, measured at the Nevada Test Site on large-sample magnetometer

[k, susceptibility; J_I, intensity of induced magnetization; J_R, intensity of remanent magnetization; I_R, inclination of remanent magnetization; J_T, intensity of total magnetization (calculated with assumed remanent azimuth direction of N. 16° E.); I_T, inclination of total magnetization; nc, indicates that magnetic intensity of sample was too low to be able to calculate inclination angles. All magnetizations given in amperes/meter]

Sample depth (feet)	k $(K_{SI}/4\pi)10^3$	J_I (A/m)	J_R (A/m)	I_R (degrees)	J_T (A/m)	I_T (degrees)
915	0.00	0.00	0.00	nc	0.00	nc
1001	.12	.06	.00	nc	.07	nc
1099	.08	.04	.00	nc	.04	nc
1107	.10	.05	.00	nc	.05	nc
1127	.11	.06	.00	nc	.06	nc
1136	.10	.05	.00	nc	.06	nc
1146	.08	.04	.00	nc	.05	nc
1156	.25	.13	.21	90	.34	79
1169	.52	.28	.41	61	.69	62
1178	.98	.52	.67	77	1.19	71
1186	.67	.36	.70	77	1.05	72
1198	1.75	.93	1.33	77	2.27	71
1222	2.68	1.42	10.76	74	12.20	73
1227	.67	.36	.48	59	.84	61
1237	1.14	.60	1.13	43	1.73	50
1248	.85	.45	.82	68	1.28	66
1260	.24	.13	.26	90	.38	81
1272	.09	.05	.10	45	.15	51
1282	1.53	.81	1.29	66	2.12	65
1290	1.35	.72	1.67	69	2.40	67
1298	1.93	1.02	2.55	47	3.57	52
1309	2.00	1.06	2.11	74	3.19	70
1318	1.08	.57	.85	37	1.40	48
1332	.09	.05	.28	90	.32	86
1440	.00	.00	.00	nc	.00	nc
1448	.32	.17	.36	76	.53	72
1459	6.47	3.43	8.90	73	12.37	70
1462	2.16	1.14	2.06	80	3.20	74
1476	.00	.00	.00	nc	.00	nc

Table 3.--Magnetic properties of drill core samples from UE25a-3, measured at the Nevada Test Site on large-sample magnetometer--Continued

Sample depth (feet)	k $(K_{SI}/4\pi)10^3$	J_I (A/m)	J_R (A/m)	I_R (degrees)	J_T (A/m)	I_T (degrees)
1481	.00	.00	.00	nc	.00	nc
1492	2.18	1.16	4.09	75	5.26	72
1498	.95	.50	2.15	60	2.67	61
1504	.35	.19	.16	90	.34	76
1513	2.44	1.29	3.05	51	4.36	55
1527	.27	.14	.53	79	.68	75
1537	4.34	2.30	7.96	58	10.31	59
1552	1.60	.85	10.31	65	11.18	65
1567	.00	.00	.00	nc	.00	nc
1571	.00	.00	.00	nc	.00	nc
1577	2.15	1.14	5.34	76	6.48	74
1586	.00	.00	.00	nc	.00	nc
1594	.00	.00	.00	nc	.00	nc
1602	.67	.36	3.30	75	3.66	74
1609	.56	.30	3.10	80	3.39	78
1618	.57	.30	1.75	79	2.05	76
1626	1.59	.84	7.55	71	8.41	70
1634	.00	.00	.00	nc	.00	nc
1644	.71	.38	6.23	73	6.61	72
1651	3.31	1.75	16.96	68	18.76	67
1660	.28	.15	1.01	80	1.15	78
1667	.00	.00	.00	nc	.00	nc
1684	.43	.23	1.18	77	1.41	75
1694	.64	.34	2.28	80	2.62	78
1704	.87	.46	4.83	61	5.30	62
1713	.39	.21	1.85	76	2.05	75
1727	.11	.06	.56	77	.62	75
1736	.29	.15	2.02	87	2.17	85
1745	.30	.16	.93	80	1.09	77
1756	1.15	.61	7.36	70	7.98	69
1764	.81	.43	5.91	83	6.32	82
1774	.55	.29	3.34	80	3.63	78
1784	.45	.24	3.60	78	3.83	77
1795	.62	.33	4.00	84	4.32	82
1804	.35	.19	1.93	76	2.12	74
1812	.57	.30	3.05	85	3.34	83
1824	.57	.30	1.84	74	2.15	73
1834	.87	.46	2.32	71	2.78	69
1846	2.00	1.06	8.88	73	9.96	72
1856	1.35	.72	5.18	73	5.90	72
1868	.97	.51	5.98	77	6.50	76

Table 3.--Magnetic properties of drill core samples from UE25a-3, measured at the Nevada Test Site on large-sample magnetometer--Continued

Sample depth (feet)	k $(K_{SI}/4\pi)10^3$	J_I (A/m)	J_R (A/m)	I_R (degrees)	J_T (A/m)	I_T (degrees)
1886	.79	.42	3.01	79	3.42	77
1896	1.36	.72	6.55	84	7.25	82
1943	.27	.14	1.87	72	2.02	72
1951	.00	.00	.00	nc	.00	nc
1958	.00	.00	.00	nc	.00	nc
1967	.00	.00	.00	nc	.00	nc
2009	.40	.21	4.70	86	4.90	85
2020	1.52	.81	17.58	82	18.37	81
2033	.60	.32	5.64	88	5.94	86
2044	.26	.14	1.29	81	1.43	79
2064	.19	.10	1.26	90	1.36	88
2074	.40	.21	4.37	90	4.56	89
2085	.20	.11	1.99	90	2.09	89
2096	.19	.10	.50	72	.60	70
2112	1.35	.72	10.25	81	10.95	80
2139	.61	.32	3.87	80	4.19	79
2149	.00	.00	.00	nc	.00	nc
2160	2.35	1.25	13.23	82	14.45	80
2170	1.07	.57	7.00	86	7.54	84
2180	.64	.34	5.94	88	6.26	86
2188	.93	.49	8.34	89	8.80	87
2200	2.97	1.57	26.55	83	28.08	82
2212	3.08	1.63	21.47	86	23.02	85
2221	.00	.00	.00	nc	.00	nc
2229	.00	.00	.16	nc	.16	nc
2239	.00	.00	.00	nc	.00	nc
2248	.09	.05	.15	nc	.18	nc
2261	.00	.00	.00	nc	.00	nc
2268	.00	.00	.16	nc	.16	nc
2279	.10	.05	.23	nc	.28	48
2289	.10	.05	.16	nc	.19	14
2299	.00	.00	.17	nc	.17	nc
2310	.00	.00	.17	nc	.17	nc
2320	.00	.00	.00	nc	.00	nc
2331	.00	.00	.00	nc	.00	nc
2342	.00	.00	.00	nc	.00	nc
2353	.00	.00	.17	nc	.17	nc
2363	.00	.00	.17	nc	.17	nc
2372	.00	.00	.16	nc	.16	nc
2384	.00	.00	.00	nc	.00	nc
2393	.00	.00	.00	nc	.00	nc
2405	.00	.00	.00	nc	.00	nc

Table 3.--Magnetic properties of drill core samples from UE25a-3, measured at the Nevada Test Site on large-sample magnetometer--Continued

Sample depth (feet)	k $(K_{SI}/4\pi)10^3$	J_I (A/m)	J_R (A/m)	I_R (degrees)	J_T (A/m)	I_T (degrees)
2416	.00	.00	.00	nc	.00	nc
2425	.00	.00	.00	nc	.00	nc
2435	.00	.00	.00	nc	.00	nc
2455	.00	.00	.00	nc	.00	nc
2462	.00	.00	.00	nc	.00	nc
2472	.00	.00	.00	nc	.00	nc
2482	.00	.00	.00	nc	.00	nc
2492	.00	.00	.00	nc	.00	nc
2502	.00	.00	.00	nc	.00	nc
2513	.00	.00	.16	nc	.16	nc
2522	.00	.00	.00	nc	.00	nc

Table 4.--Demagnetization data (with comparisons of large and small samples) including remanent intensities, remanent azimuths, and remanent inclinations

[Susceptibilities (K_{SI}); remanent intensities (J_R), in Ampers/meter; remanent azimuths (A_R); and remanent inclinations (I_R). Samples were measured at the Nevada Test Site (large) and with a spinner magnetometer (small) in Denver. * indicates values of samples with high remanent inclination; nc, indicates samples for which values of measurements on large samples were too low to calculate inclination.

Sample	Susceptibility $(K_{SI}/4\pi)X10^3$		J_R (A/m)		A_R (degrees)	I_R (degrees)		Peak demagnetizing
	Large	Small	Large	Small		Large	Small	field (gauss)
1440	0	0	0.00	0.0133	327	nc	56	---
				.0131	325		58	25
				.0127	325		57	50
				.0121	323		57	75
				.0114	324		58	100
				.0093	329		54	150
				.0077	329		54	200
1498	.95	.97	2.15	1.74	352	60	31	---
				1.58	350		31	50
				1.08	349		30	100
				.659	351		31	150
				.404	351		32	200
1626	1.59	2.91	7.55	4.32	246	71	53	---
				1.92	249		42	100
				.567	248		40	200
				.202	248		39	300
1660	.28	.50	1.01	.564	35	80*	55	---
				.379	31		56	50
				.219	31		54	100
				.133	34		57	150
				.0823	32		54	200
1694	.64	.57	2.28	.835	88	80*	64	---
				.619	97		59	50
				.359	100		56	100
				.219	105		56	150
				.137	110		56	200
1736	.29	.11	2.02	1.82	9	87*	80	---
				.364	292		86	100
				.111	225		67	200
				.0424	223		62	300

Table 4.--Demagnetization data (with comparisons of large and small samples) including remanent intensities, remanent azimuths, and remanent inclinations--Continued

Sample	Susceptibility $(K_{SI}/4\pi)X10^3$		J_R (A/m)		A_R (degrees)	I_R (degrees)		Peak demagnetizing field (gauss)
	Large	Small	Large	Small		Large	Small	
1795	.62	.48	4.00	1.11	357	84*	65	---
				.962	333		68	25
				.670	318		65	50
				.455	312		61	75
				.304	310		59	100
				.164	308		58	150
				.0946	313		54	200
				.0397	313		53	300
1824	.57	.89	1.84	1.87	279	74	71	---
				1.31	265		62	50
				.556	260		61	100
				.280	260		58	150
				.154	260		55	200
1868	.97	1.48	5.98	1.20	217	77*	79	---
				.25	327		72	100
				.0648	330		48	200
				.0278	331		46	300
1886	.79	1.07	3.01	.974	32	79*	61	---
				.662	28		60	50
				.391	27		58	100
				.227	26		57	150
				.139	30		59	200
1967	.00	.05	.00	.0033	325	nc	59	---
				.0031	326		55	50
				.0028	324		55	100
2009	.40	.65	4.70	2.19	54	86*	80	---
				1.62	44		85	25
				.609	24		81	50
				.295	11		77	75
				.186	0		73	100
				.126	355		70	125
				.0915	357		66	150
				.0608	355		63	200
				.0266	351		62	300
2064	.19	.32	1.26	.923	94	90*	82	---
				.231	74		72	50
				.106	72		63	100
				.0596	68		58	150
				.0423	68		56	200
				.0212	68		57	300

Table 4.--Demagnetization data (with comparisons of large and small samples) including remanent intensities, remanent azimuths, and remanent inclinations--Continued

Sample	Susceptibility $(K_{SI}/4\pi)X10^3$		J_R (A/m)		A_R (degrees)	I_R (degrees)		Peak demagnetizing field (gauss)
	Large	Small	Large	Small		Large	Small	
2096	.19	.10	.50	.207	339	72*	79	---
				.106	359		75	50
				.0787	316		63	100
				.0639	316		60	150
				.0519	315		59	200
2160	2.35	X	13.2	5.35	175	82*	83	---
				2.32	98		72	50
				.939	83		58	100
				.556	79		57	150
				.354	78		57	200
2212	3.08	5.29	21.47	10.8	14	86*	80	---
				6.52	354		77	25
				2.93	327		68	50
				1.79	317		60	75
				1.16	318		55	100
				.837	315		53	125
				.625	314		51	150
				.481	313		50	175
				.376	311		47	200
				.245	308		45	250
				.159	308		45	300
2221	0	0	.00	.0097	246	nc	58	---
				.0075	245		57	100
				.0061	247		55	200
2320	0	0	.00	.0315	120	nc*	74	---
				.0229	129		73	50
				.0136	135		64	100
				.0092	135		61	150
				.0062	129		60	200
2455	0	0	.00	.0012	139	nc	72	---
				.0001	199		35	100
2522	0	0	.00	.0005	259	nc	58	---
				.0003	285		54	100

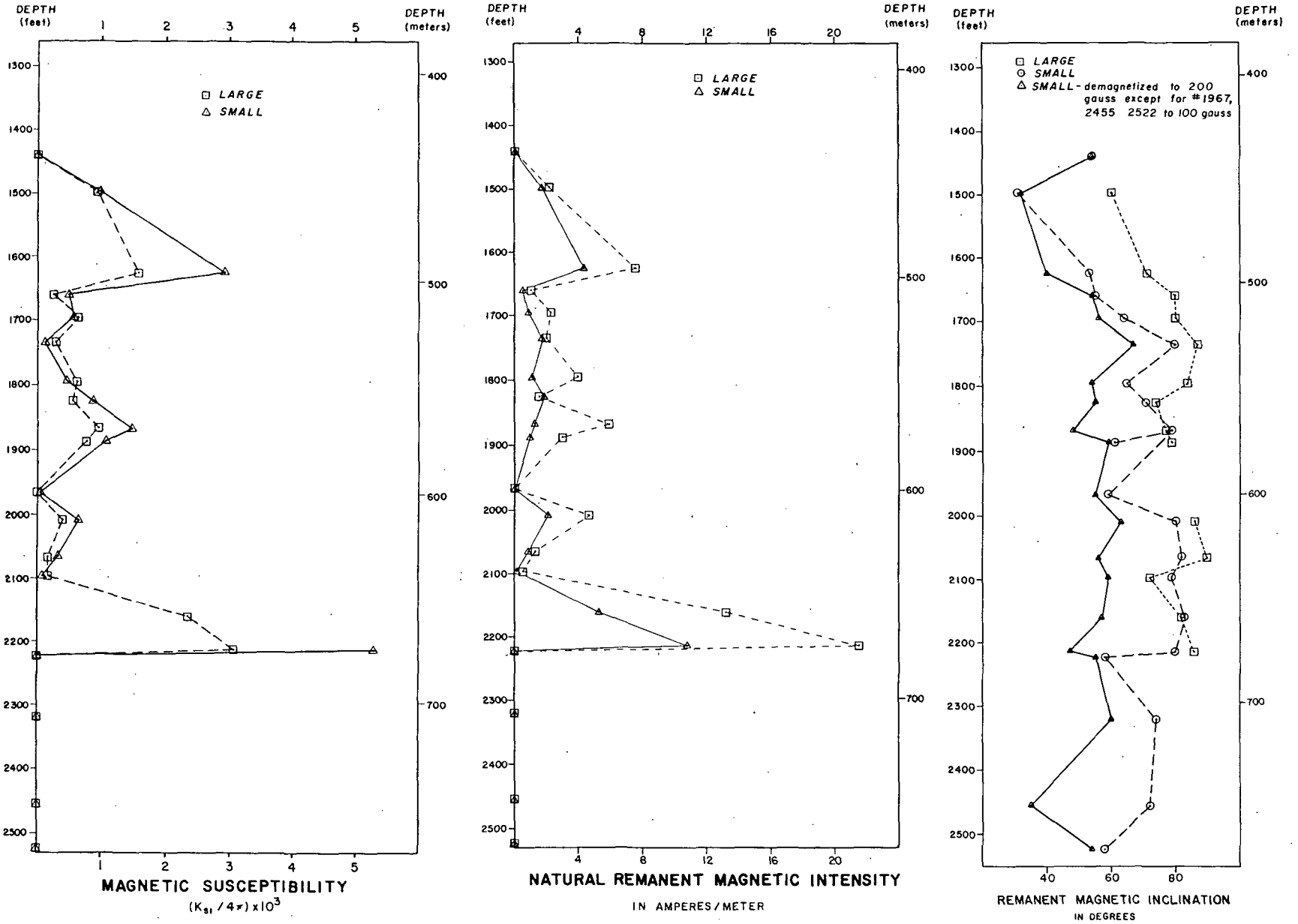

Figure 6.--Magnetic properties of small cores drilled from UE25a-3 core showing results of demagnetization or remanent inclination and comparing values of susceptibility, remanent intensity, and remanent inclination for large and small cores.

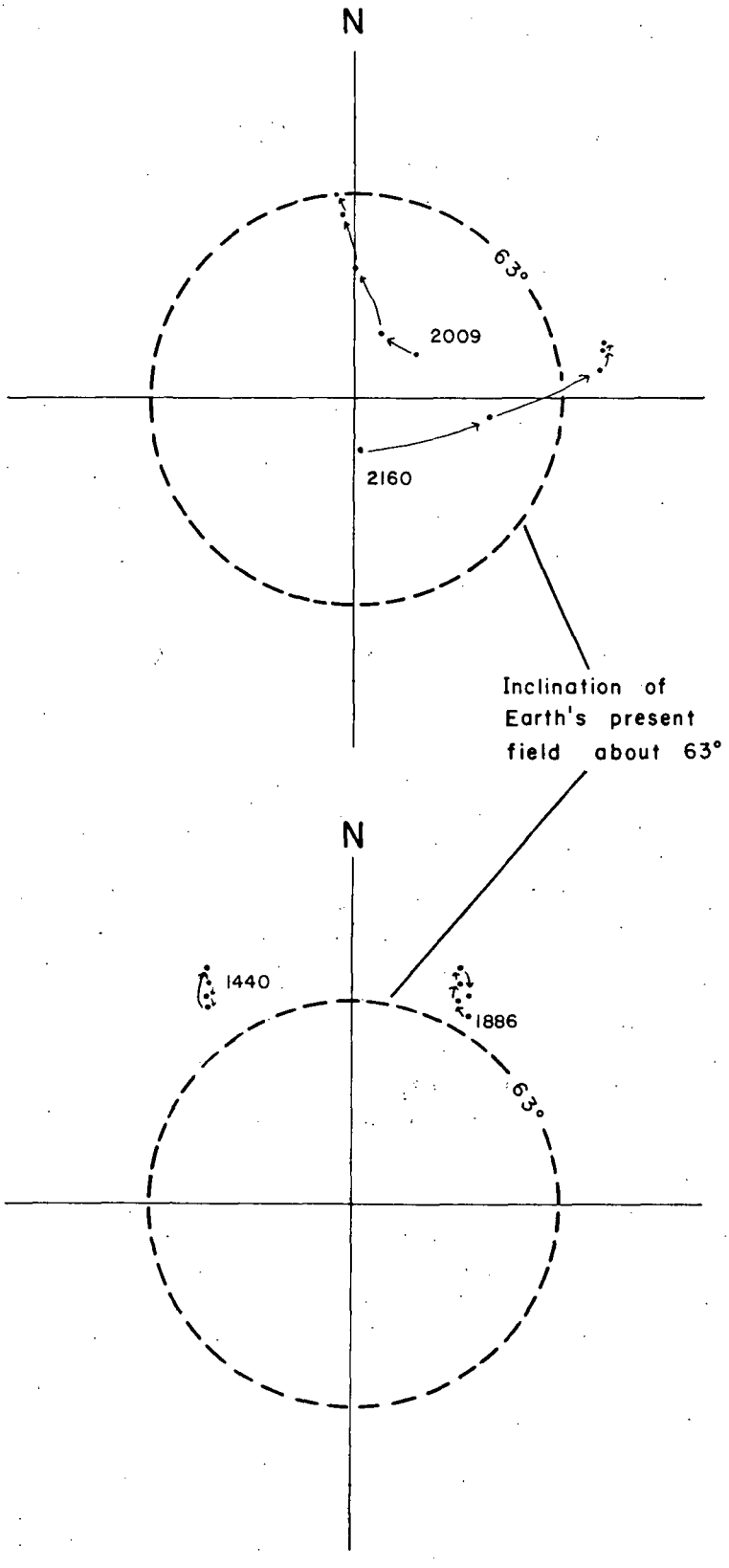

Figure 7.--Stereoplots of remanent magnetic directions before and during progressive alternating-field demagnetization of samples from four depths in drill hole UE25a-3.

Large-sample versus Small-sample Measurements

Work on two sizes of samples from the same depth gave two different values for magnitudes of magnetization, as well as for inclination angle (fig. 6 and table 4. Twenty samples that had previously been measured with the large-sample equipment at the NTS (average remanent intensity 3.55±1.88 A/m), tended to show lower values after recoring and cutting for measurement on the spinner magnetometer (average remanent intensity 1.7±1.30 A/m). There is a greater difference between two measurements of a strongly magnetized sample than for a weakly magnetized sample.

The difference in values between the large core samples and the small samples drilled from them may indicate instrumental or procedural errors, inhomogeneous distribution of magnetic minerals, or unstable magnetization. As a test of the effect of sample homogeneity on magnetic properties, and to assure ourselves that there was not some procedural error in measurements, we chose five core samples of a fairly homogeneous volcanic rock from the nearby vertical drill hole UE25a-1 (fig. 1) and two more argillite samples from drill hole UE25a-3, to compare large and small sample measurements on the same equipment. The magnetization of a small core drilled from a large sample may or may not be representative of the large sample. This problem is particularly acute if the magnetic minerals are concentrated in some manner other than being evenly disseminated through the rock. The differences probably should not always be in the same direction. If most of the magnetic mineral is concentrated (perhaps along fractures), a disproportionate number of small samples will show a relatively low magnetic moment.

We subjected the rocks to as little handling and transport as possible. We measured the remanence of the cores on the NTS large-sample magnetometer by the method described above, using the same methods of cutting and measuring core as we did for the main body of data. We then cut 2.5-cm cores out of the large cores and measured them at the NTS using a small sample-holder with the magnetometer. After these measurements, the samples were sent to Denver and measured on the spinner magnetometer. Table 5 shows that remanence values of the volcanic rock from drill hole UE25a-1 remained about the same between measurements.

The remanent magnetizations of the argillite from drill hole UE25a-3 were quite different in the first two sets of measurements, as they were in the main body of data presented above. However, they did not change further when remeasured in Denver on the spinner magnetometer (table 5). Also, inclination angle was relatively stable in demagnetizing fields up to 400 gauss in peak value. Sample 1651 changed inclination from 69° to 67°, and sample 2074 changed from 84° to 77°.

To check for the presence of unstable magnetism, we measured the susceptibility of each pair of large and small argillite samples. Susceptibility mainly reflects the abundance of magnetic material in a sample, and should not be affected by drilling or transport of samples. Thus, if the difference in remanent magnetizations between large and small samples is due to differences in concentrations of the magnetic mineral, and not due to instability of remanence, this should be reflected in susceptibility measurements. Figure 6 and table 4 give susceptibility and remanence values for large and small samples. It can be seen that differences in

Table 5.--Comparison of magnetic properties of drill core showing differences between large and small sample sizes for different rock types

[All intensities of magnetization are given in amperes/meter; k, susceptibility; J_I, intensity of induced magnetization; J_R, intensity of remanent magnetization; I_R, inclination of remanent magnetization]

Sample depth (feet)	Rock type	k $(K_{SI}/4\pi)10^3$	J_I (A/m)	J_R (A/m)		Denver spinner J_R	I_R (degrees)		Denver spinner I_R (degrees)
				Large	Small	Small (A/m)	Large	Small	Small
UE25a-1 136	tuff	0.59	0.31	1.48	1.35	1.53	-36	-33	-42.9
UE25a-1 153	tuff	.38	.20	2.30	2.13	2.34	-37	-41	-40.4
UE25a-1 166	tuff	.10	.05	1.30	1.29	1.38	-37	-43	-42.3
UE25a-1 183	tuff	.05	.03	.52	.44	([1])	-32	-42	([1])
UE25a-1 1016	tuff	.33	.18	2.29	3.26	3.49	49	47	48.1
UE25a-3 1651	argillite	3.31	1.75	14.27	9.95	10.53	68	69	69.2
UE25a-3 2074	argillite	.40	.21	4.06	1.08	.948	90	90	84.4

[1]Sample too large to fit in holder for Denver spinner.

susceptibility and remanent magnetization between large and small samples do not reflect each other. This indicates that inhomogeneity of the rock, and not unstable remanence is probably responsible for the differences between large and small samples.

The results of the comparison of large and small core samples indicate that there was no calibration problem with our equipment. Though some of the differences may be due to instability of remanent magnetism, inhomogeneity of the Eleana argillite is their probable cause.

A more elaborate study of the effects of sample handling and magnetic stability involved experimental drilling of samples. First, we simulated a sample by casting a 2.5-cm by 2.5-cm cylinder using a mixture of water-putty and powdered magnetite. After demagnetizing this sample, we drew it through a drill bit similar to the ones we had used for sample preparation. We had found by measurement that such bits have an induced magnetization of about 1,350 A/m while they are upright in the Earth's magnetic field. The bit we used had been further magnetized in a coil, however, and retained an additional intensity of 27,000 A/m. This latter magnetization was in the same direction that the bit would be magnetized in the Earth's field during the drilling process. The sample picked up a soft vertical component of magnetization in the same direction that the bit was magnetized. The vertical component of magnetization was increased from 2.6 to 9.9 A/m. It decreased spontaneously to 6.9 A/m while sitting overnight opposite to the Earth's magnetic field, and the additional magnetization was eliminated when the sample was gradually withdrawn from a decreasing 60-Hz alternating magnetic field of 138 gauss.

Our synthetic sample was about two and a half times more susceptible to magnetization than the most susceptible sample listed in table 3. Moreover, the magnetite was concentrated from Minnesota taconite and might behave differently from the magnetic component of the Eleana Formation. For these reasons we designed an experiment to test the effect of drilling Eleana Formation rocks with a magnetized bit. We continued to use the stronger bit magnetization value of 27,000 A/m, in the hope of magnifying any effect.

Next, we selected sample pairs of Eleana Formation argillite from seven different depths in hole UE25a-3. The samples are indicated by depth in table 6. Samples designated A and B in table 6 indicate the pieces of original core sawed off into cylinders with length approximately nine-tenths of their diameter. We obtained only one sample from 1858. The A samples were drilled with an unmagnetized bit and the small 2.5-cm by 2.5-cm cylindrical samples cored from them are designated A (A' for second sample). Samples designated B (B' for second sample) were cored from the B pieces in a similar way, except that a bit magnetized to 27,000 A/m was used. Sample 1858 was cored with the magnetized bit. The drilling was done vertically downward on a press, and the bit was magnetized in that direction. The bit was checked for magnetization after each drilling, and remagnetized to 27,000 A/m. Typically, less than 10 percent of the magnetization was lost during the drilling unless the sample shattered and the bit heated up. The original samples from which the small cores were drilled were then remeasured. The designation D has been used in the table to indicate these pieces.

Table 6 shows the variability from sample to sample that is often encountered in magnetic-properties measurements when replication is

Table 6.--Comparison of samples drilled with unmagnetized and magnetized drills

Sample depth		$k_{SI}/4\pi$ X10^3	J_I (A/m)	J_R (A/m)	I_R (degrees)
1647	A	7.2	3.8	38.1	79
	a	10.6	5.6	27.7	58
	B	10.4	5.5	53.0	82
	b	15.4	8.1	47.5	59
	b'	8.4	4.5	23.6	62
1677	A	8.0	4.3	35.3	82
	a	5.7	3.0	13.1	75
	B	4.2	2.2	15.1	82
	b	2.3	1.2	8.1	82
	b'	3.3	1.7	10.6	84
	BD	4.0	2.1	18.2	83
1766	A	2.4	1.3	13.3	85
	a	1.3	.7	4.8	76
	a'	2.7	1.5	9.7	79
	AD	3.0	1.6	14.0	77
	B	4.8	2.6	27.8	86
	b	3.5	1.8	11.4	68
	b'	.8	.4	2.4	76
	BD	5.0	2.7	34.9	86
1772	A	13.6	7.2	41.9	83
	a	28.9	15.3	62.0	67
	a'	1.8	.9	4.1	62
	AD	13.2	7.0	46.8	86
	B	32.9	17.4	117.3	79
	b	20.8	11.0	37.6	81
	b'	51.7	27.4	132.7	75
	BD	29.4	15.6	128.0	84
1836	A	10.4	5.5	28.2	74
	a	10.4	5.5	15.0	66
	a'	5.5	2.9	8.6	61
	AD	10.9	5.8	33.2	75
	B	10.6	5.6	29.7	72
	b	7.4	3.9	20.2	66
	b'	8.7	4.6	17.0	46
	BD	11.1	5.9	34.6	76
1858		15.2	8.1	50.3	84
	small	16.8	8.9	40.7	78
1867	A	23.3	12.3	112.3	77
	a	9.0	4.8	11.9	71
	AD	22.9	12.2	121.4	79
	B	12.2	6.5	56.7	77
	b	7.4	3.9	29.5	72
	b'	12.1	6.4	33.7	74

attempted. There is no clearly apparent systematic difference between samples drilled with the unmagnetized and magnetized bits. Neither do the small samples show remanent magnetization that is systematically different from that of the large samples out of which they were drilled.

DISCUSSION AND CONCLUSIONS

Our measurements on samples from the magnetic portion of Unit J of the Eleana Formation in the Calico Hills area penetrated by drill hole UE25a-3 indicate an average total magnetization of 3.89 A/m (3.89×10^{-3} emu) with a declination assumed to be 16° east of north, and directed downward 74° (thus, the unit is considered to be normally magnetized). This magnetic layer is approximately 366 m (1,200 ft) thick.

These Eleana rocks have a much higher susceptibility and total magnetization than Eleana rocks elsewhere. This is probably because alteration of the argillite unit has produced a magnetic phase (magnetite?) which fills fractures and is inhomogeneously disseminated throughout the rock. The bedding dips of the rocks of drill hole UE25a-3 were quite variable, ranging from nearly horizontal to as much as 38° in the sampled interval (Maldonado and others, 1979). The angles of our measured magnetic inclinations were so consistent, however, that we assume the rocks were magnetized after their structural deformation.

The measured average total magnetization of 3.89 A/m may be too high a value for the in situ magnetic interval of the Eleana Formation. Many of the samples possessed a large, soft, steeply inclined component of remanence which may have been imparted during the drilling process or some other phase of sample preparation. A limited study involving drilling this rock with a magnetized bit did not confirm such a soft component or its origin. It did demonstrate the variability of the magnetic properties of the rock.

REFERENCES

Bath, G. D., 1968, Areomagnetic anomalies related to remanent magnetism in volcanic rocks, Nevada Test Site: Geological Society of America Memoir 110, p. 135-146.

Daniels, J. J., and Scott, J. H., 1980, Borehole geophysical measurements for hole UE25a-3, Nevada Test Site, Nuclear Waste Isolation Program: U.S. Geological Survey Open-File Report 80-126, 30 p.

Jahren, C. E., and Bath, G. D., 1967, Rapid estimation of induced and remanent magnetization in volcanic rocks, Nevada Test Site: U.S. Geological Survey Open-File Report 67-122, 29 p.

Maldonado, F., Muller, D. C., and Morrison, J. N., 1979, Preliminary geologic and geophysical data of the UE25a-3 exploratory drill hole, Nevada Test Site, Nevada: U.S. Geological Survey Report USGS-1543-6, 47 p.

McKay, E. J., and Williams, W. P., 1964, Geology of the Jackass Flats quadrangle, Nevada: U.S. Geological Survey Geologic Quadrangle Map GQ-368, scale 1:24,000.

Orkild, P. P., and O'Connor, J. T., 1970, Geologic Map of the Topopah Spring quadrangle, Nevada: U.S. Geological Survey Geologic Quadrangle Map GQ-849, scale 1:24,000.

Poole, F. G., 1974, Flysch deposits of the Antler Foreland Basin, Western United States, in Tectonics and Sedimentation, Dickinson, W. R., ed.: Society of Economic Paleontologists and Mineralogists Special Publication No. 22, p. 58-62.

Poole, F. G., Houser, F. N., and Orkild, P. P., 1961, Eleana Formation of Nevada Test Site and vicinity, Nye County, Nevada: U.S. Geological Survey Professional Paper 424-D, p. D104-D111.

Sheriff, R. E., 1973, Encyclopedic Dictionary of Exploration Geophysics: Tulsa: Society of Exploration Geophycists, 266 p.

Snyder, D. B., and Oliver, H. W., 1981, Preliminary results of gravity investigations of the Calico Hills, Nevada Test Site, Nye County, Nevada: U. S. Geological Survey Open-File Report 81-101, 42 p.

U.S. Geological Survey, 1979, Aeromagnetic map of the Timber Mountain area, Nevada: U.S. Geological Survey Open-File Report 79-587, scale 1:62,500.

GPO 835-788

Partial copy 73 p. p. 1-3, p. 45-50, p. 54-56, p. 63-65, p. 68-72

USGS-OFR-85-49

need 66,67

UNITED STATES
DEPARTMENT OF THE INTERIOR
GEOLOGICAL SURVEY

PRELIMINARY INTERPRETATION OF PALEOMAGNETIC AND MAGNETIC PROPERTY DATA FROM DRILL HOLES USW G-1, G-2, GU-3, G-3, AND VH-1 AND SURFACE LOCALITIES IN THE VICINITY OF YUCCA MOUNTAIN, NYE COUNTY, NEVADA

Rosenbaum, Joe (303) 236-1304

In Tiva large variations in susceptibility

lot of Δ in magnetic properties are related to grain of microcrystalline Fe oxides

super paramagnetic - cannot hold remanent

Open-File Report 85-49

Prepared by the U.S. Geological Survey

for the

Nevada Operations Office
U.S. Department of Energy
(Interagency Agreement DE-AI08-78ET44802)

Denver, Colorado
1984

UNITED STATES
DEPARTMENT OF THE INTERIOR
U.S. GEOLOGICAL SURVEY

PRELIMINARY INTERPRETATION OF PALEOMAGNETIC AND MAGNETIC PROPERTY DATA FROM DRILL HOLES USW G-1, G-2, GU-3, G-3, AND VH-1 AND SURFACE LOCALITIES IN THE VICINITY OF YUCCA MOUNTAIN, NYE COUNTY, NEVADA

By

J. G. Rosenbaum and D. B. Snyder

ABSTRACT

Measurements of magnetic properties and paleomagnetic directions have been made on thousands of samples of Miocene age volcanics from drill core and surface localities in and around Yucca Mountain at the Nevada Test Site. The directional data have firmly established paleomagnetic polarities for the various members of the Paintbrush and Crater Flat Tuffs, and for the Tuffaceous Beds of Calico Hills. In addition, the Lithic Ridge Tuff is found to have a highly unusual paleomagnetic direction (southwest and nearly horizontal). Changes in inclination of remanence with depth in the Tuffaceous Beds of Calico Hills indicate that this unit was emplaced over a substantial period of time relative to secular variation of the geomagnetic field, and that the relatively thin sequence of tuffs of this unit encountered at the USW G-1 locality correlates roughly with the basal 125 m of the much thicker sequence penetrated in drill hole USW G-2.

Paleomagnetic data obtained for the Topopah Spring Member of the Paintbrush Tuff from cores from drill holes at Yucca Mountain and from outcrop at Busted Butte demonstrate that the remanence directions of this unit vary with depth. The cause of this variation is presently unknown and its presence severely limits the usefulness of the paleomagnetic method as a tool for examining structural rotations affecting the Topopah Spring Member. In contrast, the Tiva Canyon Member of the Paintbrush Tuff yields essentially one direction of remanence everywhere it has been sampled at Yucca Mountain. The near coincidence of paleomagnetic directions obtained for Tiva Canyon sites from throughout Yucca Mountain indicates that the change in strike of eutaxitic foliation and of the base of this unit in the vicinity of Drill Hole Wash cannot be due to structural rotation about a vertical axis, but does not rule out rotations of a few degrees about horizontal axes.

Four widespread units, the Tiva Canyon and Topopah Spring Members of the Paintbrush Tuff and the Bullfrog and Tram Members of the Crater Flat Tuff, are identified as potential sources of significant magnetic anomalies by measurements of remanent intensity and susceptibility. The measurements also demonstrate large variations in remanent intensity and susceptibility within individual ash-flow sheets. In some cases these variations are closely

related to geologically recognizable breaks in ash-flow tuff deposition. These variations provide the possibility of using magnetic field logs not only to locate major stratigraphic contacts but also to map subunits within the major ash-flow sheets.

INTRODUCTION

The strata underlying Yucca Mountain comprise a thick sequence of Miocene age volcanic rocks. The Tiva canyon Member of the Paintbrush Tuff is exposed over most of the surface of Yucca Mountain. Nearly 2 kilometers of ash-flow tuffs and related bedded tuffs were penetrated in drill holes USW G-1, G-2, GU-3, and G-3. In descending stratigraphic order the units are the Tiva Canyon, Yucca Mountain, Pah Canyon, and Topopah Spring Members of the Paintbrush Tuff, the tuffaceous beds of Calico Hills, the Prow Pass, Bullfrog and Tram Members of the Crater Flat Tuff, unnamed rhyodacite and dacite lava flows and flow breccias, the Lithic Ridge Tuff, and unnamed older lavas and tuffs. Detailed lithologic descriptions of the drill core are provided by Spengler and others [1981], Maldonado and Koether [1983], and Scott and Castellanos [1984].

Measurements of remanent magnetization and magnetic susceptibility of samples of volcanic rocks from bore holes and surface outcrops in the vicinity of Yucca Mountain have been used as stratigraphic correlation tools, as limitations on structural interpretations [Spengler and Rosenbaum, 1980], and as guides to the interpretation of magnetic anomalies in the area [Bath and Jahren, 1984]. Also these data should prove useful in the interpretation of in-hole magnetic-field and magnetic-susceptibility logs.

While the direction of remanent magnetism is useful in volcanic stratigraphic correlation and in the solution of structural problems, the direction and intensity of total magnetization, $\vec{J}_t$, is needed for the interpretation of magnetic anomalies. The total magnetization of a rock specimen is the vector sum of its remanent and induced magnetizations, so that

$$\vec{J}_t = \vec{J}_r + \vec{J}_i = \vec{J}_r + \frac{K\vec{B}}{\mu_0}$$

where $\vec{J}_t$, $\vec{J}_r$, and $\vec{J}_i$ are total, remanent, and induced magnetizations in amperes per meter (Am^{-1}), respectively; K is the bulk susceptibility (dimensionless); B is the magnetic flux ($\vec{B}$ has a magnitude of about 0.517×10^{-4} = 51,700 γ tesla (T) at NTS); and μ_0 is the permeability of free space ($\mu_0 = 4\pi \times 10^{-7}$ TmA^{-1}). $\vec{J}_r$ and K can be easily measured in the laboratory. 51,700 nT

The purpose of this report is to document magnetic property data for specimens collected during 1980-83 from drill holes USW G-1, G-2, GU-3, G-3, and VH-1 as well as from surface sampling localities on and around Yucca Mountain. Preliminary interpretations are also presented.

SAMPLING PROCEDURE

Cylindrical samples, approximately 2.5 cm in both length and diameter, were collected from outcrops and drill core. A sun compass was used to orient outcrop samples [Creer and Sanver, 1967]. Orientation with respect to the drill hole axes was maintained for all samples collected from drill core. In addition, samples from oriented core segments were collected in a

manner which preserved the orientation information [Spengler and Rosenbaum, 1980].

Sampling of outcrops has the advantage that accurate orientation of all samples is easily obtained by standard techniques. However, outcrop sampling has a number of disadvantages: (1) sampling is restricted to the limited stratigraphic section exposed in the area; (2) sampling vertically through a unit is often difficult due to incomplete exposure; (3) magnetic properties of samples may have been affected by weathering and therefore may not be representative of a large volume of rock; and (4) remanent magnetism at some localities has been altered by lightning strikes. Sampling cores from deep drill holes eliminates these problems. However, oriented core was obtained for only a small percentage of the drilled section because azimuthal orientaion of deep drill cores is difficult and expensive. Also the magnitude of the errors involved in the orienting procedure are much greater than those for outcrop sampling. Thus, the declination of magnetic remanence cannot be obtained for most of the samples taken from the deep drill holes. Moreover, it should be noted that inclination values from unoriented core cannot be corrected for deviation of the drill hole from vertical. Therefore, directional data from oriented samples presented on equal-area projections and in tables have been corrected for the drill hole orientation, whereas the inclination data for all samples plotted versus depth is oriented with respect to the drill hole axis.

LABORATORY PROCEDURES

The natural remanent magnetism (NRM) of each specimen was measured with a spinner magnetometer or, in some cases, with a cryogenic magnetometer. All outcrop samples were subjected to progressive alternating field (af) demagnetization to isolate a stable remanence direction. Selected samples from each unit encountered in the drill cores were also subjected to progressive af demagnetization to peak fields of 80 or 100 mT. In most cases it was found that the direction of these samples changed little during the cleaning process. All subsurface samples were demagnetized at a peak field of 10 mT.

Susceptibilities were determined on a precisely calibrated [Rosenbaum and others, 1979], highly sensitive bridge [Cristie and Symons, 1969]. A value of 51,700 nT was used for the earth's field in calculating the induced magnetization.

For the purpose of calculating total magnetization, each sample from drill core was assigned a remanent declination. In most cases the declination was obtained by averaging directions from measurements made on oriented specimens from the same geologic unit. In a few instances a declination of 0° (180°) was assigned to units which appeared to be normal (reversed) based on inclination data alone. In the text which follows "polarities," "directions," and "intensities of magnetization" refer to remanent magnetization unless otherwise specified as referring to total magnetization.

Tram Member: The Tram Member was sampled in drill holes USW G-1, G-2 and G-3. At Yucca Mountain the Tram can be divided into upper (lithic-poor) and lower (lithic-rich) zones. Both zones occur in holes USW G-1 and G-3, but only the lithic-rich zone occurs in USW G-2 [Spengler and others, 1981; Maldonado and Koether, 1983; Scott and Castellanos, 1984].

Oriented specimens obtained from USW G-1 and G-3 yield reversed directions with south-easterly declinations (Figure 14 and Table 14). Although the data from USW G-1 give a smaller α_{95} and larger precision parameter than those from USW G-3, it is likely that the G-3 data is more representative since the number of samples and the stratigraphic interval sampled are much greater for this hole than for USW G-1.

Inclination data for the Tram Member from USW G-3 remain quite uniform from near the top of the unit to a depth of about 1080 m (Figure 17). No substantive change in inclination occurs across any of the thin bedded intervals which occur at depths of 860, 911, 934.1, and 952.4 m [Scott and Castellanos, 1984] indicating that the entire unit was emplaced rapidly with respect to secular variation. Below this depth the inclination record becomes increasingly irregular. This zone is also characterized by increasing alteration (to zeolites and clay) of the tuff with depth [Scott and Castellanos, 1984], suggesting that the greater variations in the inclination record is a result of the acquisition of secondary components of remanence during the alteration of the tuffs. The inclination record from USW G-1 is relatively uniform in the upper 20 m, rather irregular for the next 50 m, again relatively uniform for 100 to 125 m, and then increasingly erratic in the lowermost 90 m of the unit (Figure 17). No reason is readily apparent for the irregular record between the depths of 825 and 875 m. However, as in USW G-3, the irregular record from the lower portion of the Tram Member corresponds to a zone of increased alteration [Spengler and others, 1981]. The Tram Member encountered in USW G-2 is relatively thin, lithic-rich and argillized [Maldonado and Koether, 1983]. It yields an extremely erratic inclination record throughout its thickness.

The upper lithic-poor portion of the Tram Member is characterized by high remanent intensities (Table 15) which increase from values of a few tenths to one Am^{-1} near the top of the unit to maxima in the interior of the unit of nearly 6 and 15 Am^{-1} at USW G-1 and G-3, respectively (Figure 18). As the magnetization decreases below these maxima the degree of welding also tends to decrease while the lithic content and the degree of alteration increase [Spenger and others, 1981; Scott and Castellanos, 1984]. Within this upper zone, changes in susceptibility correlate highly with changes in remanent intensity.

The lithic-rich lower zone is characterized by much lower remanent intensities than the upper zone (Table 15). Maldonado and Koether [1983] divide this portion of the Tram Member in drill hole USW G-2 into two parts, a unit consisting of more than 50% lithics above a depth of 1135 m and one comprising less than 50% lithics below this depth. As can be seen in Figure 18 both susceptibility and remanent intensity curves change abruptly at this depth. Although magnetization remains low throughout the lower lithic-rich altered portion of the Tram Member in USW G-1 and G-3, susceptibilities between 995-1060 m in USW G-1 and in the lowermost 75 m of the unit in USW G-3 are of about the same magnitude as those in the lithic-poor upper portion.

Table 14. Directional data for the Tram Member

Site	Lat.	Long.	N	D_R	I_R	a_{95}	K	af	Comments
USWG-1	36.867	116.458	6	135.8	-50.6	1.6	1762.8	10	Depth 935.5-938.5 m.
USW G-3	36.818	116.467	26	138.7	-42.6	3.2	81.1	10	Depth 819.5-948.5 m.

For explanation of headings see Table 1.

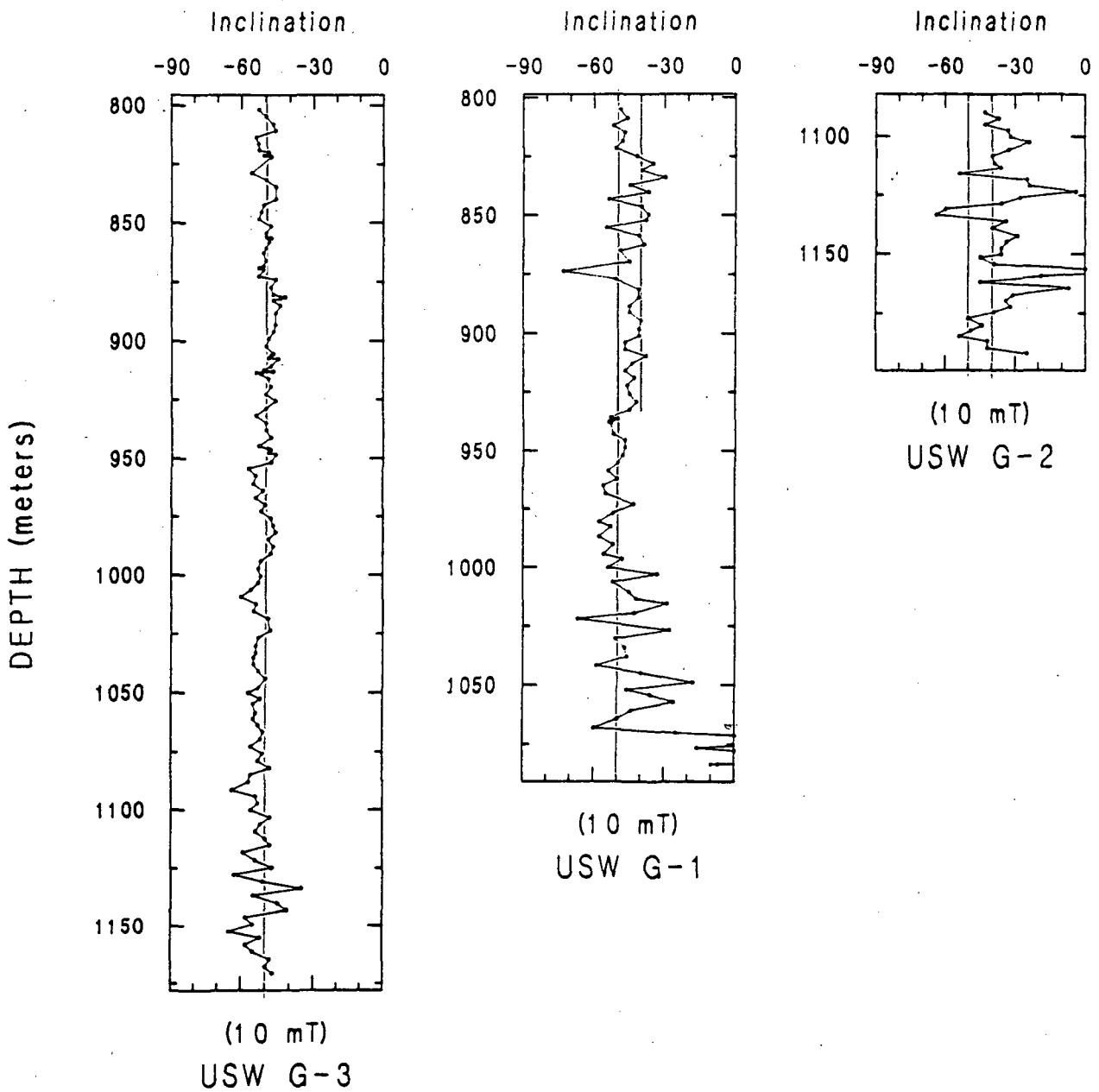

Figure 17.—Paleomagnetic inclinations versus depth for the Tram Member of the Crater Flat Tuff after a demagnetization at a peak field of 10 mT.

Table 15. Magnetic Property data for the Tram Member

Site	N	J_{NRM}	Sus.	Q	D_T	I_T	J_T	Comments
USW G-1	86	1.29±1.37	3.46±2.19	7.69	131	-30	1.20±1.30	Assumed D_R=144°.
	48	2.20±1.20	4.80±1.27	10.7	141	-42	2.04±1.17	Depth 805.0-945.5 m. Upper Tram
	38	.137±.143	1.73±1.87	3.89	117	-4	.125±.115	Depth 948.0-1073.5 m. Lower Tram
USW G-2	41	.217±.601	1.43±2.17	2.71	124	-1	.187±.546	Assumed D_R=144°.
USW G-3	139	1.90±2.40	2.90±1.65	13.3	134	-41	1.81±2.36	Assumed D_R=145°.

For explanation of headings see Table 2.

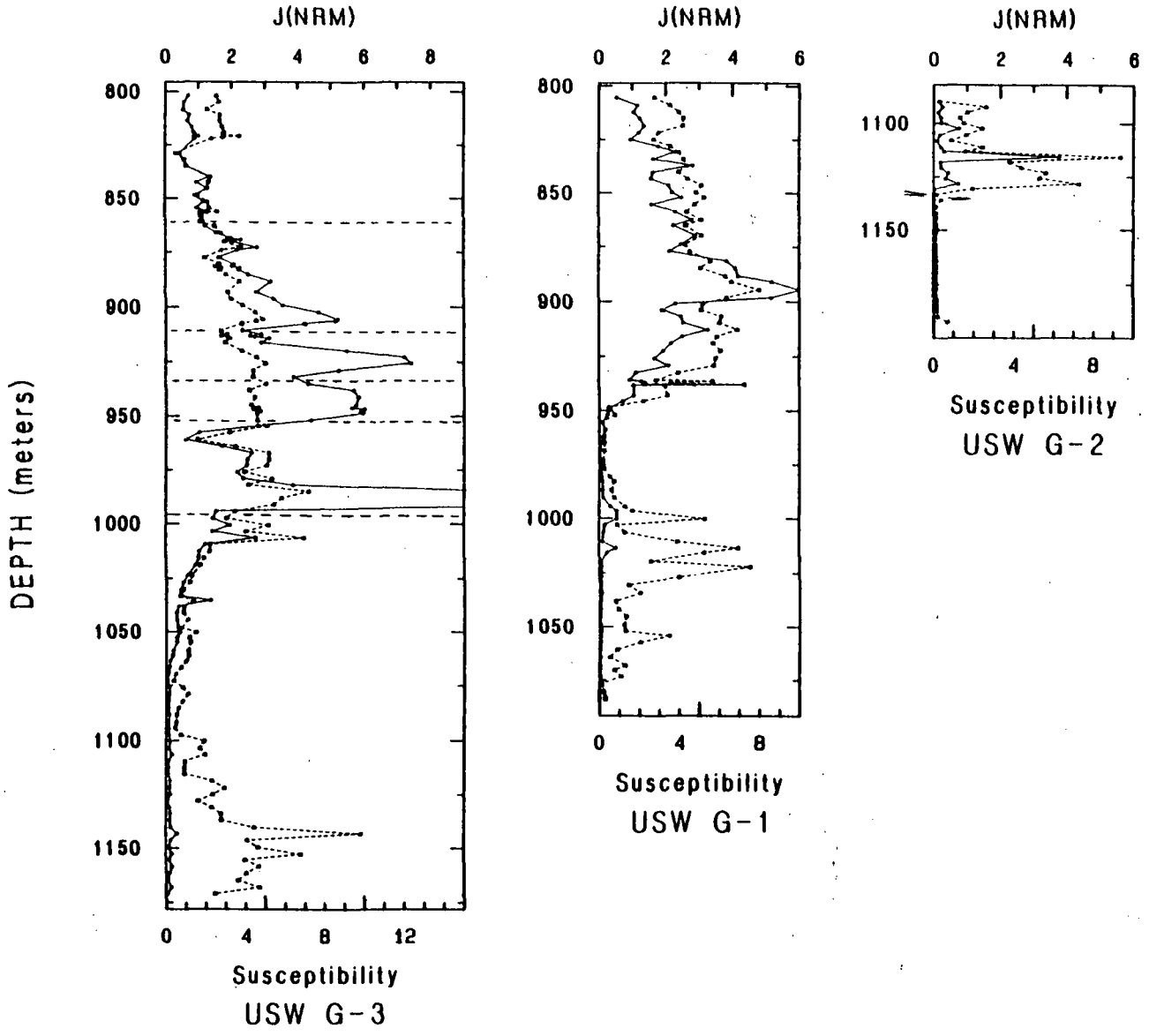

Figure 18.--Intensity of natural remanent magnetization, J(NRM), in Am^{-1} (circles and solid line) and SI susceptibility X 10^{3} (squares and dashed line) for the Tram Member of the Crater Flat Tuff. Horizontal dashed lines in plot of USW G-3 data represent depositional breaks [Scott and Castellanos, 1984].

Comparison of the magnetic properties to the lithologic description of the Tram Member from drill hole USW G-3 [Scott and Castellanos, 1984] reveals a good correspondence between geologically recognizable breaks in deposition and changes in magnetic properties. Scott and Castellanos [1984] recognized at least five depositional breaks. The upper four occur at depths of about 860, 911, 934 and 952.4 m and are marked by the presence of thin bedded tuffs. The fifth occurs at about 994 m at the base of an ash flow and was recognized by a minimum in the degree of welding. One of the four largest remanent intensity maxima occurs between each pair of adjacent depositional breaks (Figure 18) and the breaks fall at or near intensity and susceptibility minima. The largest of these maxima occurs just below a vitrophyre (982.1-983.7 m) [Scott and Castellanos, 1984]. A similar relationship between magnetic properties and a depositional break was noted for the Bullfrog Member. These observations and those of Hatherton [1954a; 1954b] indicate that at least some of the variation in magnetization may be related to the depositional history of the tuff. The mechanisms responsible for these variations are unknown but may include: (1) variation of the composition (i.e. magnetite content) of the erupted magma with time; (2) post-emplacement growth of fine-grained magnetic phases which occurs to a greater extent in one portion of the flow than another (perhaps more time for growth in the more slowly cooling interior than at the flow margins); and (3) greater oxidation of fine-grained magnetite at the top and bottom of the flows either at high temperature (during cooling) or at low temperture. Regardless of the mechanism, the correlation between remanent intensity variations and depositional breaks suggests that these variations could provide a useful tool for mapping the internal stratigraphy of thick compound cooling units.

Other Units

Lava Flows and Flow Breccias between Tram Member and Tuff of Lithic Ridge: The dacite and rhyodacite lava flows and flow breccias underlying the Tram Member in the northern part of Yucca Mountain [Spengler and others, 1981; Maldonado and Koether, 1983] were sampled throughout their vertical extent in drill holes USW G-1, G-2, and at four depth intervals in USW H-6. These units are not present in USW G-3.

The inclination data from USW G-1 and G-2 vary to such a degree that even a magnetic polarity (normal or reversed) for these rocks cannot be determined from these data (Figure 19). This erratic record may be due to alteration of the rocks, or it may indicate that the individual blocks comprising the breccia had cooled sufficiently to acquire their remanence prior to emplacement. In contrast, the dacite lava flows from USW H-6 yield exclusively downward directed magnetic vectors with inclinations ranging between 25° and 40° (Figure 19). Therefore, the unit is considered to be of normal polarity (D_R=0°, was assigned for the calculation of the total magnetization, see Table 16).

In samples from USW G-1 and G-2 remanent intensity averages only a few tenths of an Am^{-1}; however, susceptibility values are quite high (Figure 20 and Table 16). Intensities from two levels in USW H-6 are of similar magnitude to those in USW G-1 and G-2, and at two levels are much greater. Only samples of vitrophyre from a depth of 1100 m in USW H-6 have susceptibilities of the level observed in the other holes.

The rock obtained from USW H-6 appears to be much less altered than that from USW G-1 and G-2. In addition, values of Q computed for the various levels sampled in USW H-6 are substantially greater than those obtained from USW G-1 and G-2. These observations suggest that alteration has destroyed much of the fine-grained magnetite at the USW G-1 and G-2 localities, and that if these rocks were unaltered they would possess much higher remanent intensities.

Lithic Ridge Tuff: The Lithic Ridge Tuff was sampled throughout its thickness in drill holes USW G-1, G-2, and G-3. Oriented specimens were obtained from all three of these holes as well as from outcrop at the type locality at Lithic Ridge (site JR81-10) [Carr and others, 1984]. Although the inclination data from the entire unit as a whole are extremely erratic (Figure 21), af demagnetization of the oriented specimens yielded mean directions of remanent magnetization from each of the three drill holes that are to the southwest and nearly horizontal (Table 17). The mean directions of remanent magnetism of the outcrop samples after af demagnetization at 5, 10 and 20 mT differ significantly from those obtained from the drill holes (Figure 22 and Table 17). However, the average direction of vectors removed during demagnetization between 5 and 20 mT is in good agreement with the directions determined from the three holes (Figure 22f). The outcrop samples apparently possess both a soft remanence (probably a viscous remanence), which is largely removed by af demagnetization in a peak field of 5 mT (Figure 22b), and a rather hard, secondary magnetization (probably a chemical remanent magnetization) which remains after demagnetization at 20 mT (Figure 22a). These components tend to obscure the initial remanence of the unit. Similar components may be present in the drill hole samples and account for the irregular inclination records.

It should be noted that the directions presented in Table 17 and Figure 22 have not been corrected for tectonic rotation. This implies that the Lithic Ridge Tuff at Yucca Mountain has a similar attitude to that at the type locality. Nevertheless, the good agreement of directions from this unit at Yucca Mountain and at the type locality strongly supports the equivalence of these rocks.

Variations in remanent intensity of the Lithic Ridge Tuff with depth display a high degree of correlation with susceptibility variations (Figure 23). Average intensities from the drill holes are less than 0.2 Am^{-1} and from outcrop only slightly higher (Table 18). Both susceptibility and intensity generally decrease with depth. This may be due to increasing alteration with depth, although such a change is not evident from petrographic descriptions of the core [Spengler and others, 1981; Maldonado and Koether, 1983; and Scott and Castellanos, 1984].

Older Tuffs of USW G-1, and Lava Flows and Flow Breccias of USW G-2; Spengler and others [1981] divide the older tuffs encountered in drill hole USW G-1 into three units, A, B, and C. Inclination data from these tuffs are for the most part erratic. Because of the highly altered nature of these rocks it is impossible to confidently interpret magnetic polarities for these ash-flow tuffs. Nevertheless, two zones from which oriented samples were obtained yield reasonably consistent directions. One, from unit C at the bottom of drill hole USW G-1, is normal; the other, from rocks at the bottom of USW G-3 which correlate with unit A [Scott and Castellanos, 1984], is reversed (Table 19).

Table 17. Directional data for the Lithic Ridge Tuff

Site	Lat.	Long.	N	D_R	I_R	a_{95}	K	af	Comments
JR81-10	36.933	116.269	16	260.6	41.9 N	14.2	7.7	20	Type locality [Carr and others,1984]. *
			16	305.0	64.6 N	18.4	5.0	NRM-5	Removed vector.
			13	243.5	5.4 –	5.6	55.4	5-10	" "
			13	239.6	-0.3 –	6.7	30.8	5-20	" "
			13	238.4	-3.1 –	7.6	30.8	10-20	" "
USW G-1	36.867	116.458	8	225.3	-7.0 R	5.1	118.2	30	Depth 1229.0-1285.0 m.
USW G-2	36.890	116.459	10	229.4	-8.5 R	11.4	18.9	10	Depth 1313.0-1322.0 m.
USW G-3	36.818	116.467	9	236.2	-7.1 R	10.1	26.8	10	Depth 1183.5-1310.0 m.

For explanation of headings see Table 1.

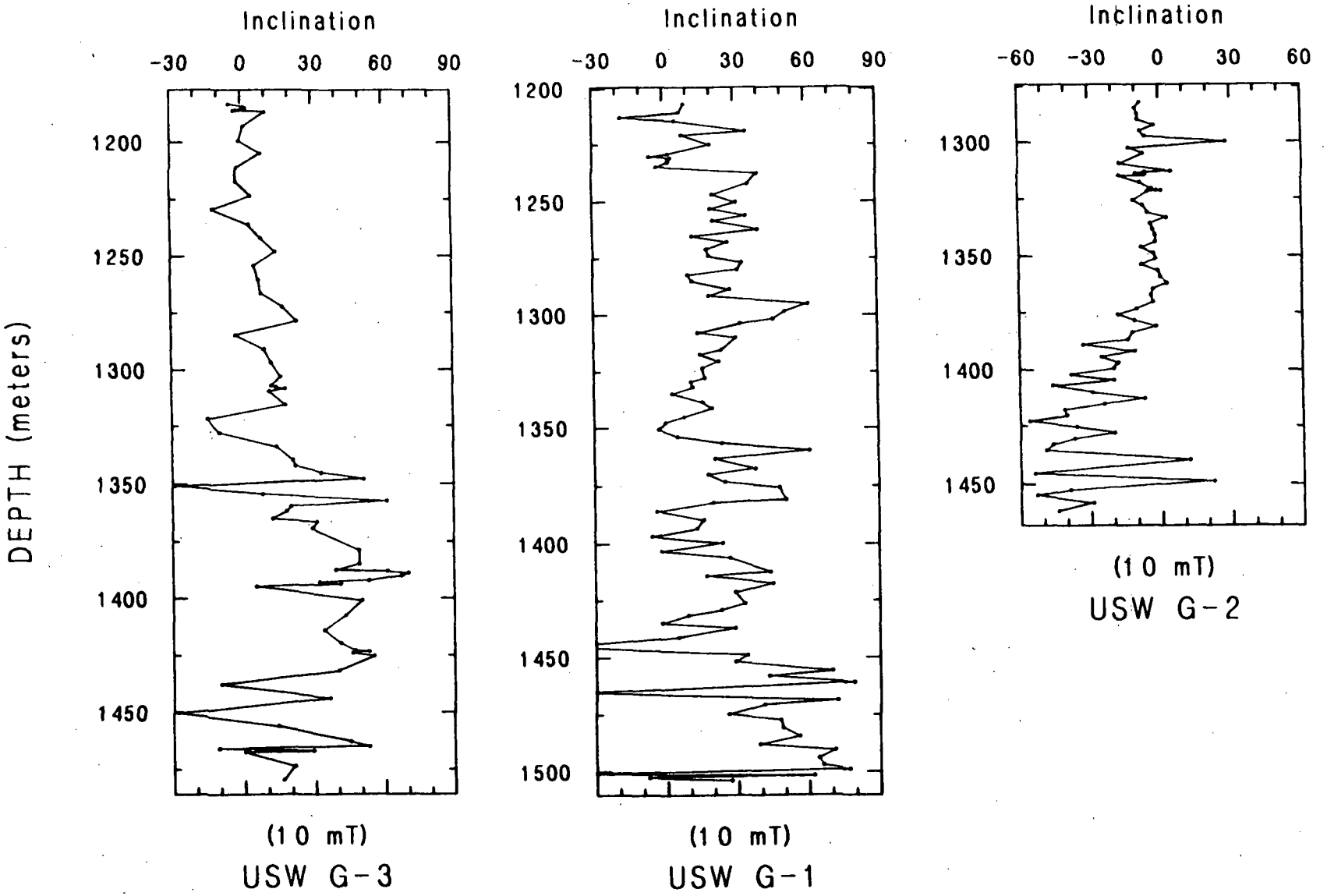

Figure 21.—Paleomagnetic inclinations versus depth for the Lithic Ridge Tuff after af demagnetization at a peak field of 10 mT.

Table 18. Magnetic Property data for the Lithic Ridge Tuff

Site	N	J_{NRM}	Sus.	Q	D_T	I_T	J_T	Comments
JR81-10	16	.265±.072	4.59±0.73	1.41	260	42	.290±.087	
USW G-1	95	.171±.165	3.14±2.20	1.19	251	69	.222±.182	Assumed D_R=225°.
USW G-2	73	.134±.134	2.58±1.91	1.23	249	48	.132±.121	Assumed D_R=225°.
USW G-3	75	.175±.142	3.72±2.71	1.19	264	62	.226±.138	Assumed D_R=235°.

For explanation of headings see Table 2.

The thick sequence of older ash flows penetrated in the bottom of USW G-1 is not present in USW G-2. Only a single thin ash-flow tuff which apparently correlates with a thin tuff at the top of unit C represents this part of the section [Maldonado and Koether, 1983]. A sequence of lava flows and flow breccias occurs below this tuff at the locality of USW G-2. With increasing depth the composition of these flows changes from rhyolite, to quartz latite, and finally to dacite. These rocks are highly altered. All but two of 33 samples of the rhyolite have negative remanent inclinations, whereas all 40 samples of the quartz latite and 21 samples of the dacite have positive inclinations. Therefore, the rhyolite appears to be of reversed polarity while the older more mafic lavas are of normal polarity.

The average magnetic properties for units penetrated in drill holes USW G-1, G-2 and G-3 below the Lithic Ridge Tuff are summarized in Table 20. Total magnetizations for these rocks are plotted in Figure 24.

The uppermost part of unit A in USW G-1 and all of the unit sampled from USW G-3 are characterized by extremely low remanent intensities ($<<0.1$ Am^{-1}) and susceptibilities ($<2 \times 10^{-3}$ SI). Both intensity and susceptibility values then rise so that J_t averages about 0.45 Am^{-1} in the lower part of unit A in USW G-1 (Figure 24). Total magnetization of unit B averages about 0.3 Am^{-1} near the top of the unit, falls to extremely low values near the middle, and then rises sharply near the base of the unit. Unit C from USW G-1 is on average more magnetic than units A and B, although its total magnetization curve varies erratically.

Low J_R
Low χ

The composition of the lavas and flow breccias which occur beneath the Lithic Ridge Tuff in USW G-2 (and presumably stratigraphically below Unit C of USW G-1) progress from rhyolite, to quartz latite, to dacite with depth [Maldonado and Koether, 1983]. Although these rocks are highly altered, they become more magnetic with depth and as their compositions become more mafic.

DISCUSSION AND SUMMARY

The interpretation of these data bear on stratigraphy, structure, and potential sources of magnetic anomalies in the vicinity of the Nevada Test Site. The data also raise several questions about the magnetism of welded tuffs.

Based upon the paleomagnetic directional data, declinations and inclinations from oriented specimens and inclination data from unoriented samples, the units can be assigned the polarities given in Table 21. Due to various uncertainties, such as the directional variations demonstrated in the Topopah Spring Member of the Paintbrush Tuff and orientation errors of unknown magnitude in obtaining oriented cores from drill holes, and due to the fact that nearly all the data come from the Yucca Mountain block, no attempt has been made to define a precise direction of remanence for any of the units.

The polarity of the units is useful as a stratigraphic aid. For instance the petrographically similar Topopah Spring and Tiva Canyon Members of the Paintbrush Tuff are easily distinguished by their opposite polarities. In addition, the Lithic Ridge Tuff possesses very unusual (southwesterly and nearly horizontal) remanent direction. Because the geomagnetic field would not be expected to maintain a direction such as this for extended periods or

(p. 67 missing)

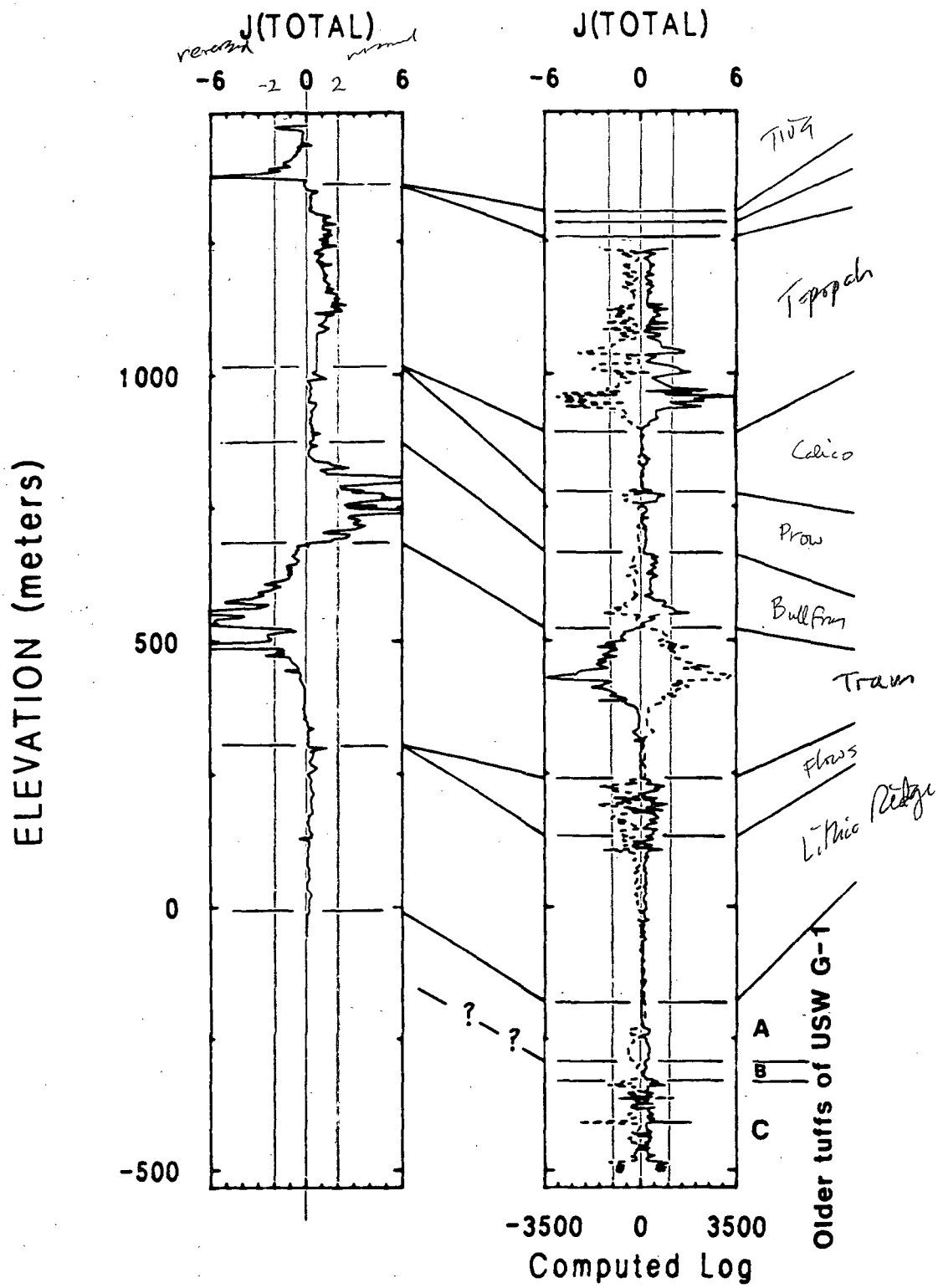

Figure 24.—Total magnetization (Am^{-1}) versus depth (solid lines) for drill holes USW G-1, G-2, GU-3, and G-3, and modeled total field log (dashed

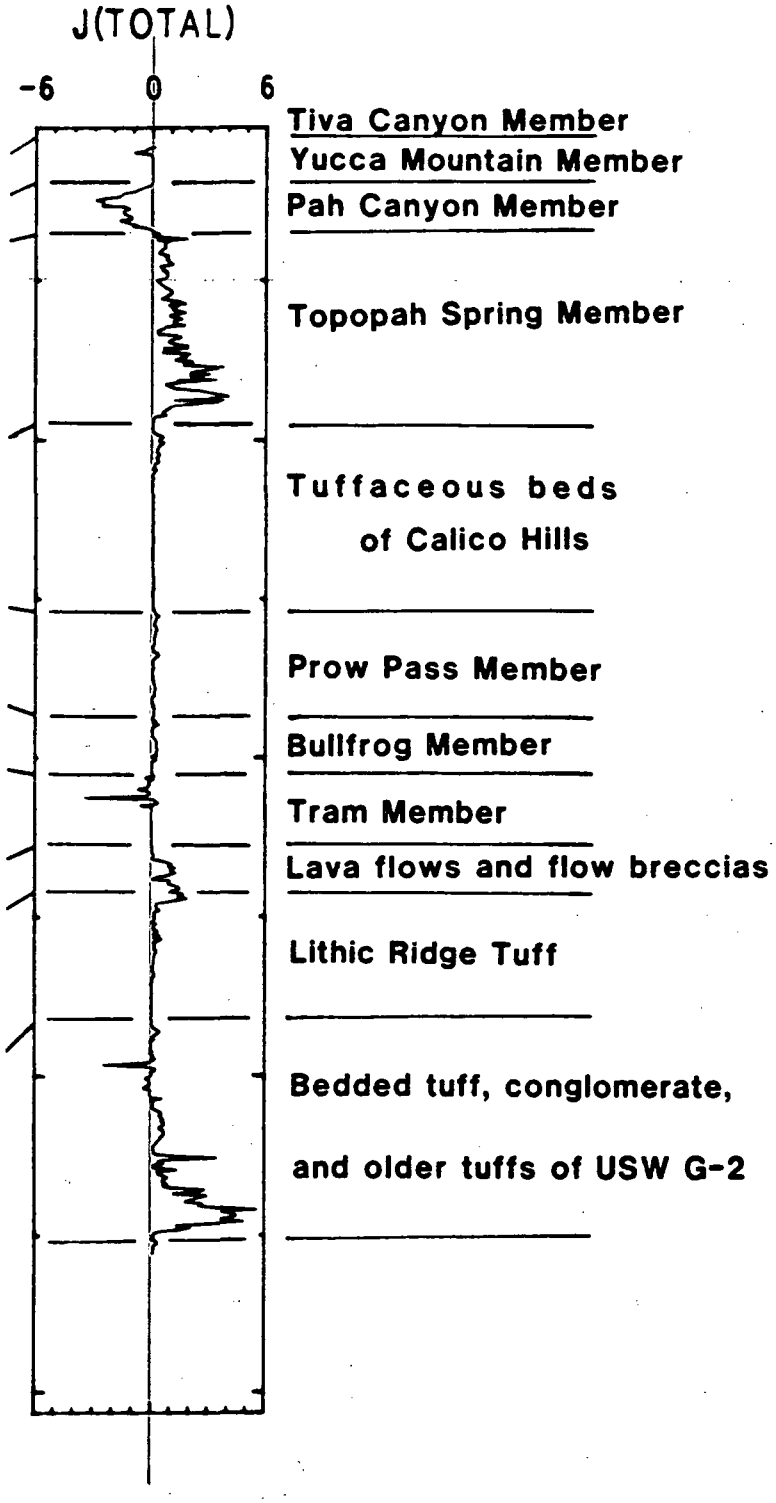

line) for drill hole USW G-1 (nT). Geologic contacts are from Spengler and others [1981], Maldonado and Koether [1983], and Scott and Castellanos [1984].

to frequently occupy such a position, determination of this direction from other localities would strongly support correlation to the Lithic Ridge Tuff.

In addition, inclination data from the tuffaceous beds of Calico Hills suggest that the relatively thin section encountered in drill hole USW G-1 is correlative with only the lowermost 125 m or so of the much thicker section encountered in drill hole USW G-2.

Two points bearing upon the structure of Yucca Mountain should be emphasized. First, paleomagnetic directions from the Tiva Canyon Member of the Paintbrush Tuff indicate that there has been no relative rotation of more than a few degrees between the sampling sites after emplacement of this unit. Therefore, the rather large, sharp change in strike observed in both the eutaxitic foliation and the base of the Tiva Canyon Member is not due to rotation about a vertical axis, and may be either a depositional feature or due to small rotations about horizontal axes. Second, the acquisition of data demonstrating very large directional variations of the remanent magnetism of the Topopah Spring Member largely invalidate the paleomagnetic evidence for left-lateral strike-slip movement on faults within Drill Hole Wash [Spengler and Rosenbaum, 1980].

Bath and others [1983] have arbitrarily set the following limits to characterize rocks for the purpose of describing their potential for producing magnetic anomalies:

$$\text{nonmagnetic} < 0.05\ \text{Am}^{-1}$$
$$0.05\ \text{Am}^{-1} < \text{weakly magnetic} < 0.50\ \text{Am}^{-1}$$
$$0.50\ \text{Am}^{-1} < \text{moderately magnetic} < 1.50\ \text{Am}^{-1}$$
$$1.50\ \text{Am}^{-1} < \text{strongly magnetic.}$$

Inspection of Figure 24 reveals that there are four arealy extensive ash-flow sheets which possess moderate to strong magnetizations throughout substantial stratigraphic thicknesses, and are therefore considered to be likely sources of magnetic anomalies. These units are the Tiva Canyon and Topopah Spring Members of the Paintbrush Tuff, and the Bullfrog and Tram Members of the Crater Flat Tuff. The Tiva Canyon and Tram Members are reversed, and the other two units are of normal polarity. Although data from only three samples of the tuff of Chocolate Mountain (the intracaldera equivalent of the uppermost layers of the Tiva Canyon Member) are available, this unit appears to be highly magnetic and certainly must be considered as a possible anomaly source. The reversely magnetized Pah Canyon Member is also moderately to strongly magnetic. However, it is not considered to be an important source of magnetic anomalies because it is thin and of limited areal extent. Also, the lavas between the Tram Member of the Crater Flat Tuff and the Lithic Ridge Tuff reach moderate to strong magnetizations (Figures 20 and 24, and Table 18). The thickness of this unit varies greatly (Figure 20), and it therefore must be considered a possible anomaly source.

In addition to the units penetrated in drill holes at Yucca Mountain there obviously may be deeper anomaly sources. Possible deep sources include other volcanic rocks, plutonic rocks, and altered sediments like those encountered in drill hole UE25a-3 at Calico Hills [Baldwin and Jahren, 1982].

The results raise two major questions about the magnetization of welded tuffs. The cause of variations in the directional data from the Topopah

p.70 missing

Spring Member are presently unknown. Several possible explanations are: 1) that the entire unit was emplaced over a relatively long period of time with respect to secular variation; 2) that the unit was emplaced quickly but cooled over a relatively long period; and 3) that internal deformation of the cooling unit took place at temperatures below that at which much of the magnetization was acquired. Regardless of the cause, such variations severely limit the usefulness of paleomagnetic directions from the Topopah Spring Member as an aid to structural interpretation.

The other question concerns the origin of the large lateral and vertical variations of magnetic properties observed within single cooling units. Mechanisms which could contribute to the variations include: (1) differences within the magma in composition, quantity, and grain size of the magnetic phase at the time of eruption; (2) post-emplacement growth of differing quantities and grain sizes of magnetic phases; and (3) varying degrees of alteration with attendant oxidation of highly magnetic magnetite to less magnetic hematite. The position of remanent intensity maxima between depositional breaks in the Bullfrog and Tram Members of the Crater Flat Tuff encountered in drill hole USW GU-3 and G-3 (Figures 16 and 18) strongly suggests some relation of the magnetic property variations to emplacement history.

Figure 24 displays a calculated magnetic field log for drill hole USW G-1. The model used to generate the log consists of a large number of thin sheets. Each sheet corresponds to a sample and extends half the distance to the overlying sample and half way to the underlying one. Each sheet was assigned a uniform magnetization equal to the total magnetization computed for the corresponding sample. The magnetic field produced by the model was calculated at about 3 m (10 ft) depth intervals at the center of a hexagonal hole approximately 0.3 m (1 ft) in diameter. The modeling results indicate that the magnetic field variations should have amplitudes of several hundred to several thousand nT. There is therefore a good possibility of using magnetization variations, as determined from in-hole magnetic logs in closely spaced holes, as an aid in locating not only major stratigraphic contacts but also to map zones within complex compound cooling units.

REFERENCES CITED

Baldwin, M. J., and Jahren, C. E., 1982, Magnetic properties of drill core and surface samples from the Calico Hills area, Nye County, Nevada, U. S. Geological Survey, Open-File Report 82-536, 27 p.

Bath, G. D., and Jahren, C. E., 1984, Interpretations of magnetic anomalies at a potential repository site located in the Yucca Mountain area, Nevada Test Site, U. S. Geological Survey, Open-File Report 84-120, 53 p.

Bath, G. D., Jahren, C. E., Rosenbaum, J. G., and Baldwin, M. J., 1983, Magnetic investigations, Chapter C in Geologic and Geophysical investigations of Climax Stock intrusive, Nevada, U. S. Geological Survey, Open-File Report 83-377,p. 40-77.